CONTRIBUTIONS TO THE STUDY OF SPRAYING OPERATIONS IN THE CONTEXT OF SUSTAINABLE AGRICULTURE

by

Muhammad Nadeem

Submitted in partial fulfilment of the requirements
for the degree of Doctor of Philosophy

at

Dalhousie University
Halifax, Nova Scotia
August 2019

DEDICATION

*This PhD thesis dissertation is dedicated to my wife**, Bushra Nadeem**, who has been an amazing source of support and encouragement. I am truly thankful for having you in my life. This work is also dedicated to my parents, **Ghulam Farid** and **Haleema Bibi**, whose hard work and guidance have allowed me to accomplish my goals.*

Muhammad Nadeem

TABLE OF CONTENTS

LIST OF TABLES

LIST OF FIGURES

ABSTRACT

The global agriculture sector faces many challenges in its mission to meet the growing demand for food and fiber. Climate change, increasing population growth, emergence of crop diseases, damages to crops from rodents and critters, and shrinking farming land in some regions are among these challenges. The application of agrochemicals has proven to be an efficient answer to some of these challenges. Through three themes, this thesis investigates how spraying configuration can contribute to the reduction of spray losses in the context of sustainable agriculture.

The first theme introduces a method for fluid quantification from a sprayer jet using a Particle Image Velocimetry (PIV) system in combination with imaging processing. Experimental results revealed that fluid flow measurement through PIV is reliable and PIV can be used to predict the spray pattern accurately and reveal velocity distribution.

The second theme investigates the velocity distribution of an extended flat fan nozzle to determine the weak jet areas, which have high risks of droplet drift, using the Particle Image Velocimetry (PIV) method and Computational Fluid Dynamics (CFD) with volume of fluid (VOF) simulation approach. Particles in the central region of the spray sheet have maximum kinetic energy and have the ability to hit the right target on the plant surface, while liquid particles in the surroundings of this central area have less velocity with minimum kinetic energy and have maximum chances to be off-target during spraying.

The third theme deals with the development of a mathematical model to jointly minimize spraying time and drift losses. The obtained bi-objective model is solved for a case study published in the crop protection literature. The results show that valid and reasonable solutions can be obtained by selecting the appropriate combination of boom height, nozzle spacing, nozzle type and tractor travel speed.

RESUME

Le secteur agricole mondial est confronté à de nombreux défis dans sa mission consistant à répondre à la demande croissante d'aliments et de fibres. Les changements climatiques, la croissance démographique croissante, l'apparition de maladies des cultures, les dommages causés aux cultures par les rongeurs et les bestioles, et la contraction des terres agricoles dans certaines régions figurent parmi ces défis. L'application de produits agrochimiques s'est révélée être une réponse efficace à certains de ces défis. À travers trois thèmes, cette thèse étudie comment la configuration de pulvérisation peut contribuer à réduire les pertes de pulvérisation dans le contexte d'une agriculture durable.

Le premier thème présente une méthode de quantification de fluide à partir d'un jet de pulvérisation utilisant un système de vélocimétrie par image de particules (PIV) en combinaison avec un traitement d'imagerie. Les résultats expérimentaux ont révélé que la mesure du débit de fluide à travers le PIV est fiable et que le PIV peut être utilisé pour prédire le modèle de pulvérisation avec précision et révéler la distribution de la vitesse.

Le deuxième thème étudie la distribution des vitesses d'une buse à jet plat et allongé afin de déterminer les zones de jet faibles présentant un risque élevé de dérive des gouttelettes, à l'aide de la méthode de vélocimétrie par image de particules (PIV) et de la dynamique des fluides numérique (CFD) avec volume de fluide (VOF) approche de simulation. Les particules dans la région centrale de la feuille de pulvérisation ont une énergie cinétique maximale et peuvent frapper la bonne cible à la surface de la plante, tandis que les particules liquides aux alentours de cette zone centrale ont une vitesse inférieure avec une énergie cinétique minimale et ont un maximum de chances d'être présentes. hors cible pendant la pulvérisation.

Le troisième thème concerne l'élaboration d'un modèle mathématique visant à minimiser conjointement le temps de pulvérisation et les pertes par dérive. Le modèle à deux objectifs obtenu est résolu pour une étude de cas publiée dans la littérature sur la protection des cultures. Les résultats montrent que des solutions valables et raisonnables peuvent être obtenues en choisissant la combinaison appropriée de hauteur de flèche, espacement des buses, type de buse et vitesse de déplacement du tracteur.

LIST OF ABBREVIATIONS AND SYMBOLS USED

A	Nozzle Spacing
ANOVA	Analysis of Variance
ASABE	American Society of Agricultural and Biological Engineers
C	Number of Tractor Direction Changes (passes) $c = \lceil WF/LB \rceil$
C_a	Area Coefficient
CCD	Charged Coupled Device
C_d	Coefficient of Discharge
CFD	Computational Fluid Dynamic
cm	Centimetre
CMOS	Complementary Metal Oxide Semiconductor
C^o	Degree Centigrade
C_v	Velocity Coefficient
D	Diameter of Nozzle orifice (m)
D_b	Fraction of Applied Spray which is Lost During Spraying and/or after Application
d_d	Distance Travelled by the Spray Particles in Wind Direction (m) (1m, our study)
DF	Degree of Freedom
DS	Total Specific Drift Proportion
F_{110}	Flat Fan Nozzle with Spray Angle of 110^o
H	Plant Height from Ground to Canopy (m)
H_j	Boom Height Level j from the Ground (m)
Hp	Horse Power

I	Index for Tractor Speed Levels
IA	Interrogation Area
J	Index for Boom Height Levels
K	Turbulence Kinetic Energy
K	Index for Nozzle Pressure Levels
kPa	Kilo-Pascal
L	Litres
l	Spacing between Consecutive Nozzle Attachments (m)
L_B	Boom Length (m)
LD 110	Low Drift Nozzle with Spray Angle of 110^o
L_F	Farm Length (m)
m	Meter
mL	Milli Litres
mm	Milli Meters
MMC	Multiple Mean Comparison
MS	Mean Square
n	Index for Nozzle Types
N_1	Total Number of Droplets Released from Sprayer (Calculated Manually)
N_2	Total Number of White Pixels
N_3	Total Number of Droplets Released from Sprayer in Fixed Time
N_n	Nozzle Type
O	Index for spray angle levels
O_{max}	Maximum Spray Sheet Overlap Allowed

O_{min}	Minimum Spray Sheet Overlap Required
Θ_o	Spray Angle Level o in Degrees (^{o})
O_v	Overlapping of Nozzle Sheets volume (m) Calculated as a Function of A, Hj and θ
PDA	Phase Doppler Anemometer
PDPA	Phase Doppler Particle Analyzer
PEI	Prince Edward Island
PIV	Particle Image Velocimetry
P_k	Nozzle Pressure (bars)
PLIF	Planar Laser Induced Florescence
PSV	Particle Streak Velocimetry
PTV	Particle Tracking Velocimetry
Q	Flow Rate (m^3/s)
R	Radius of Nozzle (m)
R^2	Coefficient of Determination
R_e	Reynold Number
S_i	Tractor Driving Speed Level i (km/h)
STP	Standard Temperature and Pressure
T	Average Air Temperature (^{o}C)
T_d	Total Drift (%)
T_s	Total Spraying Time (h)
V_1	Volume of Water Measured by PIV and Image Processing (mL)
V_2	Manually Measured Volume (mL)

$V_{3.25m}$	Average Wind Velocity at Height of 3.25 m above the Ground level (m/s)
V_{drop}	Average Volume of One Droplet
V_j	Jet Velocity (m/s)
VOF	Volume of Fluid
$V_{PIV\text{-}water}$	Total Volume of Water Measured using PIV
V_{water}	Total Volume of Water Released from Sprayer Nozzle
W	Watts
W_F	Farm Width (m)
WSP	Water Sensitive Paper
x	0.5 for Turbulence Flow
YLF	Yttrium Lithium Fluoride
Z	Objective Function
A	Marker Function (0-1)
E	Dissipation Rate
ζ_{H2O}	Absolute Humidity (weight of water vapors in grams per kg of dry air)
ρ	Liquid Density (kg/ m^3)
% E	% Absolute Error
Δ p	Total Pressure Drops (pa)
μ	Kinematic Viscosity (m^2/s)
2D	Two Dimensional

ACKNOWLEDGEMENTS

The work presented in this thesis was accomplished under enthusiastic guidance, sympathetic attitude, inexhaustible inspiration and enlightened supervision of *Prof. Dr. Tri Nguyen-Quang.* His effort towards hard work and maintenance of professional integrity will always serve as an appreciation, gratitude, and indebtedness for his valuable guidance.

I offer my cordial and profound thanks to a dignified personality and my co-supervisor, Prof. Dr. Claver Diallo for his knowledgeable guidance and continued support that has helped me to accomplish my project. I am very thankful to my committee members Prof. Dr. Uday Venkatadri and Prof. Dr. Peter Havard for their support, guidance, time and expertise throughout my project deliverables. All my committee members have provided a vast amount of advice and inspiration over the past four years. I have been blessed to have such an excellent group of researchers in my supervisory committee. Many thanks are given to Dr. Young Ki Chang who helped me in the initial stage of this project.

I want to thank University of Agriculture, Faisalabad, Pakistan for providing funding during my doctorate degree. I wish to acknowledge Canada Foundation for Innovation (CFI) Grant No 31188, Nova Scotia Research and Innovation Trust (NSRIT) and Natural Sciences and Engineering Research Council of Canada (NSERC) Grant No 34119 of Dr. Tri Nguyen-Quang for providing research funding to complete this thesis.

My gratitude remains incomplete if I do not mention the contribution of my sincere friends and teachers Mr. Anwar Saeed, Dr. Manzoor Ahmad, Dr. Muhamamd Iqbal, Dr. Abdul Jabbar, Dr. Tariq Aziz, Mr. Shafique Anwar and Syed Mashood ul Hassan, Syed

Muhammad Aslam who selflessly encouraged me with sympathetic attitude throughout the course of this research endeavor.

My thanks are also due to the kindness and love of my friends and lab mates Dung Tri Nguyen, Kateryna Hushchyna, Van Hai, and Kayla McLellan.

I wish to express my sincere feelings of gratitude and cordial thanks to my beloved brothers Muhammd Shafique, Waseem Akram, Muhammad Naeem, Mudasar and my beloved sister Samina Farid and her husband Farooq Asghar. I would like to say thanks to my brothers in law Mr. Ghulam Jelani, Sharjeel Hussain, Usman Shahid and my sisters in law Muntaha Jelani, Dr. Sidhra Sharjeel, Dr. Asma Ikram, Charity Miller and my mother in law Sheri Tirrel, and all above my beloved wife Bushra Nadeem and my son Muhammad Roshaan Musa who have always wished to see me glittering on the skies of success. Their hands always raised in prayers for me and without their support the present cherished goal merely would have been a dream for me.

CHAPTER 1: INTRODUCTION

1.1 SUSTAINABLE AGRICULTURE

The agriculture sector is responsible for providing the food and fibre needs of the almost eight billion inhabitants of our planet (Velten et al., 2015). Nowadays, the agriculture sector is facing a number of problems in its quest to fulfil the needs of a global population that is increasing by about 80 million people each year (Azadi et al., 2011a). Some of the challenges that must be tackled are: air, soil and water contamination through pesticides application; labor shortage; rapid climate changes; loss of biodiversity; depletion of available water resources; land degradation (soil erosion, soil compaction, salinity); and increasing production costs (decreasing number of farms). The existing agricultural system faces these problems; some are considered as major problems even in this modern age (Rivera et al., 2013; Koohafkan et al., 2012). The traditional agriculture cannot address these challenges. Thus, there is a need to move a sustainable agriculture which aims at developing practices that reduce the environmental degradation along with optimizing the operational efficiency and reduce the cost of operation. Several definitions of sustainable agriculture can be found in the literature:

1. It is an "*integrated system of plant and animal production practices having a site-specific application that will, over the long term: (a) satisfy human food and fiber needs; (b) enhance environmental quality; (c) make efficient use of non-renewable resources and on-farm resources and integrate appropriate natural biological cycles and controls; (d) sustain the economic viability of farm operations; and (e) enhance the quality of life for farmers and society as a whole*" (Farm Bill, 1990).

2. *"For a sustainable farm, high-quality food must be produced in adequate amounts, protect its resources and be both environmentally safe and profitable. Instead of depending on purchased materials such as fertilizers, a sustainable farm relies as much as possible on beneficial natural processes and renewable resources drawn from the farm itself*" (Reganold et al*.,* 1990).
3. Sustainable agriculture is a system of "*management procedures that work with natural processes to conserve all resources, minimize waste and environmental impact, prevent problems and promote agroecosystem resilience, self-regulation, evolution and sustained production for the nourishment and fulfillment of all*" (MacRae et al., 1989)

In summary, sustainable agriculture is a farm, food and fiber production system that respects the natural balance of different available natural resources while minimizing its environmental impacts. Sustainable agriculture aims to reduce the cost of operation, optimize the operational efficiency (economic viability), prevent environmental degradation (protect the environment) and all these practices should be acceptable for human being (socially acceptable). These goals constitute the three pillars of sustainable agriculture (Figure 1-1). Suitable agriculture aims to treat the problematic location instead of applying a blanket treatment for the whole field as in conventional agriculture.

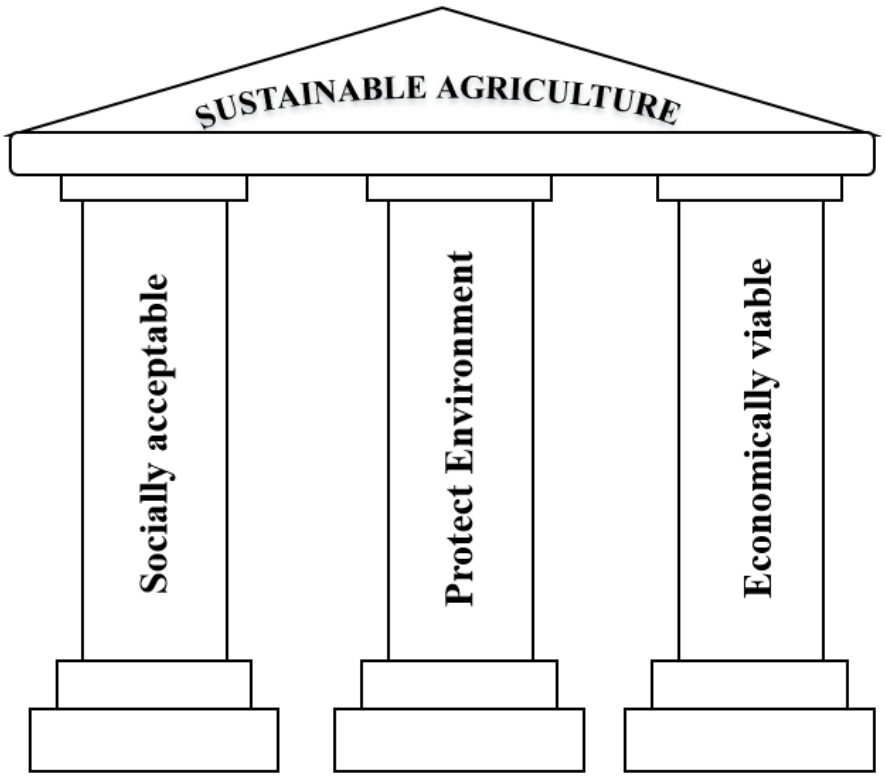

Figure 1-1: Three pillars of sustainable agriculture

1.2 AGROCHEMICALS AND ENVIRONMENT

The increasing trend of applying agrochemicals in field crops is an integral part of modern agriculture as a response to the growing demand for food and fiber. According to one study, in the United States, 3 million kg of agrochemicals costing 40 million US dollars are used annually (Al-Heidary et al., 2014; Pimentel, 2005). Agrochemicals can save 45% of the world food supply by protecting crops from different insects and pests (Oerke, 2006). On the other hand, this heavy use of agrochemicals has increased the risk of air, soil and water pollution. During the application of these chemicals in the field, small spray particles move away from the intended areas (spray drift) and cause contamination (Huang et al., 2011). Almost 30% of agricultural chemicals are wasted due to off-target spray drift

(Bahrouni et al., 2008; Miller and Butler, 2000). This off-target spray drift can create health issues for animals and humans, damage nearby sensitive crops, contaminate water sources and soils. However, Nuyttens et al., (2007a) noted that, reduction of the dosage of these chemicals may unfortunately reduce their effectiveness and could result in loss of money and chemicals. Therefore, spray drift became an important issue not only for public health policy makers but also for the scientific community. Spraying time is another important factor during the farm operation. In the modern agriculture world, timely execution of farming operations are required to ensure the efficiency of the activities by reducing activity durations, energy (fuel) use, labour hired and overall cost (which is one pillar of sustainable agriculture) (MacRae et al., 1989).

These agrochemicals are also a serious threat for aquatic life (Hilza and Vermeer, 2013). The increasing demand for food and fiber encouraged the farmers to apply agrochemicals. Therefore, spray drift became a serious issue not only for public health but also for the scientific community.

Volatile organic compounds from various agrochemicals are a significant source of air contamination (William and Smith, 2004). During spraying application, emission of volatile compounds cause air pollution while the runoff of agrochemicals from agriculture sites can enter waterways and pollute water and soil (Giles et al., 2011). With the increasing population, the world needs to use these non-renewable sources more wisely (Azadi et al., 2011b).

Tilman et al., (2002) introduced new policies and intensive production practices to be implemented in existing agricultural systems to ensure their sustainability and increase yield without compromising the environmental integrity. These intensive production

practices are as, increasing the nutrient use efficiency, increase water use efficiency, dieses and pest control, maintain and restoring the soil fertility and sustainable livestock production. Azadi et al., (2011b) focused on introducing the new rules and regulations of tax incentives coupled with agricultural subsidy to meet the required goal of suitability.

At one stage, organic farming was seen as a solution for sustainable agriculture. In organic farming, the negative effects of agrochemicals were reduced to zero because all the produce was grown without application of agrochemicals (Pelletier et al., 2008). However, this caused significant yield reduction. For this reason, organic farming is not a good substitute for conventional farming (Azadi et al., 2011b). The next section will discuss health issues related to spray drift in Canada under conventional farming.

1.3 HEALTH ISSUES IN CANADA

Health professionals in Canada agree that exposure to pesticides should be reduced (Labchuk, 2012). The Canadian Government banned the domestic application of pesticides for house lawns. According to Canadian Cancer Statistics 2015, cancer is a leading death causing disease in Canada. For example, in Prince Edward Island (PEI), the cancer disease rate is 12 % higher than national average (Canadian Cancer Statistics, 2015). Canadians inhale cancer-causing pesticides with every breath (Labchuk, 2013). In PEI, potato is grown on large areas and is considered as monoculture crop (Labchuk, 2012). Blight is a widespread potato disease all over the world. When the blight spores get humid in warm climate as in summer time, they multiply and kill potato plants. Most farmers prefer to cover the leaves of potato crops with a layer of fungicides to protect the crops from this disease (Kuepper and Sullivan, 2004). These fungicides constitute 80% share of all

pesticides used in PEI and are carcinogens (chemicals known to cause cancer or reproductive toxicity) (Labchuk, 2012).

In the late 1980s, potato acreage increased by 70%. Potatoes were grown near populated areas such as schools, daycares and houses. Fields are sprayed up to 20 times during each growing season. The spray blows around with the wind and contaminates the air (Janine et al., 2011). The concentration of Chlorothalonil (major organic compound found in fungicides) is found everywhere in air, even in control areas (Labchuk, 2012). The soil of PEI is sandy so leaching of these chemicals can also contaminate ground water and also a big threat for human life

Besides cancer related risks, the emerging threat of multi-drug resistant fungi such as *Candida Auris* has recently been linked to use of azole fungicides (penconazole, difenoconazole, tetraconazole, and tebuconazole) for crop protection in agriculture (Arikan-Akdagli et al., 2018).

These examples show how imperative it is to improve the efficiency of the spraying systems at the design and operation stages.

1.4 SPRAYER DESIGN AND DRIFT LOSSES MEASSUREMENT

A sprayer system (Fig. 1-2) usually consists of the following components: a tank, a sight gauge; an agitation device; a strainer and/or filter, a pumping system, nozzles, hoses and lines, control valve, pressure gauges, and a boom arm. Detailed explanations for each element follow.

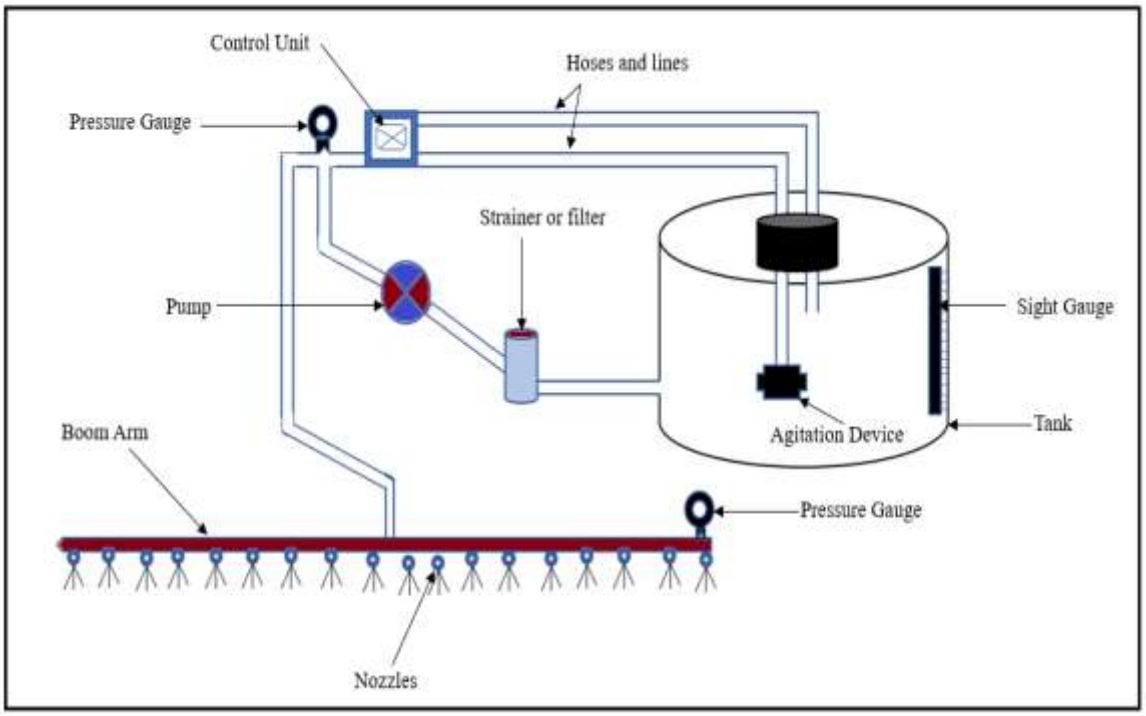

Figure 1-2: Principal components of Sprayer system

1. **Tank:**

   The tank is main storing unit for agrochemicals and water. It is available in many shapes (rectangular, cylindrical and spherical). The capacity of the tank varies according to the available horsepower of the tractor (Fig. 1-2).

2. **Sight Gauge:**

   The sight gauge consists of a transparent plastic scale along the sprayer tank to monitor the level of chemicals in the tank (Fig. 1-2).

3. **Agitation device:**

   The agitation device is very important element of the sprayer system. This device works inside the tank to mix the agrochemicals with water at a desired quantity and ensure homogeneity of the spraying fluid (Fig. 1-2).

4. **Strainer:**

   The strainer is a type of mesh used to stop debris, large dust particles and other foreign materials from going into the pipelines and pump. The strainer plays an important role as it keeps all hoses, pipes and lines clean. Hence, it prevents the clogging of the sprayer nozzles. Strainers are available in different sizes according to the orifice size of the nozzles used (Fig. 1-2).

5. **Pump:**

   Every sprayer system is equipped with a pump, whose main role is to push the agrochemicals towards the sprayer nozzles and maintain pressure. Different types of pumps are available. Centrifugal pump, piston pump, diaphragm pump and roller types are the most common types of pumps used in sprayer systems (Fig. 1-2).

6. **Hoses and lines:**

   Hoses and lines are the different types of pipelines used to connect the sprayer tank with the nozzles. The diameter and material of these lines are chosen to avoid clogging and blockage (Fig. 1-2).

7. **Control valves:**

   Control valves are used to control the flow of agrochemicals in different directions. Mostly control valves consist of six outlets, three for left right and central boom, one for agitator, one for overflow and one for pressure gauge. The main function of these values is to control the flow in all directions and sometimes these valves are used to increase and decrease the pressure in the hoses (Fig. 1-2).

8. **Pressure gauges:**

Pressure gauges are used to monitor the pressure at different locations of sprayer system. The pressure gauges installed near the control valve are used to measure the actual pressure at the inlet of sprayer nozzles (Fig. 1-2).

9. **Boom arm:**

The boom arm is a tubular structure attached behind the tractor and to which nozzles are affixed. Typically, a sprayer system has three types of booms: a central boom, a left-hand side boom and a right-hand side boom. All these three booms can be operated independently or all at same time (Fig. 1-2).

10. **Nozzles:**

Nozzles are the last elements traversed by the flow of chemicals during the spraying operations. Nozzles are made of different materials (aluminum, copper, brass, stainless steel, ceramic and nylons), and different types (flat fan, cone type, hollow cone, straight etc.) (Fig. 1-3).

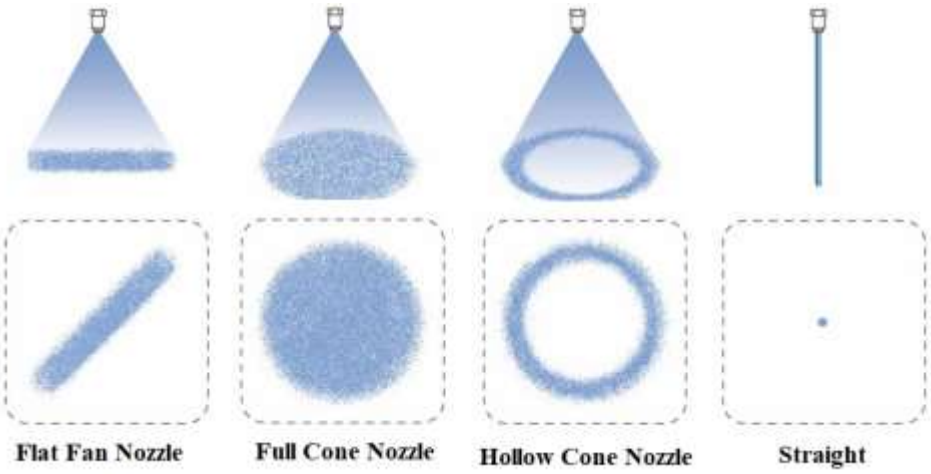

Figure 1-3: Different shapes of nozzles

[Source: *https://www.tecpro.com.au/technical-info/spray-engineering/*]

The main role of the nozzle is to provide uniform application of spray at the target surface. Nozzle selection depends upon different factors such as crop type, crop height, crop growth stage, pressure requirement, and droplet size and velocity (Fig. 1-4)

Losses during field spraying operations constitute a significant problem. Previous research showed that uniform distribution of spray is very important, 30% of agricultural pesticide sprayed is lost during spraying due to the non-uniformity of droplet size and off-

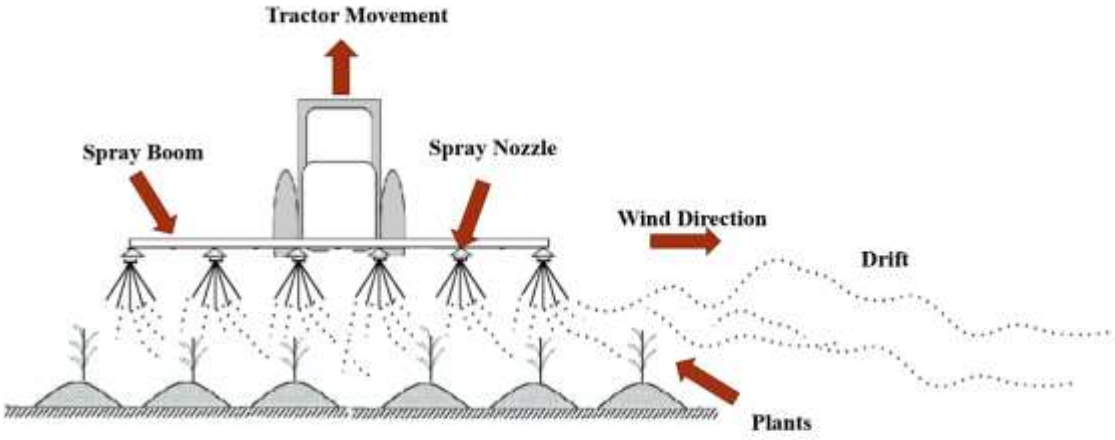

Figure 1-4: Demonstration of spray drift during field operation.

target drift (Fig. 1-4). Big droplets are lost due to gravitational effect while small droplets are lost in air (Sumner and Herzog, 2000; Bahrouni et al., 2008). There is hence an urgent need to test the sprayer system, for different cropping systems and find ways to improve the efficiency of spray in order to reduce the amount of pesticide sprays, reduce the amount of energy used and minimize environmental pollution. This generally requires an improvement in the design and application of spray.

Characteristics of the sprayer nozzles are important criteria in the application of different chemicals (pesticides, fungicides, etc.) for different cropping systems, because of they directly affect the efficiency of the chemicals. The structure of the spray deposits can be affected by velocity and size of droplets (Guler et al., 2007). Moreover, biological effectiveness of the applied chemical as well as environmental risks can also be influenced by the velocity and size of the droplets. Therefore, the study of the spray characteristics is very important for the ideal nozzle-velocity combination, which will maximize the spray efficiency for depositing the dose to the right targets (Miller and Butler, 2000). The efficiency of the chemical application process is influenced by the following factors: discharge of agrochemicals from sprayer nozzle, spray pattern and droplet velocity, and external conditions (Nuyttens et al., 2007a). In the following, these factors will be reviewed under three groups. The first subsection will deal with volume and droplet velocity measurements using Particle Image Velocimetry (PIV). The second subsection will review the approaches used to model nozzles for the purposes of studying spray characteristics. Finally, the third subsection examines the impacts of external factors on drift losses.

1.4.1 Volume and droplet velocity measurement using PIV

Particle Image Velocimetry (PIV) is a non-intrusive laser optical measurement technique used to obtain instantaneous velocity vector in a cross-section of gas or liquid flows (Cao et al., 2014). According to Adrian, 2005, the term PIV was first used in literature in the 1980s. In the last 30 years, significant progress has been achieved in computer techniques, image recording and evaluation techniques and laser operation that made PIV a very effective measuring tool. PIV techniques can be used to measure

instantaneous turbulent velocity fields. Tracer particles (seeded particles) are used for submerged flow and air flow measurements (Grant, 1997; Husted, et al., 2009; Dabiri, 2009; Hain et al., 2007). Tracer particles should be large enough to dampen the Brownian movement, but at the same time tracer particles should be small enough to follow the flow fields without disturbing the flow field. Most commonly, polystyrene particles are used as tracer particles (Santiago et al., 1998; Husted et al., 2009).

In general, to produce the images, tracer particles are illuminated by pulsed sheets of laser light at precise time intervals that are recorded by using a charge-coupled device (CCD) or complementary metal–oxide–semiconductor (CMOS) camera. A key element in the PIV technique is the analysis of these images to measure the particles displacements. This technique can be used for a variety of research and diagnostics into flows, turbulence, microfluidics, spray atomization and combustion processes (Hain et al., 2007). Many researchers used the PIV technique for the measurement of velocity and discharge in open channel, irrigation canals, sprinkler irrigation (Lee et al., 2010; Bown et al., 2006; Santiago et al.,1998; Meinhart et al., 1999; Morgan et al., 2013; Husted et al., 2009).

Lee et al., (2010) measured surface velocities in an irrigation canal by using PIV and converted into depth averaged velocities by a log-law curve. They also measured the discharge of irrigation canal by using Parshall flume and PIV methods. The results obtained through Parshall flume and PIV were found to be in good agreement (5% difference). The images of tracer particles on the surface of canal water were captured using a Video camera (Speed Dome) capable of taking 30 frames per second with picture revolution of 811 × 508 pixels. These results suggested that image measuring techniques

could be used to measure the discharge of irrigation canals more precisely without disturbing the canal flow.

Bown et al., (2006) measured the three-dimensional, three component velocity by using the Micron PIV and Particle Tracking Velocimetry (PTV). The algorithm of PIV has capability to correlate the 99 different images and provide the average velocity of particles while PTV only track the individual particles. They concluded that the accuracy of velocity measurement can be improved by increasing the number of images for the PIV method whereas more tracked particles were needed for the PTV. By varying the number of images, experimental uncertainties can be altered. Bown et al., (2006) also found that the uncertainty of the in-plane velocity components was higher than the uncertainty of the out-of-plane velocity components.

Santiago et al., (1998) developed a micro-PIV technique to measure the velocity fields with 3.45 μm vector to vector distances using interrogation volume of 6.9 x 6.9 x 1.5 μm. Meinhart et al. (1999) developed a micro-PIV system for the measurement of flow in a microchannel. They measured the velocity field in order of 1-μm spatial resolution. They used 200 nm diameter tracer particles of polystyrene, a pulsed Nd: YAG laser, an inverted epi-fluorescent microscope and cooled interline transfer CCD camera to record the particle images. They suggested that for making micro-PIV systems more accurate, one should use tracer particles with diameters in the range of 100 to 300 nm. These particles are illuminated with visible light of 532 nm wavelength. For this purpose, fluorescently labeled polystyrene with diameter of 100-300 nm and specific gravity of 1.055 were used in this experiment (Meinhart et al., 1999). To trace the slow flow motion, Brownian movement caused error due to particle diffusion of micro-particles (Meinhart et al., 1999).

PIV technique was also used for the measurement of velocity vectors in co-current liquid-liquid flow. Morgan et al., (2013) conducted a series of experiments on co-current liquid-liquid flow using a circular tube. Aliphatic hydrocarbon (Exxsol D80) and aqueous solution of glycerol were used as fluids for these experiments. Graticule technique was used to correct the optical distortion due to the circular tube. The concentration of glycerol was adjusted to ensure that both fluids (glycerol + water) had the same refractive indices. The flow was investigated using the following laser optical diagnostic techniques: Planar Laser Induced Florescence (PLIF), PIV and PTV. The images data obtained from PLIF agreed with the simple stratified laminar-laminar flow model (predictive model). PIV and PTV techniques were used to investigate the velocity conditions, flow pattern and velocity profile of two different fluids moving in same investigating area. The results of PIV and PTV concluded that, the velocity profile of the more viscous and heavier lower layer of fluid (glycerol/water) had characteristics of laminar flow while the characteristics of the less viscous and lighter upper layer of fluid (Exxsol D80) had characteristics of turbulent flow.

Husted et al., (2009) used PIV and Phase Doppler Anemometer (PDA) to evaluate high-pressure water mist nozzles during fire suppression. Droplet size is one key factor in fire extinguishing with water mist. A hollow cone nozzle and full nozzle cones were evaluated using PIV and PDA techniques. A PIV system was used to find out the overall spray behavior including spray spread and velocity field while PDA was used to measure the droplet size and flow velocity. In PIV, cross-correlation of images worked well to define the characteristics of spray behavior instead of individual droplets. Their study concluded that PIV is suitable for capturing the dynamics of a spray, but PDA can only be

used for steady state sprays. Based on PDA results, it is concluded that the surrounding air (boundary conditions) has significant effect on the sprayer behavior. Few other researchers used other techniques to find out the spray characteristics. Some used a combination of water sensitive papers (WSP) and imaging techniques.

Marcal and Cunha (2008) used water sensitive papers (WSP) coupled with image processing technique to observe the fraction of spray coverage, homogenity parameters, stains and droplet numbers. The number of droplets per area was calculated using different scanning resolution and data was then compared with manually counted spots on WSP. This method was found to be effective when the spray fraction coverage ranges between 7% to 50%. However, this method was not found to be suitable for more than 50% coverage on WSP due to the submergence of droplets (droplets merging with each other).

Sudheer and Panda (2000) measured the droplet size produced by sprinkler nozzles using image processing technique from Otsu (1979) to determine the threshold in image processing. The droplet size was also measured with the Pellet method (Sudheer and Panda, 2000) in a laboratory to compare the results of the images with actual results. This study revealed that droplet sizes less than 0.90 mm could not be measured with the image processing technique, but larger droplet sizes could be with more accuracy.

As reviewed above, a weakness in the current state of the literature pertains to the fact that there is little work reported on the use of PIV to measure flow and velocity of flat fan nozzles. To overcome the identified shortcoming, the first aim of this thesis will be to use PIV to study the velocity profile and flow rate of a flat fan nozzle in the context of spraying operations. The next subsection will review the modeling approaches of sprayer nozzles including mathematical and simulation models.

1.4.2 Mathematical and CFD modeling for sprayer nozzle

The modelling of high-pressure liquid flowing from one medium to another is still a difficult and developing research area. The formation of droplets after the fluid comes out of the nozzle into the air is an interesting research topic that is needed to understand the instability of the spray jet (Sinha et al., 2015). There are many studies investigating the phenomenon of liquid jet entering a liquid medium. However, less work has been reported on the study of the jet formation from nozzle-liquid medium going to the air. At low Reynolds number, the jet of water coming in lighter medium breaks up due to hydrodynamic instability mainly caused by surface tension (Sinha et al., 2015). Reynolds number, the ratio of inertial force to viscous force, is a dimensionless quantity used to identify the flow patterns in different flow conditions. Fundamental fluid mechanics showed very well that laminar flow occurs at low Reynolds number while turbulence appears at high Reynolds number, including in the jet flow (Sinha et al., 2015). The behavior of the jet flow is wavy at high Reynolds number due to the induction of aerodynamic effects. Chaudhary and Maxworthy (1980) conducted experiments on water jet behavior and concluded that density also had significant effect on the characteristics of water jet behavior. Lin and Reitz (1998) studied the injection of water jet in gas and reported the behavior of jet in four different regimes. These regimes are identified based on viscosity, density, gravity and surface tension. The four regimes are classified as 1) the Rayleigh regime, where jet diameter < droplet diameter; 2) the 1st wind induced regime, where jet diameter = droplet diameter; 3) the 2nd wind regime, where jet diameter > droplet diameter; and 4) the atomization regime, where droplet diameter is negligible as compared to jet diameter (Homma et al., 2006).

The behavior of droplet changes from 2D to 3D when injected from a high density to a low-density medium (Homma et al., 2006). In the case of water jet coming out of a nozzle, the atomization regime occurs given that the average droplet diameter (288 μm) (ASABE, 2010) is negligible when compared to the jet diameter (1500 μm) TEEJET 8003 (extended range flat fan). The characteristics of such fluid flow problems have not been adequately studied (Jiang et al., 2017). Computational Fluid Dynamic (CFD) software packages are commonly used nowadays (Jiang et al., 2017) to study spraying nozzle problems. Common CFD packages are: ANSYS Fluent, FloTHERM, ANSYS CFX and Star-CCM+ etc. Fluid flow, chemical reactions and heat transfer problems, which are difficult and time consuming to run experimentally, can be easily solved with these simulation methods. Simulation software packages have user friendly interface and allow the user to test many parameters, which would be difficult to do in real world. Recent advances in computer hardware made it easy to solve many complex industrial and academic problems related to fluid flow with more accuracy and low computation time. Heat transfer, fluid flow and chemical reactions can be analyzed with the help of computer simulation. Mathematical simulation helped solve many complex and non-viable fluid flow problems (Versteeg and Malalasekera, 1995). The real experiments are non-viable and more expensive then the computer simulation solutions. With the use of mathematical simulation many parameters (in case of nozzle operating pressure, nozzle type, nozzle shape, flow rate etc) can be altered which are very difficult and expensive to change in real world. In recent years, more advanced computers have made solving industrial and academic complex problems related to fluid flow faster and more accurate.

Validation is an important step for mathematical simulation methods. Validation is required to ensure the reliability of the results obtained by simulation (OpenFOAM, 2015). Jiang et al., (2017) worked on the velocity distribution of an irrigation nozzle. They used the numerical simulation method for measuring the velocity distribution and validated these results with the help of PIV experimental methods. In the same way Cock et al., (2014) worked on numerical modeling of mirror nozzle using OpenFOAM software and validated these results with the help of analytical solution.

Many other researchers used the mathematical modeling approach for solving multiphase problems (Mandal et al., 2008; Liu et al., 2011; Yeh et al., 2005; Anantharamaiah et al., 2007; Lv et al., 2011 and Lakdawala et al., 2014).

Altimira et al., (2009) used experimental and CFD approaches to analyze different parameters of fan sprayer nozzles used for different industrial purposes. Spray characteristics such as discharge coefficient and liquid sheet thickness are measured through numerical simulation and validated experimentally. The Volume of Fluid (VOF) method was used to simulate two different phases while the k-epsilon model was used due to the turbulence nature of the flow. Altimira et al., (2009) concluded that two-phase flow was taking place inside and near the tip of the nozzle. The internal structure of the nozzle had significant effect on the flow domain. Regarding thickness of liquid sheet, they conclude that it varies both in radial and angular coordinates. The shape of orifice significantly affects the thickness of liquid sheet. A vena contracta (the point in the fluid stream where the stream has minimum diameter and maximum velocity) is formed near the nozzle tip, which dramatically change the flow behavior.

Nuyttens et al., (2009) worked on droplet and velocity characteristics of agricultural sprayers. They evaluated 13 different nozzle-pressure combinations using Phase Doppler Particle Analyzer (PDPA) and concluded that the smaller droplets had less velocity while larger droplets had high velocity. The velocity of bigger droplets (> 400 μm) varies from 4.5-8.5 m/s depending on the nozzle type and size when operated at 3.0 bar pressure. In the same way the velocity of droplets less than 400 μm decreased consistently with the decrease in droplet size. Corresponding velocity varies from 0.5-2 m/s and it also depends upon nozzle type, pressure, orifice shape and size (Nuyttens et al., 2009).

Jiang et al., (2017) used the experimental PIV and CFD methods to visualize the velocity behavior of sprinkler irrigation nozzles. They used volume of fluid-level set approach to simulate the nozzle flow using ANSYS Fluent software. They conclude that both PIV and CFD approaches can be used for nozzle flow study. The PIV and CFD simulation give similar results with less than 10 % error difference. Pressure had significant effect on breakup length of the flow stream. PIV measurements are considered correct for flow stream before the droplet formation. After droplet formation in the flow stream, PIV could give the erroneous results. For a steady flow, simulation is a viable option, but it is very complex and complicated when dealing with turbulent flow with high Reynold numbers.

Cock et al., (2014) worked on numerical modeling of mirror nozzle using OpenFOAM software. InterFOAM solver with VOF approach was used to simulate the two-phase flow of nozzle. They observed that the analytical method and simulation were in good agreement when they studied the spray sheet away from the nozzle tip but near the nozzle tip the results were not in good agreement. They studied the sensitivity of nozzle

geometry and the flow rate from the nozzle inlet and concluded that the geometry and shape of inlet of nozzle significantly affected the downstream flow. High flow rate also impacts the homogeneity in flow: high flow rate yields higher homogeneity in droplet size.

After reviewing the different studies related to the spraying behavior and velocity of spray particles, this review will now present the different external factors linked with drift losses.

1.4.3 External conditions for drift losses and related factors

Spray drift or drift is the amount of spray particles blown or carried away from the intended crop areas to the surroundings and may cause harmful effects on the environment in the general sense (Huang et al., 2011). Spray drift is the core factor in this dissertation. There are many factors directly affecting drift losses. Researchers have studied the impact of these factors on spray drift individually. The aim of this thesis is to investigate the combination of several of these factors and propose a decision support tool to help farmers and other stakeholders carry out efficient spraying operations while minimizing spray losses. In this section, a review of the external conditions and factors that affect spray drift will be conducted. These factors can be categorized into three major classes as depicted in Fig 1-5:

- Sprayer related factors, (boom height, driving speed, nozzle angle, nozzle pressure) (De Jong et al., 2000);
- Weather conditions (temperature, humidity, wind velocity) (Nuyttens et al., 2007b);
- Crop architecture (crop type, height, and growth stage) (Al-Heidary et al., 2014).

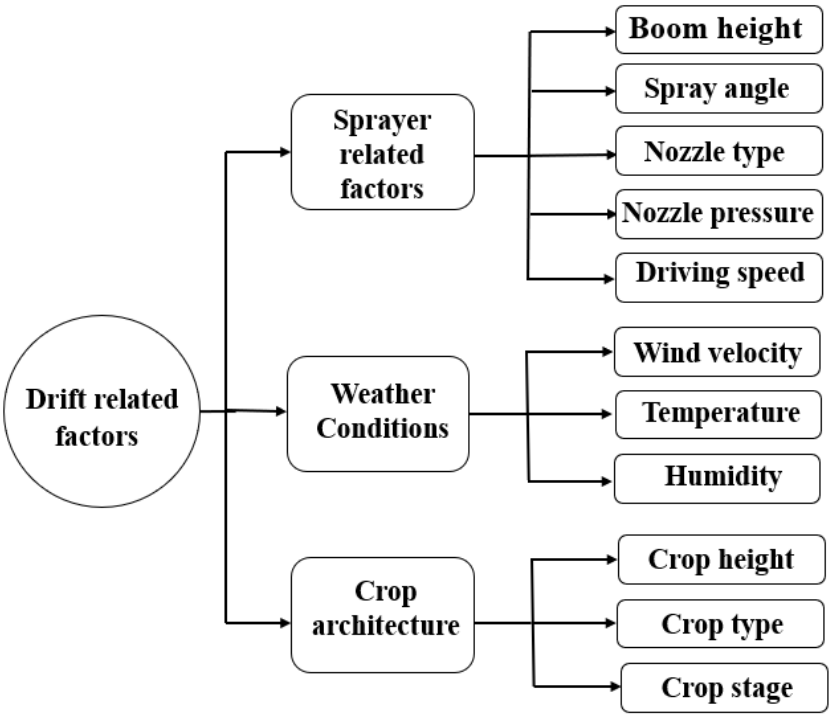

Figure 1-5: Factors affecting drift losses

Boom Height

Chao and Chengsheng, (2011); Teske and Thistle, (1999); De Jong et al., (2000); Van de Zande et al., (2000); Iqbal et al., (2005) studied the impact of boom height on spray drift. These studies concluded that drift losses decreased by lowering the boom height. Drift losses can be decreased by 80 % and 56 % when the boom height is decreased from 70 to 30 cm and from 50 to 30 cm respectively (De Jong et al., 2000).

Jan et al., (2008) researched the different crop protection products used in the last 10 years in the Netherlands. The research focused on the quantification of protection products on greenhouse plants, nursery trees, orchards and arable (cultivated) fields. The goals of this research were to find out the amount of spray deposits on the canopy of plants and the emission of spray in the environment (spray drift). Along with these effects, the

water quality along the sides of the fields was also investigated. Study concluded that by lowering the sprayer boom height, from 0.7 m (experiments 1992–1994) to 0.5 m (experiments 1997–1998) above the canopy, reduced the spray drift by 70% at 2–3 m distance from the last nozzle on boom. (Jan et al., 2008).

In a series of field experiments performed in 1999 by De Jong et al., (2000), the effect of lowering the sprayer boom height was studied for boom heights of 30, 50 and 70 cm above crop canopy. Conventional spraying was also compared with air assisted spraying. The study concluded that drift was reduced by 54% and 56 % (2-3m away from the last nozzle) when the nozzle height was reduced from 70 to 50 cm and 50 to 30 cm respectively. The use of air assistance significantly reduced the drift by 86% when compared to the conventional spray irrespective of boom height (De Jong et al., 2000).

Boom height also has a significant impact on swath width (area covered by the spray for specific height and angle). Increasing the spray height increases the swath width and more area can be covered (which is good when the crop canopy is full developed) but on other hand if the height is too high then spray particle will be at more risk to move with wind and more drift losses will be expected (Iqbal et al., 2005). There is therefore an interesting tradeoff to be had between swath width and drift losses.

Tractor Speed

During land application of agrochemicals, the boom and spraying apparatus are typically attached behind a tractor. The tractor driving speed is directly linked with the duration of the spraying operations and has a significant impact on spray drift (Miller and Smith, 1997; Ghosh and Hunt, 1998; Al-Heidary et al., 2014). Due the increasing crop acreage, timely farm operations are very important. Nuyttens et al., (2007a) and Al-Heidary

et al., (2014) conducted experiments to see the impact of driving speed on spray drift and concluded that spray drift increased by 51 % when the tractor driving speed increased from 4.0 to 8.0 km/h while these losses were 144 % when tractor speed was 16 km/h. In another experiment ran by Taylor et al., (1989), it was concluded that the spray drift increased by 4 % when tractor speed increased from 4.0 to 7.0 km/h, while spray drift increased by 90 % when tractor speed increased from 7.0 to 10 km/h.

A positive correlation relation was found between tractor driving speed and spray drift. When the driving speed was increased by 1 m/s (3.6 km/h) the drift was increased by 1%. (Arvidsson, 1997).

Nozzle Type and Pressure

Nozzle type and nozzle pressure are also important factors contributing to spray drift. (Heijne et al., 2002; Al-Heidary et al., 2014). At very high pressure (> 400 kpa), the spray particles become very fine and can cause spray drift (Al-Heidary et al., 2014). On the other hand, less pressure will lead to larger droplets size. Large droplet size is not good for many crops because these large droplets can escape from the plant surface and cause soil contamination due to runoff. In the same way, the shape of nozzle (orifice shape) also has great impact on drift losses. Nuyttens et al., (2007a) conducted experiments with flat fan, low drift and air induction nozzles, and concluded that air induction nozzles had less drift when compared to the low drift and flat fan nozzles.

Spray angle

Several studies have shown interesting effects of spray angle on spray drift for identical nozzles (Miller et al., 2011; Zamir et al., 2014). Miller et al., (2011) found that spray drift was reduced by a factor of 2 when the spray angle was reduced from 110^{o} to 80

º for a flat fan nozzle of same orifice size. Similarly, spray drift was reduced by a factor of 5 when the spray angle reduced from 110º to 65º. This meant that increasing the spray angle leads to more drift losses while decreasing the spray angle reduced the drift losses (Miller et al., 2011). On other hand increasing the spray angle also favored spray coverage (swath width). So, there should be a balance between these two parameters.

Zamir et al., (2014) studied the drift losses for banding application by using even flat fan nozzle. The effect of wind speed and spray fan angle was investigated. Three different spray fan angles 65°, 80° and 95° and three different wind speeds 1, 2 and 3 m/s were investigated in a wind tunnel. They concluded that the nozzle with less spray fan angle (65°) significantly reduced the drift losses as compared to the higher spray angle (80° and 95°). The minimum drift was found for all nozzle at a wind speed of 1m/s. The study supported the use of less spray fan angle (< 95°) with less wind speed can significantly reduce the spray drift.

Wind velocity

Wolf and Caldwell (2001) studied the influence of wind velocity on spray drift and concluded that as the wind velocity increases the drift losses increase. At same operating pressure the same nozzle may have different spray drift % depending upon the wind velocity. At 2.0 kPa nozzle pressure, the drift losses increased from 0.93 % to 1.78 % when wind velocity increased from 1.5 m/s to 2.1 m/s at 2m height from ground level. It is also recommended not to spray the field if wind velocity is 2.77 m/s or more (Tobi et al., 2011).

Temperature and humidity

Temperature and humidity had their own significance in spray drift study. High temperature and low humidity increase the risk of spray drift due to high evaporation. High

temperature and humidity will cause the suspension of spray particles in the air which will also contribute towards to air contamination (Al-Heidary et al., 2014).

Nuyttens et al., (2007b) developed a formula for the % of drift losses by considering drift distance, wind velocity, temperature and absolute humidity.

$$\text{Drift \%} = \text{Drift\_dis}^{-1.05}(13.00 + 0.5V_{3.25m} + 0.4T - 1.74\, X_{H_2O})$$

where:

Drift % = spray drift %

Drift_dis = drift distance parallel with the wind direction (m)

$V_{3.25m}$ = Average wind velocity at height of 3.25 m above the ground level (m/s)

T = Average air temperature (^oC)

X_{H_2O} = Absolute humidity (weight of water vapours in grams per kg of dry air).

Crop Architecture

Crop architecture includes crop type, crop height and crop stage. It is also important consideration in spray drift study. Gary et al. (2007) used a modeling approach to see the interaction of the plant architecture and spray techniques. They performed these experiments in L-Studio simulation environment in which a model of plant was built to see the impact of spray on the plant surface and drift was also evaluated. Wind tunnel experimental methods were used as validation of this simulation approach. They concluded that both the air induction nozzle and flat fan nozzle had the same impact on droplet deposition in broad leaves crops and weeds, but the use of air induction nozzles in these experiments had significant reduction in drift. Gary et al. (2016) used the modeling, simulations and experimental methods to see the spray retention on a whole plant of wheat and cotton. They concluded that the cotton plant had high ability to retain the applied

chemicals on its leaf surface while it is hard to wet the wheat plant. So, the less retention on wheat plant will lead to air and soil contamination. They also concluded that it is very hard to develop an accurate mathematical model for this complex phenomenon. There are many complex interactions involved in the spray retention and plant architecture (Gray et al., 2016).

1.4.4 Summary and Research Gaps

A summary of the above review is presented below along with the key shortcomings that have been identified.

1. The PIV system was previously used to quantify the amount of water in canals using different types of flume but so far, fluid flow from a sprayer nozzle has not been quantified using the PIV technique.
2. The PIV system was used to determine the velocity and spray pattern of different types of flow such as co-current liquid-liquid flow, pipe flow, canals flow, but very little work has been reported where the PIV system was used to find the velocity profiles of spray sheets for drift losses purposes.
3. The study of high-pressure liquid from one medium to another medium through a sprayer nozzle is still a stagnant topic of modeling (Multiphase flow).
4. Different researchers studied the different external factors for drift losses on an individual basis but there is a need to develop an integrated model, which will assess the drift losses for the combination of multiple factors.
5. Most studies ignore the need for timely spraying operations. Field spraying operations have economic and environmental costs which need to be balanced to offer farmers and stakeholders decisions that they can agree to and implement.

A successful transition from the traditional ways of spraying farm fields to a more sustainable practice will require an integrated approach that can combine several drift-causing factors and use mathematical modelling and optimization techniques to determine operational configurations for the spraying equipment.

1.5 RESEARCH OBJECTIVES & THESIS ORGANIZATION

This thesis investigates how spraying configuration can contribute to the reduction of spray losses in the context of sustainable agriculture. This dissertation explores the topic over three themes covering Chapters 2-4 as an integrated study combining sprayer nozzle design investigation, spray sheet velocity characterization, and spraying operation optimization. Each chapter is self-contained with its own introduction, literature review, materials and methods, model formulation, experiments, discussions and conclusions. The remainder of the thesis is organized as follows.

Water quantification without intrusion is the first theme investigated in this study. In the literature, water flow and quantity out of a nozzle is mainly quantified by contact methods which may not be precise. For precise measurement of volume of water, a non-intrusive quantification method is highly recommended by several interdisciplinary studies (sprinkler irrigation, fire sprinklers, etc). As mentioned earlier in this chapter, the efficiency of the agrochemical application process is also influenced by the quantity of agrochemicals sprayed through the nozzles. Therefore, in the first step of this dissertation, the volume of water will be determined for a flat fan nozzle using the PIV technique for spray quantification. A PIV system is used to capture images of the spray sheet and the droplet volume is subsequently calculated. This droplet volume is used for volume

quantification. The result of the PIV images is validated by an experimental manual method.

The second important factor linked to drift losses examined in this thesis is the behaviour of spray sheet under the spray nozzle. In the literature, the jet velocity is typically measured at inlet point of nozzle using modeling and experimental approaches. Very little work has been reported in which the velocity of droplet is measured at different points in the spray sheet under the nozzle. The second step or theme will examine the velocity distribution of agricultural spraying nozzles using a numerical simulation built in the commercial software ANSYS 16.0, Fluent. The obtained simulation results are compared with the jet velocity measurements yielded by the PIV method. Two outcomes of this step include: i) to provide better insight into jet behavior in terms of velocity, which will identify the weak areas of spray, and where there is the maximum probability of drift prone particles; ii) to open a new horizon in spraying system research of flat fan nozzle, which will not only decrease the experimental cost but also reduce the labor and time for nozzle analysis. The overall gain of this work can lead to building a reliable dataset that can be used for the optimization of sprayer nozzle design. Apart from quantity and velocity of spray sheet there are few other factors (sprayer related factors; weather and crop conditions) to be considered for drift and time of operation study.

For this third theme, a comprehensive model for spray drift and time of operation is developed. In this section of study, an integrated mathematical model in which multiple drift causing factors are jointly considered is proposed. The aim of this model is to give an optimal solution to balance the time of operation and spray drift. This mathematical model could be very helpful for the spraying industry and could be a part of a computer-

based program to help the farming community in balancing the time of operation (time saved for other agricultural operations) and spray drift (reducing contamination).

CHAPTER 2: WATER QUANTIFICATION FROM SPRAYER NOZZLE: PARTICLE IMAGE VELOCIMETRY (PIV) VERSUS IMAGING PROCESSING TECHNIQUES

The distribution of agrochemicals using spray nozzles is very important because there are significant losses of agrochemicals such as pesticides during spraying due to non-uniform droplets and off-target drift. Improving the efficiency of spraying would reduce energy, costs and minimize environmental pollution. In this study, jet patterns of spray nozzle flow were examined to study the performance of water distribution during the spraying process. A method of water quantification from a sprayer jet by using Particle Image Velocimetry (PIV) system in combination with imaging processing was introduced. For this study, ten sets of images were acquired with a PIV system in double frame mode. Each set of images contained different numbers of double-framed images at eight different pressures. The PIV images obtained were analysed using an image processing software for droplets and volume calculations. The results showed good agreement of both manual and PIV measurements and suggested that the PIV coupled with image processing technique can be used for a precise quantification of flow through sprayer nozzles.

2.1 INTRODUCTION AND LITERATURE REVIEW

The characteristics of spraying nozzles are important criteria in the application of different chemicals (pesticides, fungicides, etc.) for different cropping systems, because of their direct effect on the effectiveness of these chemicals. Previous research has shown that the uniform distribution of sprays is very important: 30% of sprayed agricultural pesticides are lost during spraying due to non-uniform droplet size and off-target drift (Bahrouni et al., 2008, Miller and Butler, 2000). Droplet velocity, volume, and size can affect the structure of spray deposition (Guler et al., 2007). Therefore, the study of spray

characteristics is necessary to find the ideal speed-nozzle combination, which will optimize the efficiency of the spray with the appropriate dosage for the right targets (pests or insects on the leaves, etc.) In other words, the parameters of the spray patterns such as spray rate, droplet size, volume distribution, entrained air characteristics, individual droplet structure, spray angle and the structure of the spray play an important role in the efficiency of the agrochemical application process. (Miller and Butler, 2000).

Our general research objective is to examine the properties of the liquid jet during spraying processes in order to analyze the distribution of the liquid and the uniformity of spray types on the plants in order to improve the sprayer nozzle design. This requires maximizing the uniformity of the applied spray based on operating pressures, nozzle parameters and wind effects. There are few articles in the literature dealing with this type of problem such as the work of Marcal and Cunha (2008) and Sudheer and Panda (2000).

Marcal and Cunha (2008) used water-sensitive papers (WSP), combined with an image processing technique, to observe the spray coverage fraction, the homogeneity parameters, the number of spots and the number of droplets. The number of droplets per area was calculated using different scanning resolutions and the data was then compared to the manually counted points on WSP, but this method can measure the spray fraction coverage ranging from 7 to 50%. However, this method has not proved appropriate for a coverage greater than 50% on the WSP due to the submersion of droplets (the droplets merging with each other).

Sudheer and Panda (2000) measured the droplet size produced by sprinkler nozzles using image processing technique from Otsu (1979) to determine the threshold in image processing. The droplet size was also measured with the Pellet method (Sudheer and

Panda, 2000) in a laboratory to compare the results of the images with actual results. This study revealed that droplet sizes less than 0.90 mm could not be measured with the image processing technique but larger droplet sizes could be counted with more accuracy (Sudheer and Panda, 2000).

PIV can also be used for research and diagnostics into flow, turbulence, microfluidics, spray atomization and combustion processes (Adrian, 2005; Cao et al., 2014; Hain et al., 2007). Tracers (seeded particles) are used for submerged flow and airflow measurements (Grant, 1997; Husted et al., 2009; Dabiri, 2009). Polyethylene tracers are commonly used. These tracer particles are added to the flow when it is submerged, whereas in the case where the flow is open to the air like the flow of the nozzle in the air, the water droplets are considered tracer particles. Particles are captured with a high-resolution camera and analyzed to measure velocity or volume. (Hain et al., 2007; Santiago et al., 1998; Husted et al., 2009). A key element in the PIV technique is the analysis of these images to measure the particles displacements and velocities. This method can measure an entire two-dimensional cross section of the flow field simultaneously. During the last decade, an increasing number of successful PIV applications have been reported such as indoor air flow measurements (Cao et al., 2014), micro scale fluid flow (Angui et al., 2010), liquid-liquid flow investigation (Morgan et al., 2013) etc. The need to investigate different fluid flows requires that more theoretical studies be conducted to gain a deeper understanding of the PIV performance for data measurements.

Our main objective herein is to use the PIV technique to examine the distribution and flow rate through the spray nozzles, as well as to obtain the amount of water released from the sprayer by calculating the number of droplets passing through. The result of the

PIV images was validated by the amount of water measured experimentally from the spray nozzle. This research provides a new technique for quantifying water in the context of sustainable spraying and irrigation research.

In this study, a laboratory-based research method is used to implement a new imaging technique, which consists in acquiring the information needed to support the development and implementation of an innovative spray nozzle. This will address different physical parameters of nozzle jets such as velocities, air-water flow properties, droplet size, volume distribution, entrained air characteristics, individual droplet structure. The PIV technique is used with the purpose of gaining more knowledge on jet behavior in determining relationships between velocity and pressure for sprayer system as well as to quantify the water from a sprayer jet. This technique is a non-intrusive laser optical measurement technique used to obtain instantaneous velocity vectors in a cross-section of gas or liquid flows.

2.2 MATERIALS AND METHODS

2.2.1 Experimental apparatuses

The different apparatuses used for this research, including the prototype spray nozzle and PIV setup are presented before delving into the experimental methods.

2.2.1.1 PIV

Particle Image Velocimetry (PIV) is a non-intrusive laser optical measurement technique used to obtain instantaneous velocity vectors in a cross-section of gas or liquid flows (Cao et al., 2014). This technique can be used for spray characterization and to measure the flow rate through sprayer nozzles. Based on optical principles there are different techniques, mainly include PTV, PSV and PIV (Cao et al., 2014).

In this research, two parallel methods were used to measure the quantity of water going through the sprayer nozzle: a manual measurement and the PIV technique. A schematic diagram for a PIV system is shown in Figure 2-1. The standard PIV or Two-dimensional PIV system from LPU 550 (Dantec Dynamics, New York, USA) (Fig. 2-3) was used to take the laser-illuminated images for the acquisition of the overall information of spray behavior (velocity of jet, spray spread and images for the number of droplets calculation). The droplet behavior changes from 2D to 3D when injected from a high-density to another low-density medium (Homma et al., 2006).

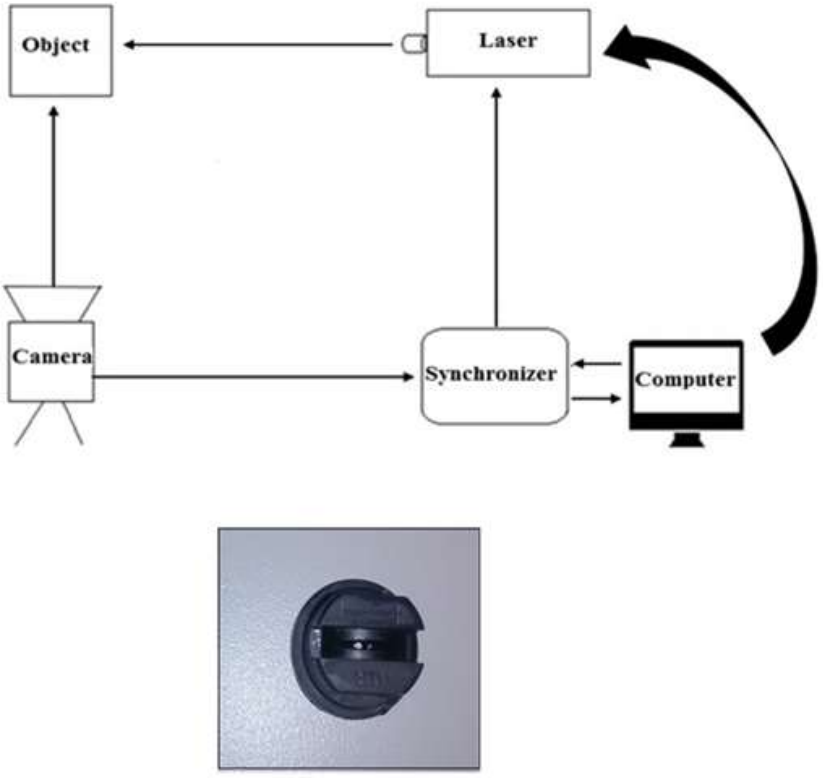

Figure 2-1: Schematic diagram of Particle Image Velocimetry (PIV) system (top), Extended flat fan nozzle (bottom)

3D Stereoscopic PIV system can be used to capture the 3D images of the droplets. This system needs at least one more camera coupled with above mentioned 2D PIV setup. Due

to the complexity of data acquisition and post processing, only 2D spray sheet is considered in this study.

2.2.1.2 Prototype of spray nozzle

A prototype was developed to adjust the nozzle at proper height and operate at required pressure. This prototype consisted of the following components: 1. Electric motor and pump; 2. Pressure gauge; 3. Flow Control valve; 4. Suction and bypass pipes; 5. Nozzle assembly; 6. Stand

1. **Electric motor and Pump:**

   A 0.4 hp (298.27 W) electric motor and pump were used to suck water from the water storage unit. This pump was fitted with a suction pipe, a delivery pipe and a bypass pipe. The main purpose of this pump was to suck the water from storage and build the required pressure at the nozzles (Fig. 2-2).

2. **Pressure Gauges:**

   Pressure gauges were mounted at two separate places of this prototype apparatus. One near the delivery pipe and the other near the nozzle section. The purpose of pressure gauges was to monitor the different pressure ranges of flow (Fig. 2-2).

3. **Flow control valve:**

   One control valve was mounted near the pump and another was mounted near the nozzle to control the nozzle flow and pressure (Fig. 2-2).

4. **Suction, delivery and by pass pipes:**

Three plastics pipes of 2.22 cm diameter were also attached to this assembly. A suction pipe was used to suck water from storage while delivery pipe delivers the water to the nozzle and a bypass pipe was used to avoid the bursting of pipes due to excusive pressure (Fig. 2-2).

5. **Nozzle assembly:**

An adjustable stainless-steel pipe was mounted after the delivery pipe. This pipe had a nozzle assembly to attach the different types of nozzles (Fig. 2-3).

1. Electric motor 2. Pump 3. Pressure gauge 4. Flow control valve 5. Suction pipe 6. Delivery pipe 7. Bypass.

Figure 2-2: Pump and accessories of prototype

6. **Stand:**

   A four-leg adjustable steel stand was used to hold the nozzle, pressure gauge and flow control value. Thus, the height of the nozzle could be adjusted as needed during the experiments. This stand is also fitted with leveler (Fig. 2-3).

2.2.2 Image acquisition of spray sheet by PIV

The liquid spray sheet was produced by an extended flat fan sprayer nozzle (TeeJet 8003) and an electric pump of 0.4 hp (298.27 W) using the above-mentioned prototype. The sprayer nozzle was operated for eight different pressures (25, 50, 75, 100, 125, 150,175, 200 kPa). For each pressure the system was operated for few minutes to stabilize the pressure to avoid any fluctuation in flow. Pressure gauges were used at the inlet of the nozzle and near the pump to see the change in pressure (Fig 2-3). When stable flow was reached at the sprayer nozzle, the spray sheet was illuminated by the beams of diode-pumped Nd:YLF laser (dual-cavity, pulsed laser 135-15 Dantec Dynamics, New York, USA), with pulse energies up to 30 mJ and repetition rates of up to 10 kHz. For imaging of the spray sheet, a Flow Sense EO CCD camera (Flow Sense EO 11M 9080X6231, Dantec Dynamics, New York, USA) with 6.5 frames per second at full resolution at sensor resolution 4008 x 2672 pixels, inter-frame time 300ns and pixel size 9μm was used. The CCD camera was aligned at an angle of 90° to the laser beam and it was focused on the laser and spray sheet (Fig. 2-3).

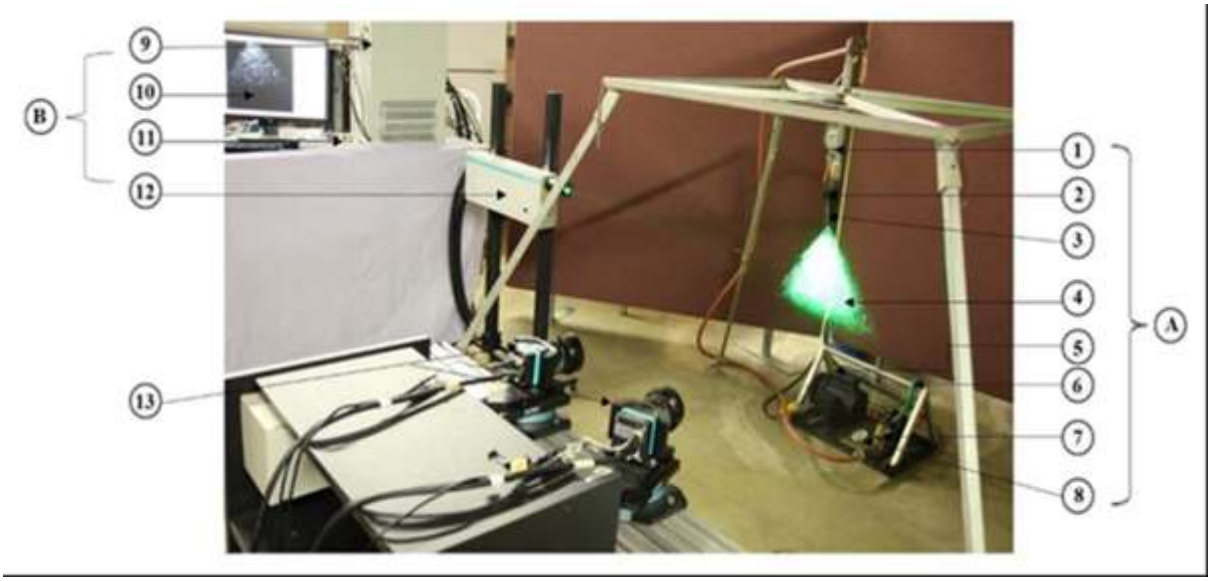

A= Prototype of spray nozzles B= Operational components of PIV 1. Pressure gauge, 2. Flow control valve 3. Nozzle assembly 4. Spray sheet with laser 5. Electric motor, 6. Suction and bypass pipe 7. Pressure control valve, 8. Pressure gauge 9. Synchronizer 10. Computer, 11. Laser controller 12. YLF laser 13. CCD cameras

Figure 2-3: PIV system and prototype of sprayer nozzle

2.2.3 Droplets calculation for volume measurement

The number of droplets appearing within the double framed images for each laser sheet were measured using the ASABE S572 (ASABE, 2010). According to the ASABE S572, the diameter of one droplet for the specific nozzle TEEJET 8003 (extended range flat fan) used in the study is 288 microns (0.288 mm). The average volume of one droplet can be calculated by the following formula:

$$V_{drop} = (4/3)\,\pi r^3 = (4/3)^* \pi\, ^*(0.144)^3 = 0.012507\ mm^3 \quad (2.1)$$

the total number of droplets N_1 is hence given by:

$$N_1 = V_{water} / V_{drop} \quad (2.2)$$

where:

V_{drop}: Average volume of one droplet.

V_{water}: Real total volume of water released from the spray nozzle (manually measured)

N_1: Total number of droplets released from sprayer (calculated manually).

2.2.4 White pixels determination using custom-made program

A custom-made computer program was designed and implemented in C++ combined with Visual Studio 2010 (Microsoft®, Redmond, WA, USA). This program was used for image processing of the PIV spray sheet images, including segmentation with different thresholds and counting of the white pixels of the segmented images as well as the Otsu's threshold method (Otsu, 1979). The Otsu's method could not in fact provide an appropriate threshold in this study as experimental images did not have bimodal distribution and contained lots of various intensity pixels due to different reflected angles. Then, threshold values from 0 to 254 were compared to find the highest value of coefficient of determination (R^2) between manually measured volume and the number of white pixels after segmentation (Fig. 2-4). A threshold value (> 0) (Fig. 2-5c) showed the highest R^2 value. Moreover, the brightness of pixels was caused by an incident angle, so the threshold value (> 0) was a more reasonable choice.

The total number of white pixels (N_2) was calculated by using the above-mentioned custom-built image processing program in the laser sheet images. The program identified adjacent regions of uniform white-scale levels. This program was also used to identify all the individual droplets in the image as well as other noise-type items such as the spray nozzle and the pump close to the spray nozzle. The algorithm requires that the 256-level gray scale (8-bit gray scale) images acquired by the PIV camera be dithered to a black and white image. This was accomplished by choosing a "Threshold" value such that all values

greater than the threshold were white and all values below or equal to the threshold were all black. There is typically a range of about 60 grey-scale levels out of 256 where the number of drops identified is invariant. The threshold was set within this invariant region. From a pair of two PIV images, only the second image was used to avoid double counting of white pixels. In the meantime, manual measurement of the spraying liquid was also made. A plastic pan was used as a drop collector to measure the liquid spray volume released, equivalent to each set of images by using the same PIV system settings.

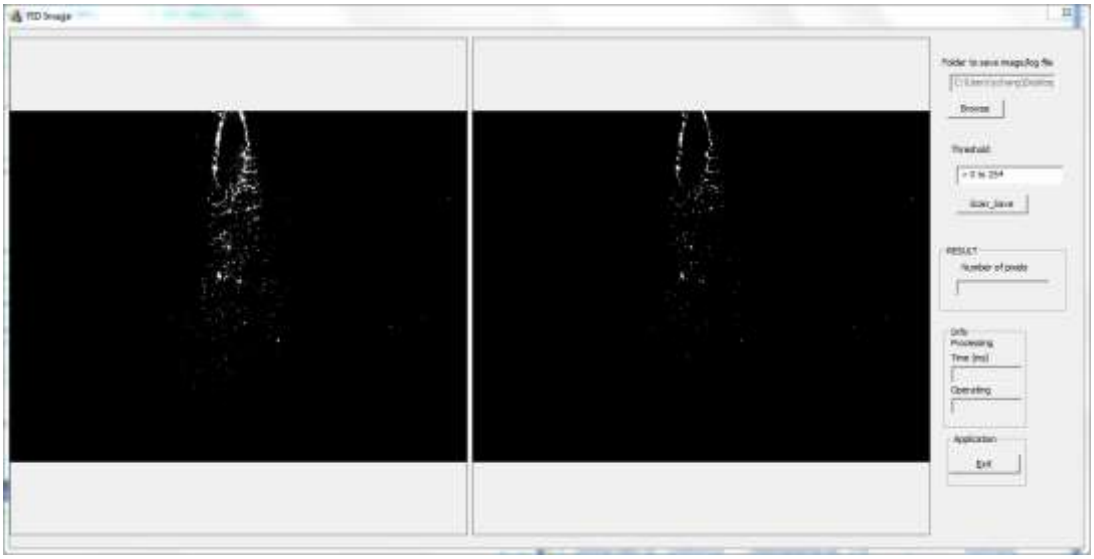

Figure 2-4: Image processing program that segments a PIV image to black/white image using different threshold values (0 to 254)

(a) **(b)** **(c)**

Figure 2-5: (a) Original image (b) Otsu threshold image (c) Threshold (>0).

2.2.5 Manual method for water quantification

For the manual measurement, a glass cylinder of 1 L was used to collect water from the nozzle (Fig. 2-6). The nozzle was operated at eight different pressures (25, 50, 75, 100, 125, 150, 175, 200 kPa) while the PIV system took the 10, 20, 30, 40, 50, 60, 70, 80, 90 and 100 images. Each time, the nozzle was operated for few minutes at one pressure to stabilize the flow and pressure. The detailed data sheet for manual data collection is presented in Appendix-A (Table A-1) of this thesis.

Figure 2-6: Collection of volume of water from nozzle at different pressures

2.2.6 Volume and absolute error calculation

The next step was to find the relationship between the size of the droplets and the number of pixels. For this, 8 graphs were plotted between the number of white pixels and the number of droplets (calculated using equations 2.1 and 2.2) at eight different pressures. A linear regression was fitted between the number of white pixels and the number of droplets calculated by the manual method were used. For example, at 25 kPa (Fig. 2-7), the regression equation indicates that one pixel in the PIV image equals to $0.5697X + 6 \times 10^6$ droplets. The regression equations for other pressures (50, 75, 100, 125, 150, 175 and 200 kPa) are tabulated in table (2-1).

$$N_3 = (0.5697 \times N_2 + 6 \times 10^6) \qquad \text{for } N_2 \geq 1.35\ 10^6 \tag{2.3}$$

Where;

N_2 = Number of white pixels in a PIV double frame images

N_3 = Total number of droplets released from the sprayer in a fixed time.

Equation (2.3) was then used to determine the number of droplets based on the count of white pixels N_3.

Finally, Equation (2.4) is used to calculate the measured volume of the water going through the nozzle.

$$V_{PIV\text{-}water} = N_3 \times V_{drop} \tag{2.4}$$

Equation (2.5) was used to calculate the percentage absolute error between the two volumes of water, one determined by PIV and the other one manually measured:

$$\text{Error} = | (V_{PIV\text{-}water} - V_{water}) / V_{water} | \times 100 \quad (\%) \tag{2.5}$$

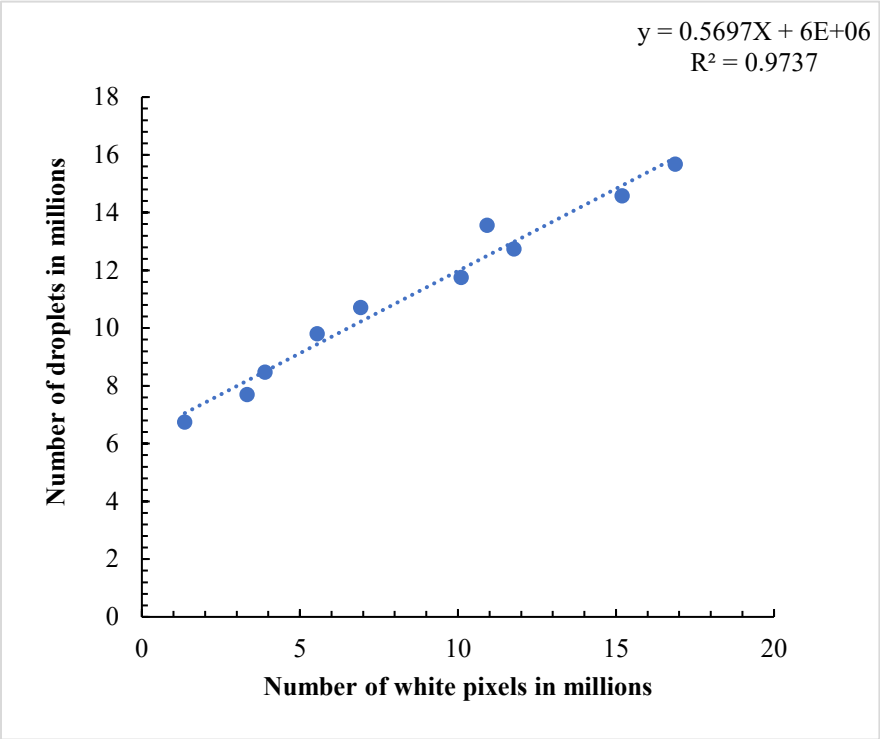

Figure 2-7: Relationship between white pixels and number of droplets at 25 kPa

Table 2-1: Regression equations and R^2 obtained from graphs at different pressures

Pressure (kPa)	Regression equation	R^2
50	$N_3 = 0.6218\ N_2 + 8E+06$	0.9907
75	$N_3 = 0.5755\ N_2 + 9E+06$	0.9952
100	$N_3 = 1.2132\ N_2 + 9E+06$	0.9877
125	$N_3 = 1.116\ N_2 + 1E+07$	0.9837
150	$N_3 = 1.0021\ N_2 + 1E+07$	0.9807
175	$N_3 = 1.0826\ N_2 + 1E+07$	0.9652
200	$N_3 = 1.0375\ N_2 + 1E+07$	0.9729

Where: N_2 = Number of white pixel and N_3 = Number of droplets measured through white pixels.

2.2.7 Statistical Analysis

A question that arises here is: what combination of number of pictures and operating pressure can give the least significant error with the well-defined PIV configuration? To answer this question, a factor analysis in which the pressure and the number of images were considered as two input factors, while the percentage of absolute error was considered as output is conducted.

The model for factorial analysis is represented as follows:

$$\mathbf{Y_{ijk}} = \mu+\alpha_i+\beta_j+(\alpha\ \beta)_{ij}+ \varepsilon_{ijk} \quad (2.6)$$

Where;

Y_{ijkl} = response variable (i.e. % error)

μ = overall mean,

α_i = Effect of "Pressure" on response at i_{th} level,

β_j = Effect of "Number of pictures" on response at j_{th} level,

ε_{ijk} = The error terms (uncontrollable/uncontrolled factors)

i = 1, 2… a, j = 1, 2… b, k = 1, 2… n.

In our study, a = 8 (number of pressures), b = 10 (number of pictures), and n = 3 (replications).

Hypothesis and statistical tests

The hypothesis was segregated in two parts (i.e. hypothesis for the main effects and hypothesis for interaction effects).

Main Effects

1. H_o: $\alpha_1 = \alpha_2 = \alpha_3 = \alpha_4 = \alpha_5 = \alpha_6 = \alpha_7 = \alpha_8 = 0 =$

H_a: at least one of the treatment effect is $\neq 0$

2. H_o: $\beta_1 = \beta_2 = \beta_3 = \beta_4 = \beta_5 = \beta_6 = \beta_7 = \beta_8 = \beta_9 = \beta_{10} = 0$

H_a: at least one of the treatment effect is $\neq 0$

Interaction Effect: Two-way Interaction effects:

1. Ho: $(\alpha\beta)_{ij} = 0$ Ha: at least one $(\alpha\beta)_{ij} \neq 0$

After checking all the assumptions of normality for the error term, constant variance and independence, the data was analyzed using the General Linear Model (GLM). The statistical analysis of the data is performed using Minitab 17 (Minitab Inc., Pennsylvania, USA).

2.2.8 Analysis process for experimental data

Acquired PIV images were analyzed to determine the velocity of the spray particles at different positions. The adaptive PIV method was used to calculate velocity vectors. This method adjusts the size and shape of the interrogation area (IA) to accommodate local seeding densities and flow gradient. The velocity information of the spray sheet was then exported as digital data for graphical representation.

For the verification of the velocity distribution uniformity, the standard classical notion of normal distribution was used. All velocity data measured by PIV were exported and treated statistically, i.e., the mean and standard deviation for velocity data at different points under the spray nozzle were calculated.

2.3 RESULTS AND DISCUSSION

2.3.1 Image acquisition by PIV experimental method

The spraying sheets of the extended range flat fan nozzle (TeeJet 8003) were illuminated by a pulsed laser sheet at eight different pressures (25, 50, 75, 100, 125, 150, 175 and 200 kPa), as shown in Fig. 2-8. Ten sets of images were acquired using the PIV system setting described in materials and methods section, with a double frame mode at a trigger rate of 4 Hz, and time between pulsed signals of 500 μs. Each set of images contained the different number of double frame images: 10, 20, 30, 40, 50, 60, 70, 80, 90 and 100. Three replications for each data set was performed. The data was processed by using Dynamic Studio v4.00 software (Dantec Dynamics, New York, USA), which contains tools for configuration, acquisition, analysis and for post-processing of the acquired data.

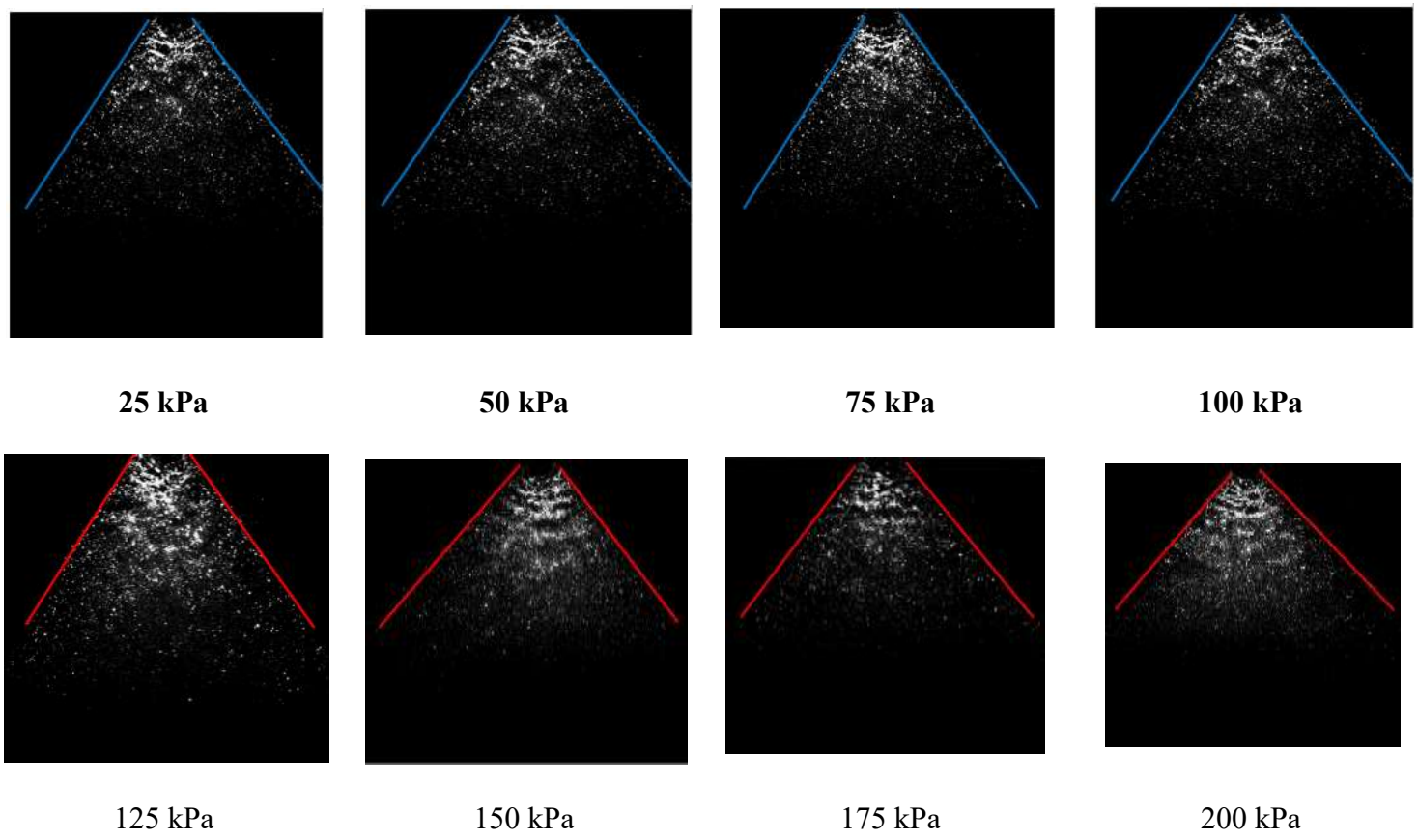

Figure 2-8: PIV Images acquired for analysis at different pressures.

2.3.2 Uniformity of velocity distribution in the spray particles

The velocity vectors at four different positions (10, 20, 50 and 70 mm) under the spray nozzle were determined after the processing of the PIV images to verify the velocity distribution. All velocity data were reported in the graphic versus their frequency (Fig. 2-9) showing that the velocity distribution follows the normal distribution equation with a mean value of 8.84 and median of 9.5. The mean and median were not very diverse, in other words, the mean value is close to the median value. It verified that the spraying water particles were uniformly distributed, i.e., there was a uniformity of spraying water around the symmetrical axis of the nozzle. In a perfect scenario, the mean value had to be the median of this distribution, which means the velocity distribution is perfectly uniform. However, due to the asymmetrical laser source (the laser beam just coming from one side), the graph cannot have a perfect and symmetrical lighting situation for each PIV image (Fig. 2-9), hence it cannot reach the perfect normal distribution.

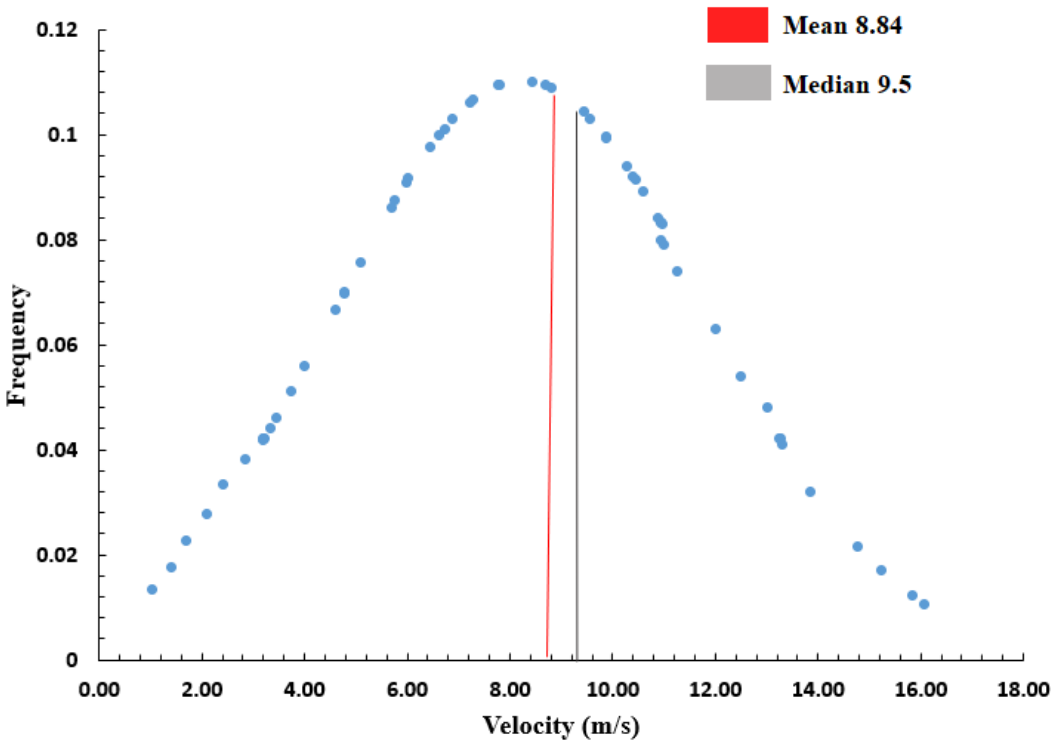

Figure 2-9: Velocity distribution under the sprayer nozzle at 200 kPa pressure

Figure 2-10 (a, b, c and d) showed the velocity profiles at 10mm, 20mm, 50mm and 70mm distances under the sprayer nozzle. From these profiles, it can be observed that the velocity has maximum value at the centre of nozzle (outlet of the flow) and the velocity field is uniformly distributed on each left and right side, but not totally perfect.

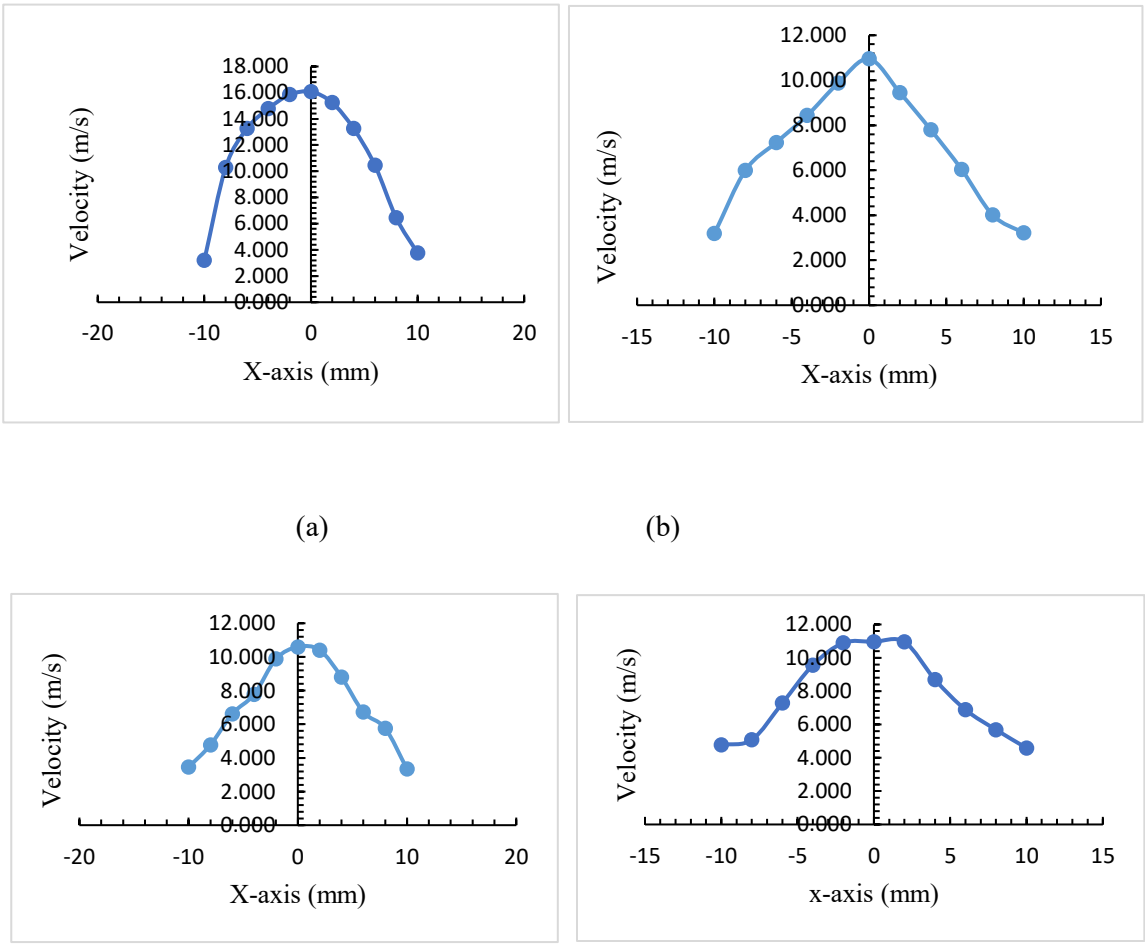

Figure 2-10: Velocity distribution profiles under the sprayer nozzle at 10 mm (a), 20 mm (b), 50 mm (c) and 70 mm (d) distance at 200 kPa pressure.

2.3.3 Manual measurements for water volume versus PIV results

After validation of the normal distribution of the spray sheets, these PIV images were used to calculate the volume of the spray sheet. The volume of a drop of spray coming out of the nozzle was calculated using equation (2.1), while the number of droplets (N_1) was calculated by dividing the volume of water collected manually and the average volume of droplets at the lowest pressure (25 kPa) (Table 2-2). All the other pressures data is

presented in Appendix -A. The calculations for the total number of droplets (N_3) was done using the data from the regression equations presented in Table 2-1.

Table 2-2: Result of calculations done for measuring the spray volume using PIV (25 kPa)

No. of pictures	N_2	N_3	$V_{PIV\text{-}water}$ (mL) $= N_3 \times V_{drop}$	V_{water} (mL) $= N_1 \times V_{drop}$	% E
10	1357707	6773485.678	84.7159	84.33	0.45373
20	3324186	7893788.764	98.7276	96.33	2.48541
30	3899246	8221400.446	102.825	106.00	2.995230
40	5546436	9159804.589	114.561	120.67	5.062
50	6922519	9943759.074	124.3665	130.00	4.333
60	10096836	11752167.47	146.9843	147.00	0.0106
70	11772475	12706779.01	158.923	159.33	0.257
80	10920085	12221172.42	152.8502	160.33	4.6672
90	15192179	14654984.38	183.2898	182.33	0.5246
100	16875515	15613980.9	195.28405	196.00	0.3652

Where: N_1 : Total number of droplets released from sprayer, N_2 = Number of white pixel, N_3 = Number of droplets measured through white pixels, $V_{PIV\text{-}water}$ = Predicted volume= Volume measured by using PIV (mL), V_{water} = Manually measured volume (mL), V_{drop} : Average volume of one droplet and E = % Absolute Error.

Equation (2.4) was used to calculate the volume of water from PIV while equation (2.5) was used for the calculation of the absolute error. These calculations were also performed for other pressure ranges including 50, 75, 100, 125, 150, 175 and 200 kPa and presented in Table 2-3.

It is observed that the manually measured volume and the PIV based volume, compared in Table 2-3, are very close to each other (relative error less than 5%) when the number of double-framed pictures at 10, 60, 70, 90 and 100, captured under the 25kPa pressure (Table 2-3). Under that pressure, the error is very significant (greater than 5%) when the number of pictures was at 40, the error is very significant (greater than 5%) when the number of pictures was at 40.

A question that arises here is: what combination of the number of pictures and the operating pressure can give the least significant error with the well-defined PIV configuration? The answer to that question is obtained by conducting a factorial analysis where the pressure and number of pictures are considered as two input factors while the error is considered as output.

Table 2-3: Result of calculations done for measuring the spray volume using PIV and manually measured methods at different pressures.

Pressure	25 kPa			50 kPa			75 kPa			100 kPa		
No. of pictures	**V_1**	**V_2**	**% E**	**V_1**	**V_2**	**% E**	**V_1**	**V_2**	**% E**	**V_1**	**V_2**	**% E**
10	84.72	84.33	0.4537	114.9	108.0	6.403	128.00	132.33	3.277	134.33	140.67	4.507
20	98.73	96.33	2.4854	129.8	132.7	2.185	145.73	146.00	0.182	155.78	163.33	4.623
30	102.83	106.00	2.9952	144.5	139.7	3.472	162.38	158.00	2.775	176.86	188.33	6.091
40	114.56	122.67	5.0620	159.9	153.0	4.515	179.07	179.33	0.149	199.35	206.33	3.386
50	124.37	134.00	4.3334	172.4	164.0	5.128	196.33	193.67	1.375	224.35	228.33	1.747
60	146.98	147.00	0.0106	186.5	184.0	1.361	213.80	209.00	2.297	262.41	250.00	4.966
70	158.92	159.33	0.2571	202.3	194.0	4.253	229.40	231.00	0.691	267.12	267.33	0.078
80	152.85	169.67	4.6672	216.6	207.3	4.481	246.73	253.33	2.607	288.88	294.67	1.965
90	183.29	182.33	0.5246	228.8	230.0	0.516	268.15	268.67	0.192	309.87	324.67	4.559
100	195.28	196.00	0.3653	243.0	240.0	1.268	284.33	282.33	0.706	333.98	345.33	3.288
Pressure	**125 kPa**			**150 kPa**			**175 kPa**			**200 kPa**		
No. of pictures	**V_1**	**V_2**	**% E**	**V_1**	**V_2**	**% E**	**V_1**	**V_2**	**% E**	**V_1**	**V_2**	**% E**
10	145.18	157.33	7.726	150.23	155.33	3.283	156.48	175.67	10.92	154.00	198.33	22.35
20	165.47	188.67	12.297	174.81	184.00	4.993	186.13	193.00	3.56	183.45	227.33	19.30
30	186.36	195.67	4.757	200.41	207.67	3.493	206.42	222.33	7.16	213.42	230.67	7.48
40	207.32	246.00	6.328	225.03	235.33	4.377	230.91	251.67	8.25	242.66	275.67	11.97
50	228.79	254.67	4.937	249.94	254.00	1.600	257.7	273.33	5.72	271.01	283.67	5.68
60	249.94	271.67	7.998	276.29	311.33	11.255	291.26	263.00	10.75	302.49	309.33	2.21
70	271.27	292.33	7.205	302.89	328.33	7.750	322.05	322.67	0.19	328.94	346.00	4.93
80	292.53	310.00	5.634	328.49	335.00	1.944	346.43	364.33	4.92	366.74	401.00	8.54
90	311.53	326.67	4.633	353.00	358.67	1.581	376.25	406.00	7.33	388.42	421.00	7.74
100	333.41	353.67	5.728	379.79	379.67	5.446	403.52	416.00	3.00	415.76	465.67	10.72

Where: V_1 = volume of water measures through PIV and image processing technique in mL, V_2 = Manually measured volume in mL and % E = % Absolute Error

2.3.4 ANOVA Test and Multiple Means Comparison (MMC)

It is very difficult to identify the pair of pressure and number of pictures which provide the least percentage absolute error from Table 2-3. A factorial analysis is carried out to answer this question by considering pressure and number of pictures as factors and percentage absolute error as a response variable. Table 2-4 shows the ANOVA results indicating the effects of pressure and number of pictures on % absolute error. In factorial experiments, if the higher order interaction is found to be significant then we can ignore the main effects because they are the part of interaction effects. Based on these results, two-way interactions (pressure x No. of Pictures) and main effect of pressure and number of pictures were found to be statistically significant. These results suggested the multiple mean comparison (MMC) of two-way significant interaction effect only.

Table 2-4: Analysis of variance

Source	DF	MS	F-Value	P-Value
Pressure	7	184.44	16.44	<0.001
No. of Pictures	9	60.95	5.43	<0.001
Pressure x No. of Pictures	63	26.37	2.35	<0.001
Error	160	11.22		
Total	239			

DF = degree of freedom MS = mean square

The results of ANOVA suggested the MMC of the significant interaction effects shown in Table 2-4. Since the experiment was performed in the laboratory, the magnitude

of the error should therefore be between moderate and high, suggesting that LS mean was used as a method for MMC only for two-way interaction.

The MMC results of important interactions are shown in Table 2-5. The non-relevant interactions are not presented here. The results of these non-relevant interactions are presented in Appendix- A (Table A-9) of this thesis. These results showed that maximum percent absolute error (22.220) was obtained when pressure = 200 kPa and number of pictures = 10. The percent absolute error obtained when the factors interacted at this level was significantly different (higher) from the percent absolute error obtained at all other combinations, except for pressure = 200 kPa and number of pictures = 10.

Table 2-5: Two-way interaction effect (pressure × number of pictures) of important

Pressure (kPa)	No. of Pictures	Mean (% Error)	Pressure (kPa)	No. of Pictures	Mean (% Error)
200	10	22.220 a	25	100	0.9754 de
200	20	19.271 ab	25	90	0.9749 de
175	60	144.937 abc	75	40	0.5454 de
200	40	11.976 abcd	75	90	0.2657 de
125	20	11.733 abcde	175	70	0.2110 e

Means with same grouping letter are not significantly different at the 5 % level of using L.

In addition, the results indicated that the minimum error was obtained when the pressure and the number of pictures interact under pressure = 175 kPa and the number of pictures = 70. The mean percent absolute error obtained when the factors interacted at this level was significantly different (lower) from the mean percent absolute error obtained

at all other combinations, except for pressure = 175 kPa and number of pictures = 70 significantly less error.

Moreover, the less perfection of the PIV system for more turbulent flow. For 10 pictures set and 200 kPa pressure the highest percent absolute error (22.220%) was observed possibly due to the accuracy of correlations and the short period of measurement time. The smallest error (0.2110%) was found with 70 number of pictures with a pressure of 175 kPa. It seems that the number of pictures is optimal for correlation and our pattern recognition processes. It should be noted that the results of different statistical analyzes showed a good agreement between these two measurements, which suggests that the quantification of the flow through the spray nozzles by the PIV technique coupled with image processing could be reliable and precise.

2.4 CONCLUSIONS

The PIV technique coupled with image processing can be used for a precise quantification of flow streams through sprayer nozzles as well as for the velocity distribution of spaying pattern. The results of this study showed that the velocity reaches the maximum value at the center of nozzle water stream and decreases continuously at the left and right sides within the spraying pattern. The field of velocity also showed a uniform and asymmetrical distribution on the entire area of spraying.

The results of this research revealed that fluid flow measurement through PIV is a reliable and can predict the spray pattern accurately. The methodology of this research can be used for quantification of water coming out of sprayer nozzles used in precision irrigation (drip irrigation, sprinkler irrigation etc.) It would open a new horizon in the future for the use of PIV technique to investigate the characteristics of sprayer nozzles air-

water flow properties, submerged flow, internal geometry of the spray, performance as well as flow rate through a sprayer nozzle.

Future research works will investigate velocity of spray particles at different points under the spray nozzle. This will provide detailed insight of the flow pattern and will help to see the weak jet areas where there are maximum chances of the spray particles to escape from the spray sheet in the form of drift. In the next chapter, the velocity distribution will be discussed in detail.

CHAPTER 3: CONTRIBUTION TO SPRAYING NOZZLE STUDY: A COMPARATIVE INVESTIGATION OF IMAGING AND SIMULATION APPROACHES.

Application of agrochemicals on crops is important for plants protection. Multiple factors influence the application of agrochemicals on plants such as climatic conditions, crop characteristics and spraying system design. Reliable, low cost and quick methods are needed to investigate these properties more precisely. In this study, the velocity distribution of an extended flat fan nozzle is investigated to determine the weak jet areas, which have high risks of droplet drift. Two different methods are used and compared: Particle Image Velocimetry (PIV) method used as an experimental approach versus a Computational Fluid Dynamics (CFD) with volume of fluid (VOF) integrating k-epsilon model as a simulation approach. The nozzle was operated at eight different pressures on a custom-made nozzle operating prototype while ANSYS 16 Fluent software was employed for the simulation approach. The results of this research showed three significant outcomes. First, the spray sheet (jet) has maximum velocity in its central spray region. Second, the particles present in the central region of spray sheet have maximum kinetic energy and this region has the ability to hit the right target on the plant surface, while liquid particles present in the surroundings of this central area have a lower velocity with minimum kinetic energy and have maximum chances to be off-target during spraying. These particles have maximum chances to move away from the targeted surfaces easily even with very low wind velocity. Third, the study also showed that PIV and CFD simulation methods were in agreement and both showed reliable ways to measure the jet velocity and plot the velocity distribution under the sprayer nozzle.

3.1 INTRODUCTION

Application of agrochemicals on crops is important for plant protection. The quality of agrochemicals plays a key role in the application of agrochemicals using different types of spray nozzles. Sprayer efficiency can be maximized by choosing the appropriate nozzle pressure combination that increases the deposition rate of agrochemicals on the plant surface (Smith et al., 2000), reduces runoff of agrochemicals on soils (Derksen et al., 2008), and reduce the dangers of drift (Nuyttens et al., 2007a, Yarpuz and Bozdogan, 2009). The effectiveness of agrochemical application depends on the characteristics of the spray, such as droplet size, operating pressure, droplet velocity, incoming air characteristics, and volume distribution characteristics (Nuyttens et al., 2009). In this study, we will discuss the characteristic behavior of the nozzle velocity of the sprayer under different pressures.

Droplet size, operating pressure and droplet velocity are the most important factors during the application of agrochemicals. Studies are available on droplet distribution of spray (Bird et al., 1996; Carlsen et al., 2006; Ozkan et al., 1997; Nuyttens et al., 2007a; Piggott and Matthews, 1999; Etheridge et al., 1999). These studies have shown that the distribution of the droplets in the spray sheet is not homogeneous and that the distribution of the droplets depends on the position of the droplet in the spray sheet.

Droplets after leaving the nozzle are three-dimensional in nature (Farooq et al., 2001). The authors reported that increasing the operating pressure of spray system not only decreases the size of the droplets, but also increases the velocity of droplets at the outlet of the nozzle. In other words, increasing the operating pressure produces more fine spray particles that are more likely to drift, but at the same time, high operating pressure increases

the droplet velocity (Ozkan, 1998). According to Miller and Butler (1997), after a certain pressure limit, spray drift decreases due to the dominance of droplet velocity.

Nuyttens et al. (2009) studied the characteristics of droplets along with the droplet velocity of spray particles for agricultural sprayers. They evaluated 13 different nozzle pressure combinations using a Doppler particle analyzer (PDPA) and concluded that the smaller droplets had a lower velocity and the larger ones had a higher velocity. The velocity of large droplets (> 400 μm) varies from 4.5 to 8.5 m/s, but depends on the type and size of the nozzle when operating at a pressure of 3.0 bar. In the same way, the droplet velocity of less than 400 μm decreases steadily with the decrease in droplet size (gravitational effect reduces and drag force increases as droplet size decreases). This speed varies from 0.5 to 2 m/s, but it also depends on the type of nozzle, operating pressure, shape and the size of the orifice (Nuyttens et al., 2009).

The study of high-pressure liquid flowing from one medium to another is still a difficult theme in modeling. The development of droplets after the fluid comes out of the nozzle into air is still an interesting topic to understand the instability of jet. For example, in our case study, water is coming out of a nozzle into a lighter medium by pressure. There are many studies underlined the phenomenon of liquid jet entering in liquid medium. However, fewer works have been reported on understanding the jet phenomenon from nozzle-liquid medium going to the air. At low Reynolds number, the jet of water coming in lighter medium brakes up due to hydrodynamic instability and surface tension is a major contributor towards this instability (Sinha et al., 2015). The behavior of the jet is wavy at high Reynolds number due to the induction of aerodynamic effects. Reynolds number, the ratio of inertial force to viscous force, is a dimensionless quantity used to ‘quantify’ the

flow patterns in different flow conditions. Fundamental fluid mechanics showed very well that laminar flow occurs at low Reynolds number while turbulence at high Reynolds number, including in the jet flow (Sinha et al., 2015); Taylor and Hoyt (1977) and Chaudhary and Maxworthy (1980) conducted experiments on water jet behavior and concluded that density also had significant effect on the characteristics of water jet behavior. Lin and Reitz itz (1998) studied injection of water jet in gas and reported the behavior of jet in four different regimes. These regimes are identified based on viscosity, density, gravity and surface tension. The four regimes are classified as 1) the Rayleigh regime, where jet diameter < droplet diameter; 2) the 1st wind induced regime, where jet diameter = droplet diameter; 3) the 2nd wind regime, where jet diameter > droplet diameter; and 4) the atomization regime, where droplet diameter is negligible as compared to jet diameter (Homma et al., 2006).

The droplet behavior changes from 2D to 3D when injected from a high-density to another low-density medium (Homma et al., 2006). In the case of water jet coming out from nozzle like in our case study, the atomization regime occurs given that the average droplet diameter (288 μm) (ASABE, 2010) is negligible when compared to the jet diameter (1500 μm) TEEJET 8003 (extended range flat fan). The characteristics of such fluid flow problems have not been sufficiently studied. CFD software are widely used today (Jiang et al., 2017) to solve such nozzle problems. Fluid flow, chemical reactions and heat transfer problems, which are difficult and take a long time to experiment, can be easily solved with these CFD simulation methods. CFD packages have a user-friendly interface and allow the user to test many parameters, which would be difficult to do in the real world. Recent

advances in hardware make it easier to solve many complex industrial and academic problems related to fluid flow with greater accuracy and reduced computing time.

For all the above reasons, it is necessary to study the behavior of the spray to reduce the spray losses. In particular, it is important to understand the behavior of the fluid jet at different pressures because it is directly related to spray losses. In this study, we examined the velocity distribution of agricultural spray nozzles using numerical simulation (commercial software ANSYS 16.0, Fluent) and validate the results with a velocity study by a PIV experiment. Velocity distribution under the spray nozzle is one of the key factors related to spray drift.

The PIV technique is a non-intrusive laser optical measurement technique used to obtain instantaneous velocity vectors in a cross-section of gas or liquid flows. The details of the experimental method PIV can be seen in our previous work (Nadeem et al., 2018).

Two objectives of this work are: i) to provide better insight into jet behavior in terms of velocity, which will identify the weak areas of spray, and where there is the maximum probability of drift prone particles; ii) to open a new horizon in spraying system research of flat fan nozzle, which will not only decrease the experimental cost but also reduce the labor and time for nozzle analysis. The overall gain of this work can lead to a reliable dataset that will be used to optimize the design of sprayer nozzle for less spraying losses. The flowchart in Fig. 3-1 represents all different steps involved in this study.

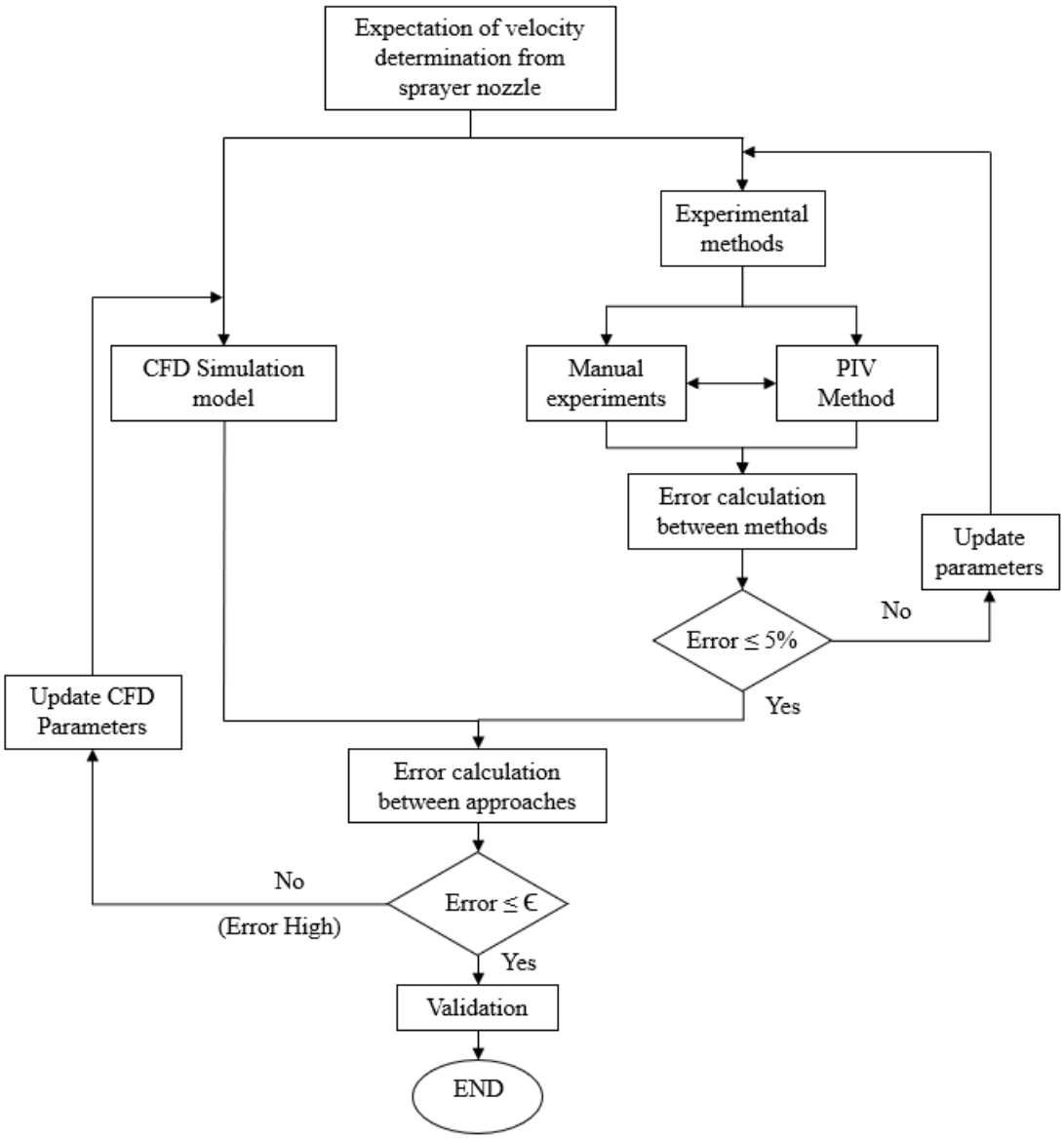

Figure 3-1: Schematic diagram of analysis for spray nozzle measurement

3.2 MATERIALS AND METHODS

3.2.1 Mathematical modeling for jet velocity

The flow chart (Fig. 3-1) is shows the schematic diagram of analysis for spray nozzle measurement. The jet velocity was calculated by two different methods: 1. CFD (Using ANSYS 16) simulation method; 2. Experimental method. In this section, the CFD mathematical modeling and PIV (experimental) approaches for velocity measurement will be discussed. We start by presenting a basic terminology used for this section.

3.2.1.1 Reynolds number:

In most of fluid flow problems, the first and foremost step is to find out the nature of flow, whether it is laminar or turbulent. Before selecting the appropriate model for simulation, the Reynolds numbers (Re) at different pressures was calculated using Equation (3.1) and presented in Table 3-1

$$\mathrm{Re} = VD/\gamma \qquad (3.1)$$

Where V : Jet velocity at inlet (m/s), D: diameter of orifice (m), γ: Kinematic viscosity (m^2/s).

The values of Reynolds numbers (Table 3.1) were very high so the flow conditions were considered as turbulent flow (Sinha et al., 2015; Iqbal et al., 2005). To deal with turbulent flow many researchers used the *k*-epsilon modeling approach (Altimira et al., 2009; Jonsen, 1992 ; Menter et al., 2003; Shirani et al., 2006; Shih et al., 1995; Tiwari et al., 2014).

Table 3-1: Relationship between pressure and Reynolds number

P (kPa)	V (m/s)	Re
25	6.837	10215.73
50	9.950	14865.66
75	12.025	17965.60
100	15.208	22721.21
125	16.504	24658.67
150	17.330	25891.61
175	18.509	27652.94
200	20.324	303650.40

P= Pressure at the tip of nozzle (kPa), V= Jet velocity at the tip of nozzle (m/s) using PIV

3.2.1.2 Turbulence regime:

The standard *k*-epsilon model was used for the simulation of turbulent flow through the spray nozzle. This model is composed of two parameters which model the turbulence kinetic energy (*k*) and the dissipation rate (ε). The standard *k*-epsilon model is based on the assumption that the flow is in fully turbulent conditions while neglecting the viscosity. This model has been found to be reliable, accurate and simple with very fast convergence and is widely used to study flow problems (Jiang et al., 2017; Sinha et al., 2015; Tiwari et al., 2014; Altimira et al., 2009; Najjar et al., 1995).

Governing Equations for k-epsilon model

$$\frac{\partial U_{i,k}}{\partial X_i} = 0 \tag{3.2}$$

$$\frac{\partial}{\partial t}\left(\rho_k U_{i,k}\right) + \frac{\partial}{\partial X_i}\left(\rho_k U_{i,k} U_{j,k}\right) = -\frac{\partial p_k}{\partial X_i} + \frac{\partial}{\partial X_i}\left[U_k\left(\frac{\partial U_{i,k}}{\partial X_j}\right)\right] \tag{3.3}$$

$$[U_i] = 0$$

$$\left[\left(\tau_{ij} \ . n_i \right) . n_i + p \right] = \sigma . k \tag{3.4}$$

$$\left[\left(\tau_{ij} \ . n_i \right) . t_j \right] = 0 \tag{3.5}$$

Where; u_i : Velocity component in corresponding direction (m/s), ρ : density of fluid **(**kg/m^3), and k : turbulence kinetic energy.

3.2.1.3 Volume of Fluid (VOF):

There are several methods listed in the literature to simulate the multiphase flow described by the conservation of mass and conservation of momentum equations. Normally these methods are classified into two major categories based on their flow domain and method of discretization (Lakehal et al., 2002).

In the first category, each phase (fluid) is considered as a deformable flow domain and solutions can be discretized to solve the mass and momentum equations at each time step (Ryskin and Leal, 1984). Interfaces between two phases (water and air) would be the straightforward boundary conditions of the different phase domains. These models used in this category encounter difficulties when dealing with highly distorted domains. In the second category, the fluid domain is considered fixed. An additional processor is used to define the interface between the two different phases (water and air). A system of differential equations for the fluid (mixture) is used to solve the fixed domain. The whole domain is modeled in such a way that different phases allow the spatial variation in fluid properties such as density and viscosity, and conditions of jumps are modeled separately. To identify the interface, there are two different methods under this category: the front tracking method and the front capturing method.

In the front tracking method, the particles of moving fluids are used to identify the interface (Harlow and Welch, 1965). In the front capturing method, the mark function (using different colors) is utilized to identify the interface. To solve this mark function, additional differential equations are solved to locate the interface. VOF is one of the popular front capturing methods (Hirt and Nichols, 1981; Gueyffier et al., 1999). VOF was used to track air and water phases during the simulation of the sprayer nozzle. VOF method defined the fraction of water and air (Albadawi et al., 2013; Lv et al., 2011; Lakdawala et al., 2014). Variable α takes a value of 0 to define regions where there is air, while a value of 1 represents water. To define both water and air in a grid, the VOF method assigns a value in-between 0 and 1 (Altimira et al., 2009; Cock et al., 2014).

Governing Equations for VOF method

$$\frac{\partial \alpha}{\partial t} + \frac{\partial}{\partial X_i}(\alpha u_i) = 0 \tag{3.6}$$

$$\rho = \alpha\rho_1 + (1-\alpha)\rho_g \tag{3.7}$$

$$u = \alpha u_1 + (1-\alpha)u_g \tag{3.8}$$

$$\frac{\partial \rho}{\partial t} + \frac{\partial \rho u_1}{\partial X_i}\left[U_k\left(\frac{\partial U_{i,k}}{\partial X_j}\right)\right] \tag{3.9}$$

$$(Fv_i) = \sigma.k.n_i.\delta \tag{3.10}$$

Where α : marker function (0 or 1), u : particle velocity (m/s), ρ : density of fluid (kg/m^3).

3.2.2 CFD simulation

3.2.2.1 CFD simulation by the commercial software ANSYS:

Modelling the turbulence flow by simultaneously using the k-epsilon and VOF approaches for a spray nozzle at different pressures is very complex due to the many factors involved.

To deal with this complex problem, the ANSYS 16.0 (Fluent) software was used. For more reliable results, many CFD packages are available with a comprehensive and easy-to-use interface for pre-processing and post-processing processes (Sinha et al., 2015).

3.2.2.2 Geometry:

The 2D model of the spray nozzle was created using the design module available in ANSYS 16.0. The model included key elements of the nozzle and the environment, consisting of water and air (Fig 3-2). The inlet zone was selected as water, while the exit zone was selected for STP air (standard temperature and pressure) (Fig. 3-2).

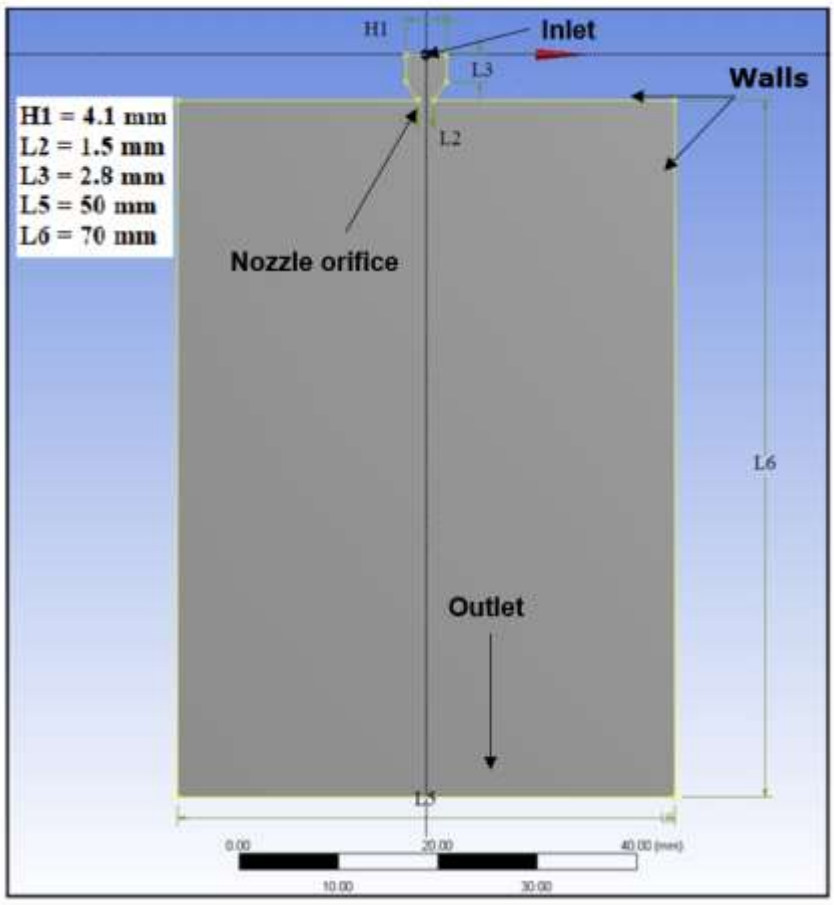

Figure 3-2: Geometry of nozzle and flow domain

3.2.2.3 Meshing:

Three different meshes were tested for this study: coarse, fine and very fine. Mesh-sensitive analysis was performed to verify the influence of the mesh on the calculation results. The mesh with 56741 nodes and 56243 elements (Fig 3-3a) was considered the best option for this study because there was no significant difference between very fine and fine meshes, except computing time, while the coarse meshes with 14380 nodes and 14127 elements were not taken into account due to significantly worse simulation results. For fine and very fine meshes, the results indicated that the results were similar and independent of the mesh. The fine mesh was selected for later simulation because it took less computing time without significantly modifying the results.

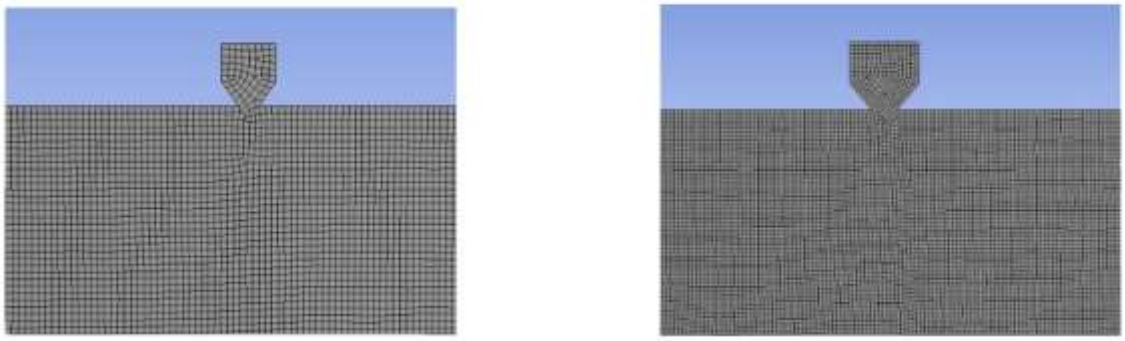

(a) Coarse mesh (b) Fine Mesh

Figure 3-3: Mesh analysis

3.2.2.4 Boundary Conditions:

The following boundary conditions for CFD simulations were used. The geometrical part of the nozzles was selected as a water fluid (density 1000 kg / m^3) with different pressure conditions. The remaining geometric portion after the tip of the nozzle was considered 100 kPa air. At the inlet, the pressure varies between 25 kPa and 200 kPa for the numerical simulation and for the experimental configuration.

3.2.3 Experimental methods for Jet velocity measurements

3.2.3.1 PIV experimental setup:

To validate the CFD modeling results the experimental setup was used to simulate the nozzle at different pressures (25, 50, 75, 100, 125, 150, 175, 200 kPa). A schematic diagram for a PIV system is shown in Fig. 3-1. The standard PIV (Two-dimensional PIV system from LPU 550, Dantec Dynamics (Fig. 2-3) was used to take the laser-illuminated images for the acquisition of spray behavior (velocity of jet). Details of all parameters were kept the same as in section 2.2.2 of this thesis.

Calibration of the PIV system was performed before acquisition of images for further processing (Fig 3-4). In calibration, the scale factor was adjusted and for accuracy purposes, absolute distance was assigned. The following procedure was adopted for calibration.

3.2.3.2 Calibration of PIV system

1. Before starting the laser for calibration, the water level in laser synchronizer was checked. The water tank was filled with the deionized water for smooth running of laser unit.

2. The key on the back side of the laser synchronizer was put ON.
3. The laser synchronizer was run for a while to attain the temperature 100°C for good results.
4. All the buttons were switched in internal mode because the laser is controlled manually. External mode could be run if it became necessary to run the image acquisition automatically.
5. Double frame acquisition setting was used for all the images captured for calibration.
6. Laser and camera were aligned first with visual observation, and then the alignment was performed by observing the images on screen as shown in Fig. 3-4.
7. For calibration and image acquisition of spray sheet the laser beam was adjusted on very thin mode.
8. A steel ruler was used to adjust the scale for calibration (Fig. 3-4). Aperture of the camera was adjusted to make the ruler clear.
9. Grid size of the image was adjusted as 32 x 32 for more accurate results.
10. After all these setting the images was captured and saved for calibration.
11. An absolute distance was assigned for calibration images, 20 cm = 200 mm.
12. After successful calibration the different images were acquired for further processing.

After calibration, the PIV system was run using the same settings as mentioned in 2.3.2 section of this thesis. The main objective of PIV imaging was to measure the particle displacement and time so that velocity of individual particles could be calculated. In the case of submerged flow, seeded particles (having same density of fluid used for simulation)

were used to mimic the flow. The displacement of these particles can be calculated by using post-processing tools available in Dynamic Studio (Computer based software). In the case of nozzle flow, water was coming out into the air directly, droplets of water were hence illuminated by laser beam and the CCD cameras were used to capture these images (Fig. 2-3).

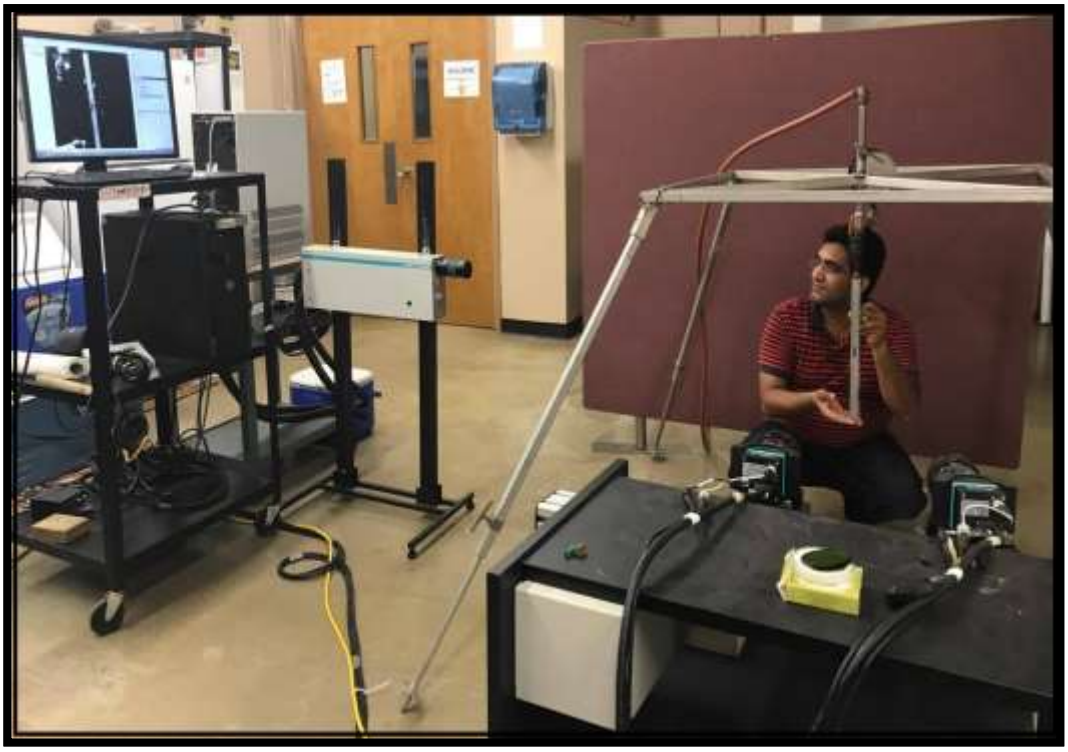

Figure 3-4: Calibration of PIV system

3.2.3.3 Post processing of acquired images:

The choice of the optimal recording parameters and the definition of the appropriate parameters for the processing requires experience, in particular the section of the interrogative zone which makes it possible to balance the robustness, the precision and the accuracy of the fields of flow. The purpose of the image interrogation was to measure the movement between different pattern images with great precision. For this purpose, the

images were divided into small areas called “interrogation area” (normally 16 x 16 and 128 x 128 pixels maximum). Then, an adaptive correlation method was used to determine the displacement value for each small area interrogation area (IA). There are no defined rules and optimal conditions for different types of flows due to variable seeding density, variable image quality and flow conditions (Theunissen et al., 2006; Dantec Dynamics, 2013). Adaptive correlation was considered an automatic adaptive method for calculating the velocity vector according to the adaptability of the flow (gradient) and the adaptability of the signal (quality of the signal). This type of automatic system leads to more precision and spatial resolution, especially in high gradient regions. (Theunissen et al., 2006). Therefore, the adaptive correlation method, a very user-friendly technique, was chosen to compute velocity vectors to improve spatial resolution, speed, and accuracy. The second main advantage of this technique is that it controls brightness, image focus, and time step (Dantec Dynamics, 2013). Our results using adaptive correlation showed a statistical matching between two images and the location of the maximum displacement value was measured as the average displacement of the particles, considered as a velocity vector.

3.2.3.4 Jet velocity calculation from the experimental discharge data

Iqbal et al. (2005) reported a formula to calculate the jet velocity at the tip of nozzle with known diameter.

Volumetric flow rate:

$$Q = V_j C_a A \tag{3.11}$$

Where

Q = flow rate or discharge (m^3/s),

V_j = Jet velocity (m/s), C_a = Area coefficient,

A= Nozzle surface area (m^2)

Jet velocity *:*

$$Vj = C_v (2 \Delta p / \rho)^x \qquad (3.12)$$

Where;

Vj = Jet velocity (m/s),

C_v = velocity coefficient

Δp = Total pressure drop (pa)

ρ = Liquid density (kg/ m^3), X = 0.5 for turbulent flow

Now substituting the value of "V_j" in equation 3.11 from equation 3.12.

$$Q = C_v (2 \Delta p / \rho)^{0.5} \; C_a A \qquad (3.13)$$

Let $C_v C_a = C_d$ then, $Q = C_d (2 \Delta p / \rho)^{0.5} A$

Where; C_d = Coefficient of discharge

$$(2 \Delta p / \rho)^{0.5} = (2gh)^{0.5} = V_j$$

So, equation (3.12) becomes $Q = C_d V_j A$

$$V_j = Q / C_d A \qquad (3.14)$$

Equation (3.13) was used to calculate the average jet velocity. For this equation, we need Q, C_d and A. For measuring the value of Q, a 1-liter graduated beaker was used to collect the volume of water for one minute and discharge was calculated by as volume/time

while the nozzle was operated at eight different pressures. This method was repeated three times and the average discharge or flow rate of the nozzle was calculated as presented in Table 3-2.

Table 3-2: Effect of pressure on discharge.

Pressure (kPa)	$(P)^{1/2}$	Q (m^3/sec)
25	5.00	4.830E-06
50	7.07	7.033E-06
75	8.66	8.500E-06
100	10.00	10.75 E-06
125	11.18	1.166E-05
150	12.25	1.225E-05
175	13.23	1.308E-05
200	14.14	1.436E-05

** P= Pressure at the tip of nozzle (kPa), Q= flow rate (m^3/s) measured manually*

The value of C_d was calculated as the slope of the line between Q and $\sqrt{p}$.

$$Q = c_d\sqrt{(2\Delta p/\rho)}\ A$$

$$Q = c_d\sqrt{(2/\rho)}\ A\sqrt{\Delta p}$$

$$Q/\sqrt{\Delta p} = c_d\sqrt{(2/\rho)}\ A = \text{slope of line}$$

So, $$c_d = Q/\sqrt{\Delta p}\ /\ \sqrt{(2/\rho)}\ A \qquad (3.15)$$

3.3 RESULTS AND DISCUSSION

Based on our framework (Fig. 3-1), the results obtained in each step will be discussed. The jet velocity was measured at the tip of sprayer nozzle using: a) the

experimental measurement including PIV and manual methods (right branch of Fig. 3-1); and b) numerical simulation by CFD (left branch of Fig. 3-1).

3.3.1 Tip velocity measurement

In the CFD numerical simulation, we used ANSYS 16 Fluent software to simulate the

Table 3-3: Comparison of jet velocity measured with experimental data and simulation

Sr #	P (kPa)	$(P)^{1/2}$	Q (m^3/sec)	Simulation "V" (m/s)	PIV "V" (m/s)	Manual "V" (m/s)
1	25	5.00	4.830E-06	6.64	6.8933	6.84
2	50	7.07	7.033E-06	9.43	8.6371	9.95
3	75	8.66	8.500E-06	11.06	11.5245	12.03
4	100	10.00	10.75 E-06	13.4	13.4137	15.21
5	125	11.18	1.166E-05	14.9	15.5234	16.50
6	150	12.25	1.225E-05	16.4	17.6296	17.33
7	175	13.23	1.308E-05	17.7	18.4578	18.51
8	200	14.14	1.436E-05	19.45	20.1845	20.32

** P= Pressure at the tip of nozzle (kPa), Q= flow rate (m^3/s), V= Jet velocity (m/s)*

nozzle at eight different pressures (25, 50, 75, 100, 125, 150, 175, 200 kPa) and results of tip velocity were tabulated in Table 3-3 (column 5).

After obtaining this CFD tip velocity, the experimental techniques, including PIV and manual methods were used to find out the tip velocity for this nozzle. The PIV method was used to capture the real-time images by using the experimental setup mentioned in the previous section. These images were processed to find out the tip velocity and tabulated in Table 3-3 (column 6). Beside the PIV method, a manual measurement was also used to quantify the tip velocity. For this approach, Equations (3.11) to (3.15) were used. Equation 3.13 was used to calculate the velocity with Q, C_d, and A as inputs. The values of Q were measured using the volumetric method and are presented in column 4 of Table 3-3. Parameter A was calculated based on the nozzle diameter as shown below.

Diameter of nozzle: D = 1.5 mm

Radius of nozzle: r = 0.00075 m

Surface area of nozzle: $\pi r^2 = 1.76 \times 10^{-6}\ m^2$

For C_d, the slope of the line from Fig. 3-5 was used.

$$Q/\sqrt{\Delta p} = = 1 \times 10^{-6}$$

According to equation (3.14), the C_d was calculated as

$$1 \times 10^{-6} / \sqrt{1000} = C_d \times (1.76 \times 10^{-6}) \times (1.4121 \times 0.03162)$$

$$C_d = 0.316 \times 10^{-6} / 0.07858 \times 10^{-6}$$

$$C_d = 0.40$$

Knowing the value of C_d, Q, and A, the jet velocity V can be obtained from Equation (3.13) and is reported in column 7 of Table 3-3.

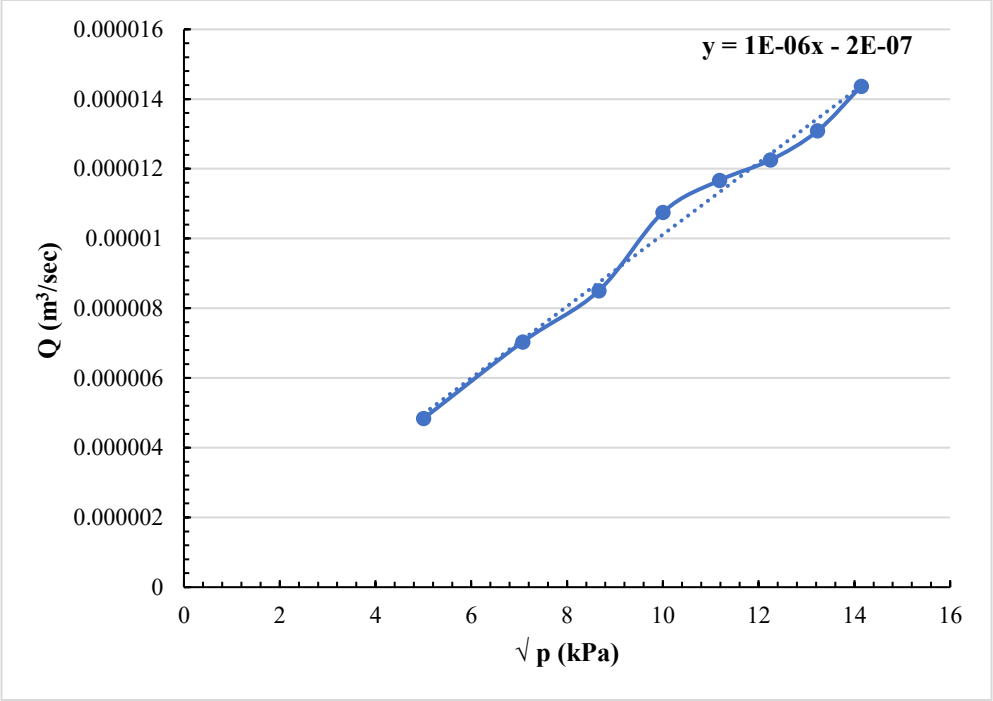

Figure 3-5: Coefficient of discharge for extended flat fan nozzle

3.3.2 Error estimation and validation

The results of these three methods (Table 3-3) showed that the tip velocity of sprayer nozzle was increasing from 25 kPa to 200 kPa using CFD numerical simulation and the same trend was observed with the PIV and manual experimental methods. The tip velocity values obtained by these three methods are very close to each other within ± 1 % error. At a pressure of 25 kPa, the tip velocities are very close to each other within ± 0.5 % error. However, the error is less than 5 % in most cases when comparing CFD numerical simulation with PIV and manual experimental methods (Table 3-3). When the pressure increases these measured values start to diverge, not as homogenously as with the 25 kPa case. This could be explained by the fact that higher pressure causes high turbulent regime governed by high Reynolds number (Table 3-1). Fig. 3-6 presents the relationships of nozzle pressure (kPa) versus jet velocity (m/s) obtained by the three different methods: CFD, PIV and manual measurements.

It is noticed that the numerical simulation velocity by CFD mostly overlapped the manual and PIV experimental results. There was however a mismatch between the CFD numerical and manual results at the pressure of 100 kPa, which can be due to human error during operation.

The results overlapped at high pressure (200 kPa) (Fig. 3-6). Fig. 3-7 illustrates the flow pattern obtained through the PIV.

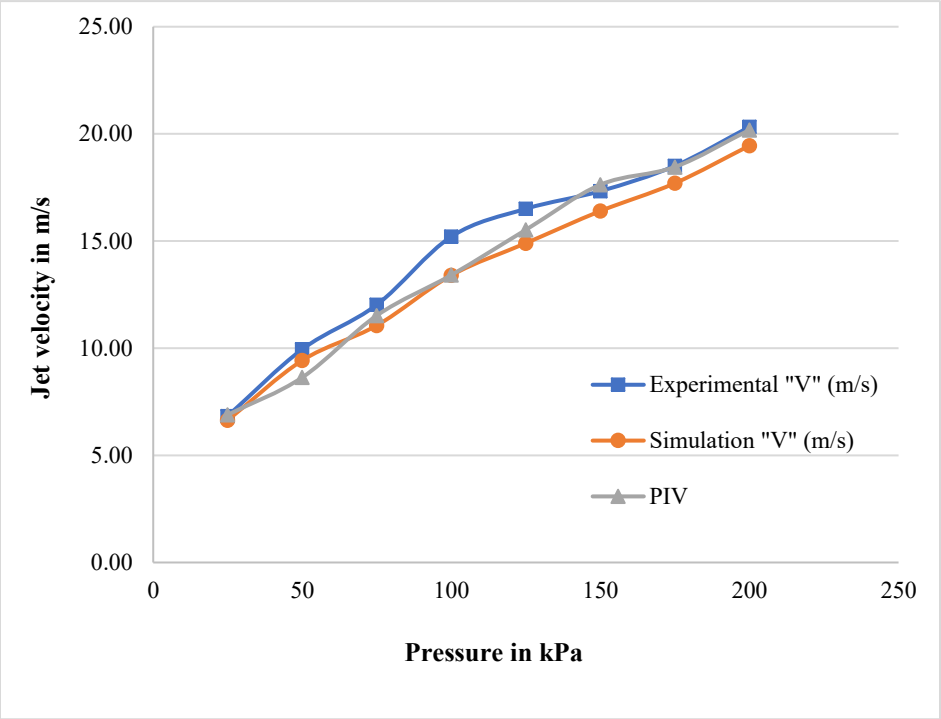

Figure 3-6: Comparison of jet velocity

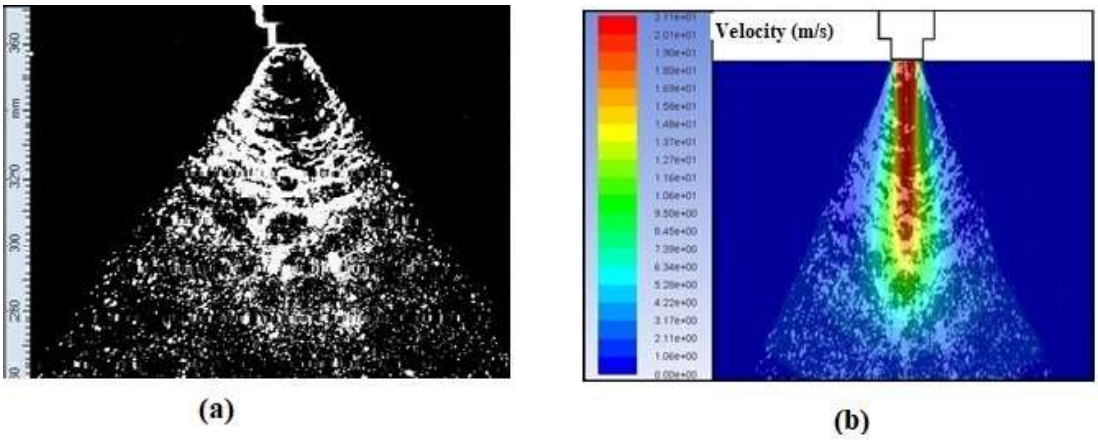

Figure 3-7: PIV image captured at 200 kPa (a), Overlapping of PIV and CFD images at 200 kPa

3.3.3 Behavior of spray velocity under nozzle tip at different positions:

Fig. 3-8 shows the velocity distribution at different points under the sprayer nozzle at 200 kPa pressure (precisely, at 10, 20, 30, 40 and 50 mm as shown in Fig. 3-8). The tip velocity changes from 20.02 m/s to 12.00 m/s along the central line of flow. It was observed that there was a deceleration of velocity from top to bottom along the central line due the impact of air.

At the 10 mm position, PIV and CFD numerical simulation results did not overlap, it may be due to the abrupt entrance of the air at tip points. The entering air at this point changed the velocity in the case of PIV. As water moved down, the velocity profiles overlapped better. The velocity distribution was also verified through PIV images at five different positions (10, 20, 30, 40 and 50 mm) under the sprayer nozzle.

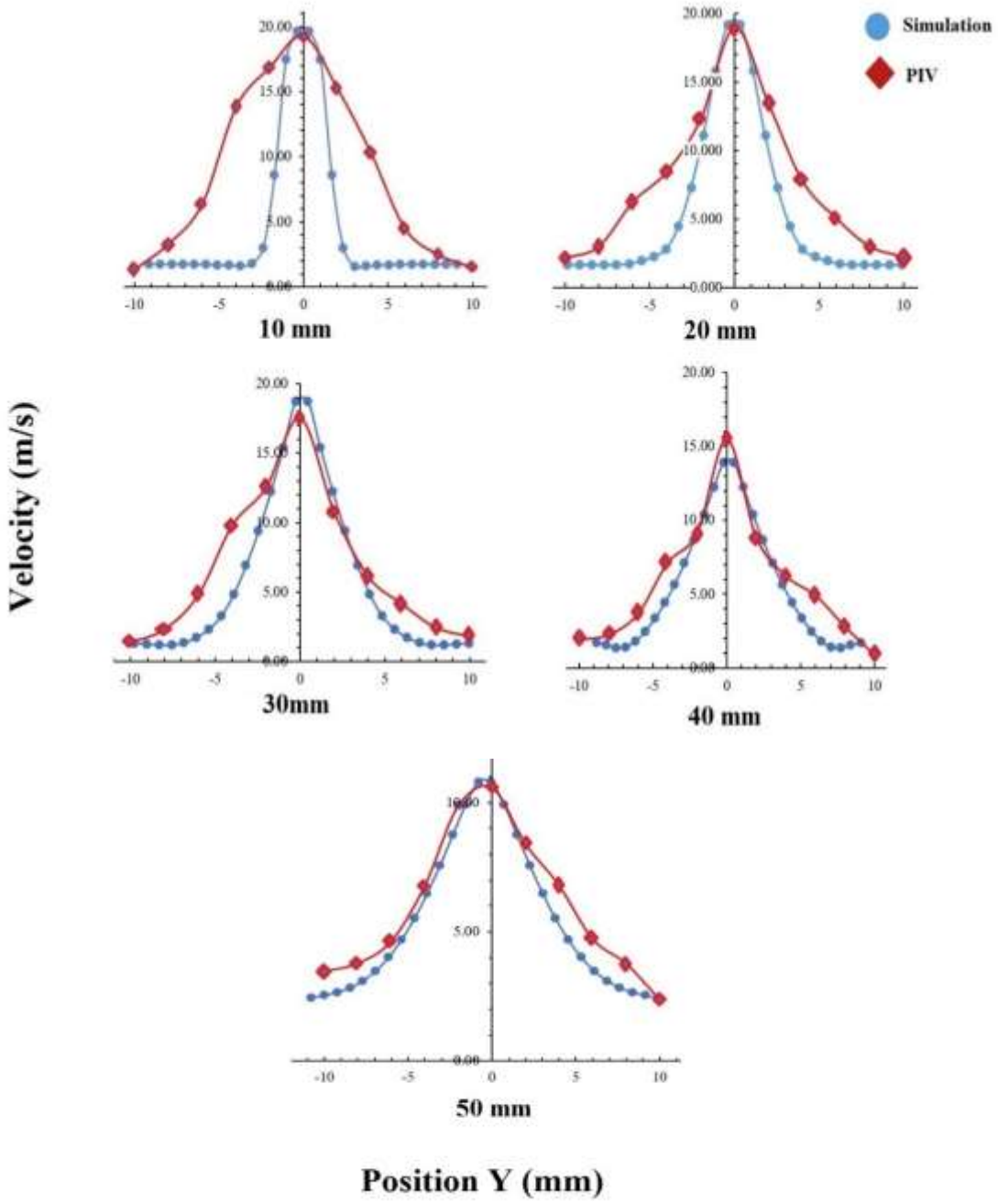

Figure 3-8: Velocity profiles at different points under the nozzle using numerical simulation and PIV.

3.3.4 Remark on the velocity values measured

At different positions, the numerical simulation and PIV methods give similar results. Fig. 3-8 shows the overlapping of velocity of these two methods. It can be also seen from this figure that the velocity of spray is decreasing in both PIV and numerical simulation cases while being at lower positions of the nozzle and the width of jet is spreading. The PIV and CFD numerical simulation given are in good agreement despite of some mismatching points between them.

The PIV method is a reliable option of measuring the jet velocity and very helpful to map the velocity distribution under nozzle. This method incorporates all the fluctuation of pressure and the changing behavior of the air around the nozzle jet.

The numerical simulation is also reliable method for mapping the velocity distribution under nozzle. But the velocity profile obtained through numerical simulation is not completely overlapping with PIV velocity profile near nozzle tip (10 mm) (Fig. 3-8). The main reason of this mismatching could be the pressure drop at tip of nozzle due to very high velocity and the surrounding air mixing with the water jet. The mixing of air at this point could result in high turbulence. The second main cause of this variation could be the slight change in pressure due to pump fluctuation.

3.3.5 Different applications from the finding of this study

The present study confirmed again that during spraying from through a nozzle, maximum velocity occurs in the center of the spray sheet which has the maximum probability to hit the right target (on plant surface). At this high velocity (16-20 m/s), there are fewer chances of droplet to escape from the spray sheet. The other good aspect of this result is that if we need to apply the spot specific application as in case of early stages of

many row crops then proper volume of chemical could be applied by using only one nozzle per row. This study showed with a more precise and qualitative way that the outer layer of spray sheet has minimum velocity. This part of spray is very sensitive to drift. Due to low velocity of spray sheet, the droplets could blow off target and could contaminate the air by suspending in the air or can cause contamination of off field soils. To avoid this situation, we recommend adjusting the boom height as low as possible in early stage of crop, while allowing the overlapping of spray sheets when crop canopy is fully developed.

The results of this study could be very useful for the uniform application of edible coating on fruits (an emerging food science topic) (Andrade et al., 2012) uniform protective coating for meat (Spraying system, 2013) fire sprinkler (Husted et al., 2009), sprinkler and drip irrigation (Yunkai et al., 2008) and to study the behaviour of nozzle injectors (Vimal and Gupta, 2015).

The results of simulation and experimental validation of jet velocity were used to predict the jet velocity behavior at high pressure. The jet velocity has a parabolic trend as shown in Fig. 3-9. The predicted pressure velocity relationship (Fig. 3-9) could be very usefully for many industrial applications (fruit coating, car painting, high-pressure fuel injection, tablet coating etc). According to this predicted jet velocity (Fig. 3-9) the velocity of spray jet had increasing trend with increase in pressure. However, the increasing pressure also had impact on decreasing the droplet size. For better penetration of spray we need to find an optimal pressure where we will attain the optimal velocity (high velocity will lead to runoff after slipping from the leaves, and low velocity will lead to more drift) with optimal droplet size because increasing the pressure will increase the risk of drift by

making mist of spray in agricultural application. At low pressure, the velocity of jet will be low and the spray sheet will be more drift prone.

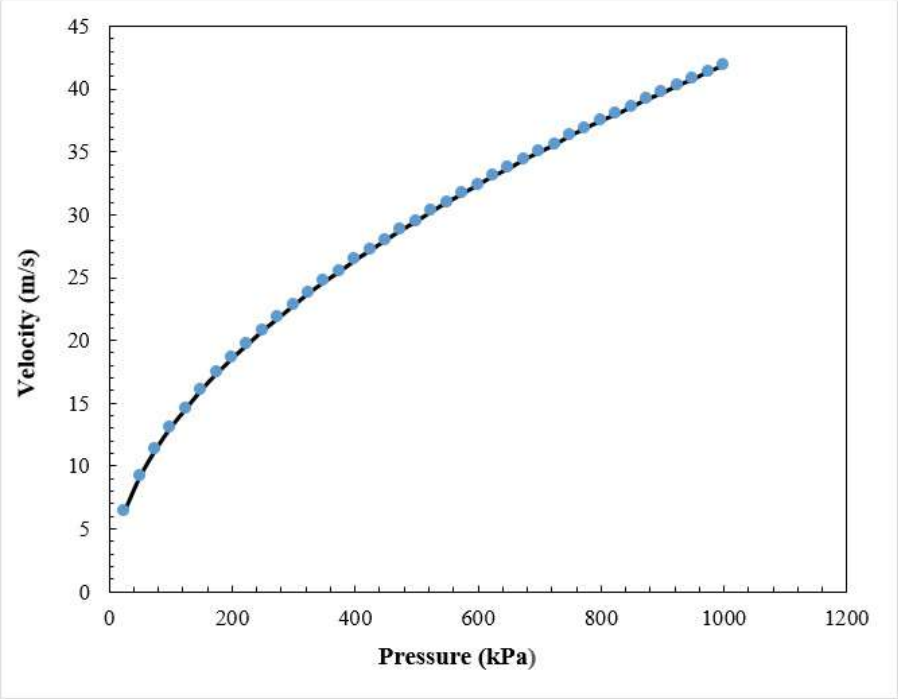

Figure 3-9: Jet velocity prediction at high pressure

Selection of proper pressure will lead to the less spray losses and uniform distribution. There is a need of comprehensive research on spray drift to consider all the possible factors, which are influencing the spray drift.

3.4 CONCLUSIONS

The results of this study showed that the spray sheet had maximum velocity at its center. The particles present in the central region of spray sheet will have maximum kinetic energy and that region have the maximum probability to hit the right target. The spray particles present in the surroundings of the central part had the less velocity that would lead

to minimum kinetic energy. This part of spray would be the more sensitive part of spray. There are maximum chances of off target drift only on these parts. Due to low kinetic energy, these particles can move away from the targets surfaces easily even with very low wind velocity.

Both PIV and ANSYS 16.0 simulation methods were proven as appropriate tools to investigate the distribution pattern of flat fan nozzles and can be considered as reliable and cost-effective research methods for such type of complex nozzles flow. Although the research result has more or less a known common sense of spraying nozzles, the performance of the study by using PIV technique confirms quantitatively some accurate and precise values of droplet velocity, validated by simulation, is our main finding here as no previous work was focusing on it.

The overall results of this study showed that the edges of spray sheet and spray away from the tip of nozzle had low velocity and these parts are at high risk for drift. The spray from these parts have maximum probability to move away from the target. This off-target spray could cause soil and water contamination. To reduce this off-target spray, there is a need of comprehensive research on spray drift to consider all the possible factors, which are influencing the spray drift.

In this chapter, a single nozzle was evaluated for velocity distribution. Figure 3-8 is clearly showing that the velocity of spray sheet is maximum in the central region so maximum spray will accumulate in this region. Fig 3-9 shows a comparison of the spraying patters of multiple nozzles before and after overlapping of volume. Overlapping of volume is an important consideration for uniform application of spray. The comparison of the nozzles

with no overlap and with overlap is clearly showing that overlapping nozzles have the potential of generating more uniformity in spray distribution (Fig. 3-10). This aspect of overlapping of spray sheets will be a key factor in the next theme.

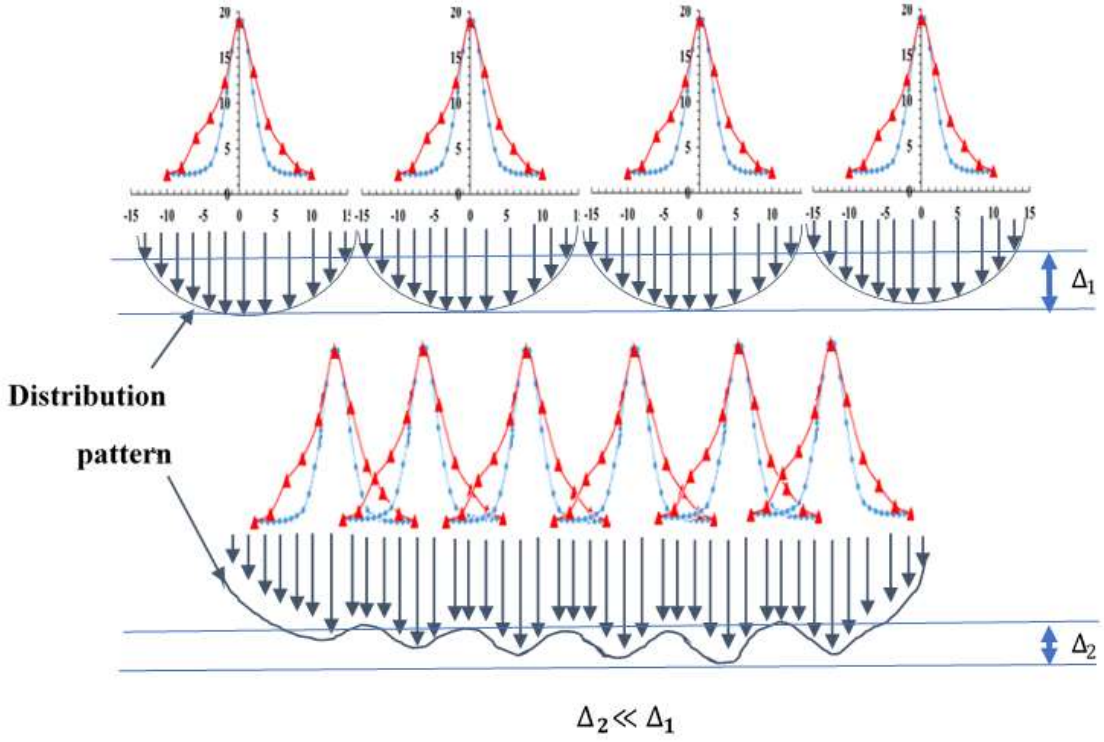

Figure 3-10: Overlapping for uniformity of spray

The next chapter of this thesis will discuss the different factors that can affect the drift losses and how these losses can be optimized along with the time of operation.

CHAPTER 4: OPTIMIZING A BI-OBJECTIVE MATHEMATICAL MODEL FOR MINIMIZING SPRAYING TIME AND DRIFT PROPORTION

The global agriculture sector faces many challenges in its mission to meet the increasing demand for food and fiber. Climate change, increasing population growth, emergence of crop diseases, damages to crops from rodents and critters, and shrinking farming land in some regions are among these challenges. Application of agrochemicals has proven to be an efficient answer to some of these challenges. However, the impacts of these products on human health and the environment combined with the increased requirement for sustainable farming requires the development of optimal spraying practices that would balance out all interests and concerns. In this study, a mathematical model is developed to jointly minimize spraying time and drift losses. The obtained bi-objective mixed integer nonlinear programming model is solved for a case study example published in the crop protection literature. Optimal solutions are obtained using the weighted sum method and the epsilon-constraint approach. The results showed that valid and reasonable solutions can be obtained by selecting the appropriate combination of boom height, nozzle spacing, nozzle type and tractor travel speed. Useful insights are obtained through various computational experiments.

4.1 INTRODUCTION

Sustainable agriculture aims at placing the agricultural inputs in such a way to reduce the environmental degradation along with optimizing the operational efficiency and reduce the cost of operation. According to the US Farm Bill (1990), “sustainable agriculture is an integrated system of plant and animal production practices having a site-specific

application that will, over the long term: (a) satisfy human food and fiber needs; (b) enhance environmental quality; (c) make efficient use of non-renewable resources and on-farm resources and integrate appropriate natural biological cycles and controls; (d) sustain the economic viability of farm operations; and (e) enhance the quality of life for farmers and society as a whole". In traditional farming, a blanket of treatment is applied throughout the field instead of treating only the problematic locations (Velten et al., 2015) without consideration for human health and contamination of the environment.

The increasing trend of applying agrochemicals in field crops is an integral part of advance agriculture. According to one study, in the United States, 3 million kg of agrochemicals costing 40 million US dollars are used annually (Al-Heidary et al., 2014; Pimentel, 2005). Agrochemicals can save 45% of the world food supply by protecting crops from different insects and pests (Oerke, 2006). On another hand, this heavy use of agrochemicals have increased the risk of air, soil and water pollution. During the application of these chemicals in the field, small spray particles move away from the intended areas (spray drift) and cause contamination (Huang et al., 2011). Almost 30% of agricultural chemicals are wasted due to off-target spray drift (Bahrouni et al., 2008; Miller and Butler, 2000). This off-target spray drift could create health issues for animals and humans, damage nearby sensitive crops, contaminate water sources and soils. However, Nuyttens et al., (2007a) noted that, reduction of the dosage of these chemicals may unfortunately reduce their effectiveness and could result in loss of money and chemicals. The increasing demand for food and fiber has forced farmers to apply agrochemicals. Therefore, spray drift became an important issue not only for public health but also for the scientific community. Spraying time is another important factor during the farm operation.

In the modern agriculture world, timely execution of farming operations is required to ensure the efficiency of the activities by reducing activity durations, energy (fuel) use, labour hired and overall cost (which is one pillar of sustainable agriculture) (MacRae et al., 1989).

There are several factors, which have direct influence on spray drift. These factors can be categorized into three major groups: 1. Sprayer related factors (boom height, driving speed, nozzle angle, nozzle pressure) 2. Weather conditions (temperature, humidity, wind velocity) 3. Crop conditions (crop type, crop height, crop stage) (Nuyttens et al., 2007a).

Different researchers studied the impact of these factors on spray drift individually. For example, Chao and Chengsheng, (2011); Teske and Thistle, (1999); De Jong et al., (2000); Iqbal et al., (2005) studied the impact of boom height on spray drift. These studies concluded that drift losses decreased by lowering the boom height. Drift losses can be decreased by 80% and 56% when the boom height is decreased from 70 cm to 30 cm and 50 cm to 30 cm respectively. Boom height has a significant impact on swath width (area covered by specific height and angle). Increasing the boom height increases the swath width and more area can be covered (which is good when crop canopy is fully developed) but on other hand if the height is too high then spray particle will be at more risk to move with wind and more drift losses will be expected (Iqbal et al., 2005).

The next important factor is tractor driving speed, which is directly linked with time of operation and has significant impact on spray drift (Taylor et al., 1989; Miller and Smith, 1997; Ghosh and Hunt, 1998; Al-Heidary et al., 2014; Nuyttens et al., 2007a; Taylor et al., 1989) conducted some experiments to see the impact of driving speed on spray drift and concluded that spray drift increased by 90 % when the tractor speed increased from 7.0

km/h to 10 km/h. Nozzle type and its pressure are also important factors regarding the spray drift (Heijne et al., 2002; Klein and Johnson, 2002; Al-Heidary et al., 2014)

Al-Heidary et al. (2014); Wolf and Caldwell (2001) studied the influence of wind velocity on spray drift and concluded that as the wind velocity increases the drift losses increased. It is also recommended not to spray the field if wind velocity is 2.77 m/s or above (Tobi et al., 2011). Temperature and humidity had their own significance in spray drift study. High temperature and low humidity will increase the risk of spray drift due to high evaporation. High temperature and high the humidity will cause the suspension of spray particles in the air which will also contribute towards air contamination (Al-Heidary et al., 2014). Crop type, crop height and crop stage are also important consideration in spray drift study. Most of the studies investigate the impact of these factors on an individual basis.

Many researchers worked on the importance of drift by considering the sprayer related, weather related and crop related factors (Al-Heidary et al., 2014; Chao and Chengsheng, 2011; Iqbal et al., 2005; Nuyttens et al., 2007b; Heijne et al., 2002 ; Klein and Johnson, 2002; De Jong et al.,2000; Teske and Thistle, 1999; Ghosh and Hunt, 1998; Miller and Smith, 1997) but very few studies dealt with spraying time. Spraying time is another important factor, which is directly linked with drift losses and cost of spraying operation. The producer has the primary responsibility to ensure that the crop they grow complies with the export regulatory guidelines. The timely application of agrochemicals can be a useful tool for farmers to apply the agrochemicals needed to maintain their crop.

Tobi et al. (2011) showed that farmers have no means to select efficient spraying speed. Their main goal is usually to finish as soon as possible given the labour and fuel costs. Thus, farmers usually opt for the highest speed possible without consideration for the fact that the selected speed could increase the hazardous effect of drift losses. Increased tractor speed will lead to the less spraying time but ultimately increases the drift. Drift losses increased by 51 % when the tractor speed increased from 4.0 to 8.0 km/h and 144% when tractor is operated at 16 km/h speed (Tobi et al., 2011). Therefore, there is a need for a trade-off between spraying time and drift.

4.2 PROBLEM DEFINITION

In this study, a bi-objective mathematical model is developed to find the optimal solution that minimizes both the spraying time and spraying drift proportion. Spraying time is affected by the tractor speed, the farm length and width, the boom length and the number of passes required. As covered in the literature review, multiple factors such as boom height, spray solution viscosity, spray angle, nozzle pressure, temperature and moisture content, evaporation affect the drift proportion (Al-Heidary et al., 2014). In this study, the following factors that affect spray drift will be considered: nozzle type, operating pressure, tractor speed, boom height, wind velocity, etc. This study deals with only these factors because these are the only ones for which drift proportion data was available from the field experiments ran by Nuyttens et al. (2007b). The proposed model can easily be extended to include all other factors enumerated by Al-Heidary et al. (2014), whenever full experimental data becomes available. It is also assumed that the factors considered in this study are independent and uncorrelated. This is reasonable as the data used to run the numerical experiments come from a field study that varied all these factors and corrected

for correlation (See Nuyttens et al., 2007b). Fig. 4-1 presents the drift causing factors along with the parameters that affect the spraying time. In general, drift amounts monotonously decrease as the measurement points get away from the point of application (Nuyttens et al., 2007a,b). Therefore, in this study all drift measurements are considered to be made at a reference point set to a predetermined distance from the end of the field. Minimizing the drift amounts at the reference point is equivalent to minimizing the drift amounts at any other point or minimizing the total drift amounts.

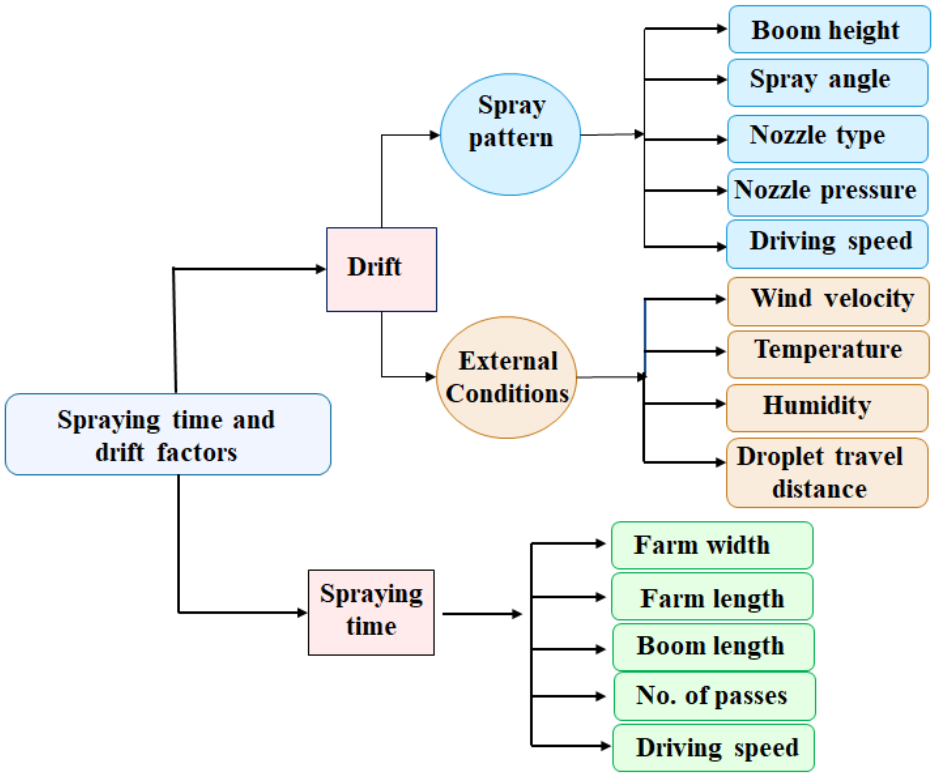

Figure 4-1: Drift causing factors and spraying speed parameters under consideration

The first objective function is the minimization of the spraying time. The second is the minimization of the spray drift proportion at a reference point. The optimization model aims at finding the best set up that will result in the best trade-offs between spraying time and drift generated.

This study focused on the development of a mathematical model which provides a trade-off between spraying time and drift so that farmers can select the optimal settings for different parameters to reduce the spraying time along with drift. Our goals are:

1. To develop a formula to calculate the spraying time by considering the farm width, farm length, boom length number of passes.
2. To develop the spray drift model by considering the external conditions and spray pattern related factors.
3. To build a model to determine spray settings that trades off the travel time and drift.

4.3 MODEL FORMULATION

4.3.1 Notation (Indices and Parameters)

The notation, (indices and parameters) used for the formulation of the bi-objective model are presented in nomenclature section of this thesis.

Decision Variables

$$X_i^S = \begin{cases} 1, & if\ tractor\ speed\ level\ i\ is\ selected \\ 0, & otherwise \end{cases}$$

$$X_j^H = \begin{cases} 1, & if\ boom\ height\ level\ j\ is\ selected \\ 0, & otherwise \end{cases}$$

$$X_n^N = \begin{cases} 1, & if\ nozzle\ type\ n\ is\ selected \\ 0, & otherwise \end{cases}$$

$$X_o^\theta = \begin{cases} 1, & if\ \text{spraying angle level}\ o\ is\ selected \\ 0, & otherwise \end{cases}$$

$$X_k^P = \begin{cases} 1, & if\ pressure\ level\ k\ is\ selected \\ 0, & otherwise \end{cases}$$

A= Nozzle spacing (multiples of attachment spacing: $\boldsymbol{A = m \times l}$ where $\boldsymbol{m = 1, 2, ...}$)

$\boldsymbol{\theta}$ = Selected spray angle in degrees (°) ($\theta = \sum_o \theta_o X_o^\theta$)

O_v= Overlapping of nozzle sheets volume (m) calculated as a function of A, H_j and θ .

4.3.2 Formulation of the spraying time

A field with a surface area of W_F x L_F (m^2) is considered as pictured in Fig. 4-2. A spraying tractor moves at a constant speed along the length (longest side) of the farm. The tractor is assumed to turn in semicircles when it reaches one end of the field to switch direction and start spraying in opposite direction without a gap in spray coverage as illustrated on Fig. 4-2.

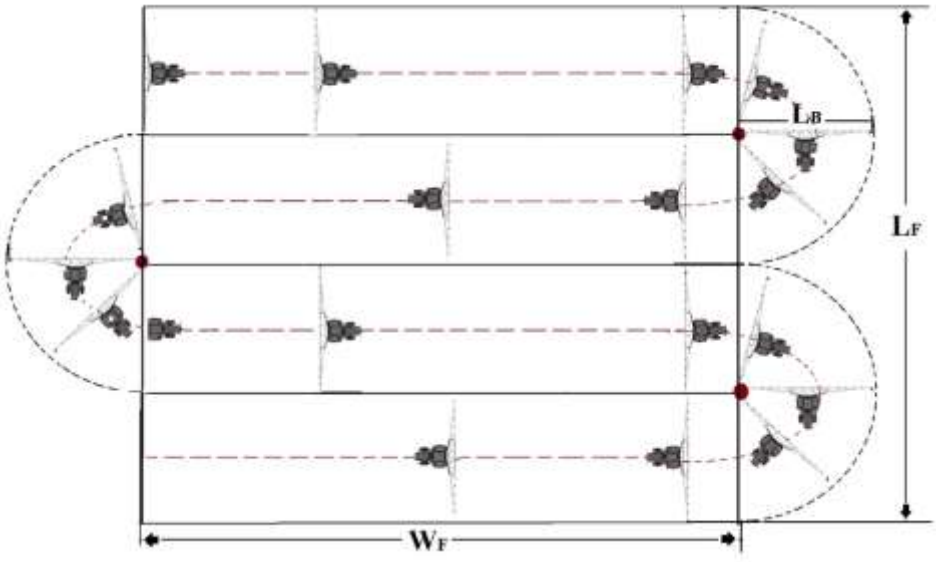

Figure 4-2: Field layout and driving directions of tractor during spraying operation (Example with 4 passes and 3 half rotations).

The total distance D traveled by the tractor is given by:

$$D = c \cdot W_F + (c-1)\pi \cdot \frac{L_B}{2} \tag{4.1}$$

For c direction changes (passes), there are (c-1) half circles to change direction. Distances traveled to and from the beginning or end of the field are not included in the optimization model.

The total spraying time is then obtained by dividing the total distance by the tractor speed S.

$$T_s = \frac{2cW_F+(c-1)\pi L_B}{2S} \tag{4.2}$$

where S is given by the selected speed level $S = \sum_i S_i X_i^S$.

4.3.3 Formulation of the drift proportion

The assessment of drift is divided into two parts based on the involved factors according to Fig. 4-1: External conditions (weather factors) and Operational aspects (Sprayer related factors).

4.3.3.1 External conditions

Humidity, temperature, wind velocity and distance (travel distance of droplets from the outer nozzle) were considered as weather related factors. All these factors are considered as independent and non-correlated and combined in a single formula by Nuyttens et al., (2007b) which constitutes a baseline drift (D_B) given by

$$D_B = d_d^{-1.05}(13.00 + 0.5V_{3.25\text{m}} + 0.4T - 1.74\,\zeta_{H_2O}) \tag{4.3}$$

where:

D_B = Fraction of applied spray which is lost during spraying and/or after

application

d_d = Distance travelled by the spray particles in wind direction (m) (1m, in our study)

$V_{3.25m}$ = Average wind velocity at height of 3.25 m above the ground level (m/s)

T = Average air temperature (°C)

ζ_{H_2O} = Absolute humidity (weight of water vapours in grams per kg of dry air).

4.3.3.2 Operational or spray related factors

The second component of the drift formulation relates to the drift proportion incurred by each of the spray related factors under consideration: speed of tractor (S_i), height of boom (H_j), nozzle pressure (P_k), and nozzle type (N_n). Using the field experiments carried out by Nuyttens et al., (2007b), a drift proportion value (Δ_u^F) is measured for each level u of each factor F. Illustrative examples of Δ_u^F are given in Table 4-1.

Thus, the total specific drift proportion (D_S) due to the four operating factors under consideration are given by:

$$D_S = \sum_n \Delta_n^N X_n^N + \sum_k \Delta_k^P X_k^P + \sum_i \Delta_i^S X_i^S + \sum_j \Delta_j^H X_j^H \quad (4.4)$$

4.3.3.3 Total Drift Formulation

The total drift (T_d) is obtained as the sum of the baseline drift and specific drift.

$$T_d = D_B + D_B \times D_S$$

$$T_d = D_B(1+\sum_n \Delta_n^N X_n^N + \sum_k \Delta_k^P X_k^P + \sum_i \Delta_i^S X_i^S + \sum_j \Delta_j^H X_j^H) \quad (4.5)$$

For a given spraying application in the field, it is assumed that the external factors do not change during the application and therefore the calculated baseline drift does not

change (remains constant), therefore this term will be dropped from the optimization model and only the specific drift proportion (DS) will be optimized. The following subsection deals with the constraints that are included in the formulation.

Table 4-1: Relative drift proportion values for each level and each factor. Values are relative to the minimum value obtained by Nuyttens et al. (2017b).

Nozzle pressure			**Height of boom**		
k	**P_k (bars)**	**Δ_k^P (%)**	***j***	**H_j (m)**	**Δ_j^H (%)**
1	$P_1 = 2$	0	1	$H_1 = 0.3$	0
2	$P_2 = 3$	3.5	2	$H_2 = 0.5$	3
3	$P_3 = 4$	6.5	3	$H_3 = 0.75$	8
Speed of tractor			**Nozzle type**		
i	**S_i (km/h)**	**Δ_i^S (%)**	***n***	**N_n**	**Δ_n^N (%)**
1	$S_1 = 4$	0.6	1	N_1 = F110 04	18.5
2	$S_2 = 6$	0	2	N_2 = F110 06	4
3	$S_3 = 8$	2.7	3	N_3 = F110 03	1.5
4	$S_4 = 10$	2.1	4	N_4 = F110 02	2
			5	N_5 = LD110 02	6.5
			6	N_6 = LD110 03	3.5
			7	N_7 = LD110 04	0

4.3.4 Constraints: levels selection, nozzle spacing and Spray sheet overlapping

Of all the speed levels available, only one has to be selected for a given spray application, therefore, the following constraint is added to the formulation:

$$\sum_i X_i^S = 1 \tag{4.6}$$

Similarly, one and only one level has to be chosen for the nozzle type, the nozzle pressure, the boom height, and the spray angle. Thus, the following other constraints are obtained.

$$\sum_n X_n^N = 1 \tag{4.7}$$

$$\sum_k X_k^P = 1 \tag{4.8}$$

$$\sum_j X_j^H = 1 \tag{4.9}$$

$$\sum_o X_o^\theta = 1 \tag{4.10}$$

Uniform application of agrochemicals is an important quality requirement for spraying systems. Overlapping of spray sheets has significant impact on the uniformity of the spray applied to the crop canopy. Furthermore, nozzles spacing can be selected to control spray overlap depending on boom height. On a typical boom, there are by design locations where nozzles can be attached. For example, the operator can attach nozzles at each location (m = 1) or skip one location (m = 2) depending on the desired spacing $A = m \times l$. The constraint then is to select at least one location for the nozzle:

$$m \geq 1 \tag{4.11}$$

Once the nozzle spacing, spray angle and boom height are set, the spray sheet overlap can be calculated using the formulas developed below and based on the relationships depicted in Figure 4-3.

For a single nozzle (Fig 4-3a.), the half swath width (b) is given by:

$$b = (H - h)\tan\left(\frac{\theta}{2}\right)$$

where $\theta = \sum_o \theta_o X_o^\theta$ and $H = \sum_j \Delta_j^H X_j^H$.

The overlap between two consecutive spray sheets (Fig. 4-3b) is given by:

$$O_v = 2b - A$$

$$O_v = 2(H - h)\tan\left(\frac{\theta}{2}\right) - A \tag{4.12}$$

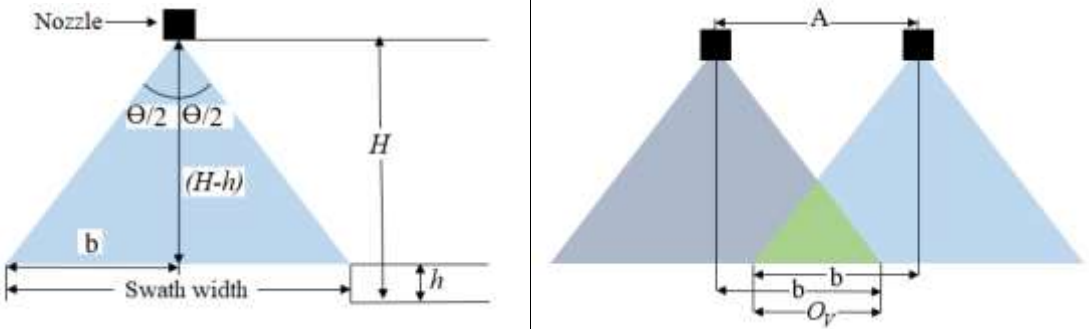

(3a) (3b)

Figure 4-3: Swath width and spray sheet overlap between consecutive nozzles

The overlap constraint, which is given as follows, ensures that the achieved overlap is between the minimum and maximum overlapping values set by the farmer or any other subject matter expert.

$$O_{min} \leq O_v \leq O_{max} \tag{4.13}$$

4.3.5 Bi-objective mathematical model

The goal of the mathematical model developed in this study is to investigate the trade-offs between the two-objective functions: spraying time (T_s called objective Z_1) and the specific drift proportion (D_s called objective Z_2). The full mathematical formulation is given below.

$$\text{Minimize } Z_1 = \frac{2\mathrm{k}\,\mathrm{W}_F + (\mathrm{k}-1)\pi\,\mathrm{L}_B}{2\mathrm{S}} \tag{4.14}$$

$$\text{Minimize } Z_2 = \sum_n \Delta_n^N \mathrm{N}_n + \sum_k \Delta_k^P \mathrm{P}_k + \sum_n \Delta_i^S \mathrm{S}_i + \sum_j \Delta_j^H \mathrm{H}_j \tag{4.15}$$

Subject to:

$$\sum_i X_i^S = 1 \tag{4.16}$$

$$\sum_n X_n^N = 1 \tag{4.17}$$

$$\sum_k X_k^P = 1 \tag{4.18}$$

$$\sum_j X_j^H = 1 \tag{4.19}$$

$$\sum_o X_o^\theta = 1 \tag{4.20}$$

$$m \geq 1 \tag{4.21}$$

$$O_{min} \leq O_v \leq O_{max} \tag{4.22}$$

$$X_i^S, X_n^N, X_k^P, X_j^H, X_o^\theta \in \{0,1\} \ and \ \ m \geq 0 \tag{4.23}$$

Constraint (4.23) states the binary variables and required *m* to be non-negative. The obtained formulation is a bi-objective mixed integer nonlinear programming model. The following section will present the approaches used to solve the mathematical model.

4.4 SOLUTION APPROACHES

Both objective functions have different units: spraying time Z_1 is in hours (h) while drift proportion Z_2 is measured in percentage (%). To solve this kind of models, several approaches are available in the literature (See Hwang and Masud, 1979; Ghayebloo et al., 2015). Here, we will use the weighted sums method and the Ɛ-constraint (epsilon-constraint) method as done by Ghayebloo et al., (2015).

4.4.1 Weighted sum method

The weighted sums method combines both objective functions into a single function by assigning appropriate weights to each objective depending on the preference of the decision maker. Equation (4.24) shows the weighted sum formulation for our problem. The single objective function is normalized to 1 by dividing each objective function by its minimum possible value (Z_{1min} and Z_{2min}).

$$\text{Minimize } Z = w\frac{Z_1}{Z_{1min}} + (1-w)\frac{Z_2}{Z_{2min}} \tag{4.24}$$

s.t.:

Equations (4.16) – (4.23).

4.4.2 Ɛ-constraint method

In this method, the multi-objective (bi-objective in our case) optimization problem is converted into single or mono objective optimization problem by retaining the objective function with highest priority (or preference) as the sole objective function and the other objective functions are rewritten and incorporated as constraints in the formulation. In this study, drift reduction is considered as the most important objective function and is retained as the sole objective function while spraying time is constrained to be less than or equal to a specific value ε ($Z_1 \leq \varepsilon$). The ε -constraint formulation for our problem is shown below.

$$\text{Minimize } Z = Z_2 \tag{4.25}$$

s.t.:

Equations (4.16) – (4.23).

$Z_1 \leq \varepsilon$

4.5 NUMERICAL EXPERIMENTS AND DISCUSSIONS

In this section, a series of numerical experiments using parameter values from the field study conducted by Nuyttens et al., (2007b) was run and discussed to demonstrate the validity and applicability of the proposed mathematical model. Managerial insights will also be drawn to guide decision making by farmers and stakeholders. All experiments were run on an Intel™i5 3.4GHz desktop computer with 16GB of RAM running Windows 7™. The model is programmed in the optimization software MPL 5.0 (Maximal Software) and solved using the nonlinear solver LINGO Release 9.0 (Lin and Schrage, 2009).

4.5.1 Experiment 1: Effects of minimum overlap in the weighted sums method:

In this experiment, 7 different nozzle types (N_n), 3 different nozzle pressures (P_k), 4 different tractor driving speeds levels (S_i), 3 different boom height levels (H_j) are used. The nozzle spacing was constant at l = 0.508m while W_F = 0.4km, L_F = 0.9km and L_B= 0.02km, h= 0.01m. Table 4-2 shows the results obtained for three values of the minimum overlap: 0, 0.40 and 0.95m. The results are obtained by varying the values of the weight (w) from 0 to 1. When w=0 then spraying time is not important and only drift reduction matters. Conversely when w=1, then only minimizing spraying time matters. Intermediate values of w represent the preference expressed by the farmer or decision-maker between spraying time and drift reduction.

Weighted sum results for 0m overlapping (Case 1)

When w = 1, all the weight is given to spraying time and the value of the normalized objective function is 1. The optimal solution is then to set m = 1 (one nozzle at each position), use a flat fan nozzle F110 02 at a pressure of 2 bars with a boom height of 0.30 m and a tractor speed of 10 km/h, which will result in a spraying time of 1.32 h. Recall that

when w = 1, drift reduction is not considered. These settings yield the fastest spraying in this study. This spray setting is very useful for row crops in their early stage when plants typically grow at a specific distance with no to little canopy. This setting is useful when applying the spray only on specific rows with less overlapping. This setting is useful only to finish the spraying operation very quickly or when the row distance equals the nozzle spacing. The boom height (0.3 m) will remain the same throughout this case due to less overlapping. It should be noted that running a 30 cm boom height at 10 km/h is only feasible for a relatively flat land as was the case for the experiments that generated the dataset being used here. On rougher terrain, the boom height will be raised from the optimal value to the nearest operationally viable height. Ideally, a dataset should be obtained for each type of terrain. Furthermore, it should be noted that any nozzle type other than F110 02 would work because drift reduction has a weight of 0. The result displayed in Table 4-2 is the first one that the mathematical model finds and reports. Other nozzle types are found on subsequent runs of the model and yield the same value of the objective function.

When the value of *w* is reduced to 0.9, the model suggests using a tractor speed of 6 km/h and nozzle LD 110 04 while maintain the other parameters as before. As soon as drift reduction comes into play, the model reduces the traveling speed and uses a low drift nozzle to reduce drift. The same solution is obtained for the remaining values of *w* in Table 4-2. The model suggests that drift reduction is considered then there is a need to reduce tractor speed and to choose an appropriate nozzle.

Weighted sum results for 0.4m overlapping (Case 2)

In this case, the minimum overlap between spray sheets is increased from 0 to 0.40m. Now changing the constraints of overlapping from 0 to 0.4m. At *w*=1, the optimal solution

is: nozzle spacing of 0.508m, nozzle type LD 110.04, pressure of 2 bars, tractor speed of 10 km/h and boom height of 0.50m. As expected, the boom height is increased to account for the need for more overlap. The switch from a 10km/h to 6km/h tractor speed occurs when w=0.5 instead of 0.9 in Case 1. Raising the boom higher generates more drift than the change in speed so the model waits for the spraying time to be less important before reducing the speed to 6km/h.

In this second case, the model also suggests the same nozzle type (LD110.04) for all values of w. The reason for this result is that the increase in drift due to the increased boom height is substantial, therefore the model suggests the nozzle with the lowest drift: LD110.04.

Weighted sum results for 0.95m overlapping (Case 3)

In this case, the minimum overlap between spray sheets is increased from 0.4 to 0.95m. To achieve the required minimum overlap, the model suggests raising the spraying boom to its highest position (0.75m). All other settings remain the same as in Case 2. The switch from a 10km/h to 6km/h tractor speed occurs when w=0.4 instead of 0.5 in Case 2. Increasing boom height will lead to the higher overlapping and increase the spray uniformity. This is useful when crop canopy is fully-grown and covers the whole farm field. The spray sheet has maximum volume and velocity in its central part (Nadeem et al., 2018). Therefore, higher overlap may be needed for uniform application.

Table 4-2: Results of the weighted sums method for minimum overlapping of 0, 0.4 and 0.95m.

Case # 1: 0m minimum overlap											
w	0	0.1	0.2	0.3	0.4	0.5	0.6	0.7	0.8	0.9	1
Z	1.00	1.07	1.13	1.20	1.27	1.33	1.40	1.47	1.53	1.60	1.00
T_S	2.20	2.20	2.20	2.20	2.20	2.20	2.20	2.20	2.20	2.20	1.32
H	0.3	0.3	0.3	0.3	0.3	0.3	0.3	0.3	0.3	0.3	0.3
O_V	0.349	0.349	0.349	0.349	0.349	0.349	0.349	0.349	0.349	0.349	0.349
A	50.8	50.8	50.8	50.8	50.8	50.8	50.8	50.8	50.8	50.8	50.8
n	LD110.04	LD110.04	LD110.04	LD110.04	LD110.04	LD110.04	LD110.04	LD110.04	LD110.04	LD110.04	**F110.02**
P	2	2	2	2	2	2	2	2	2	2	2
s	6	6	6	6	6	6	6	6	6	6	**10**
Case # 2: 0.40m minimum overlap											
w	0	0.1	0.2	0.3	0.4	0.5	0.6	0.7	0.8	0.9	1
Z	1	1.07	1.13	1.20	1.27	1.33	1.28	1.21	1.14	1.07	1
T_S	2.20	2.20	2.20	2.20	2.20	2.20	1.32	1.32	1.32	1.32	1.32
H	0.5	0.5	0.5	0.5	0.5	0.5	0.5	0.5	0.5	0.5	0.5
O_V	0.9201	0.9201	0.9201	0.9201	0.9201	0.9201	0.9201	0.9201	0.9201	0.9201	0.9201
A	50.8	50.8	50.8	50.8	50.8	50.8	50.8	50.8	50.8	50.8	50.8
n	LD110.04	LD110.04	LD110.04	LD110.04	LD110.04	LD110.04	LD110.04	LD110.04	LD110.04	LD110.04	LD110.04
P	2	2	2	2	2	2	2	2	2	2	2
s	6	6	6	6	6	6	**10**	**10**	**10**	**10**	**10**
Case # 3: 0.95m minimum overlap											
w	0	0.1	0.2	0.3	0.4	0.5	0.6	0.7	0.8	0.9	1
Z	1	1.07	1.13	1.20	1.16	1.13	1.11	1.08	1.05	1.03	1
T_S	2.20	2.20	2.20	2.20	1.32	1.32	1.32	1.32	1.32	1.32	1.32
H	0.75	0.75	0.75	0.75	0.75	0.75	0.75	0.75	0.75	0.75	0.75
O_V	1.63	1.63	1.63	1.63	1.63	1.63	1.63	1.63	1.63	1.63	1.63
A	50.8	50.8	50.8	50.8	50.8	50.8	50.8	50.8	50.8	50.8	50.8
n	LD110.04	LD110.04	LD110.04	LD110.04	LD110.04	LD110.04	LD110.04	LD110.04	LD110.04	LD110.04	LD110.04
P	2	2	2	2	2	2	2	2	2	2	2
s	6	6	6	6	6	**10**	**10**	**10**	**10**	**10**	**10**

w = weight, *Z*= Normalized objective function, T_S= spraying/travel time (h), A= Nozzle Spacing (m), *H* = Boom height (m), O_V=Overlap (m), n = Nozzle Type, *P*= Nozzle Pressure (bars), s= Speed (km/h).

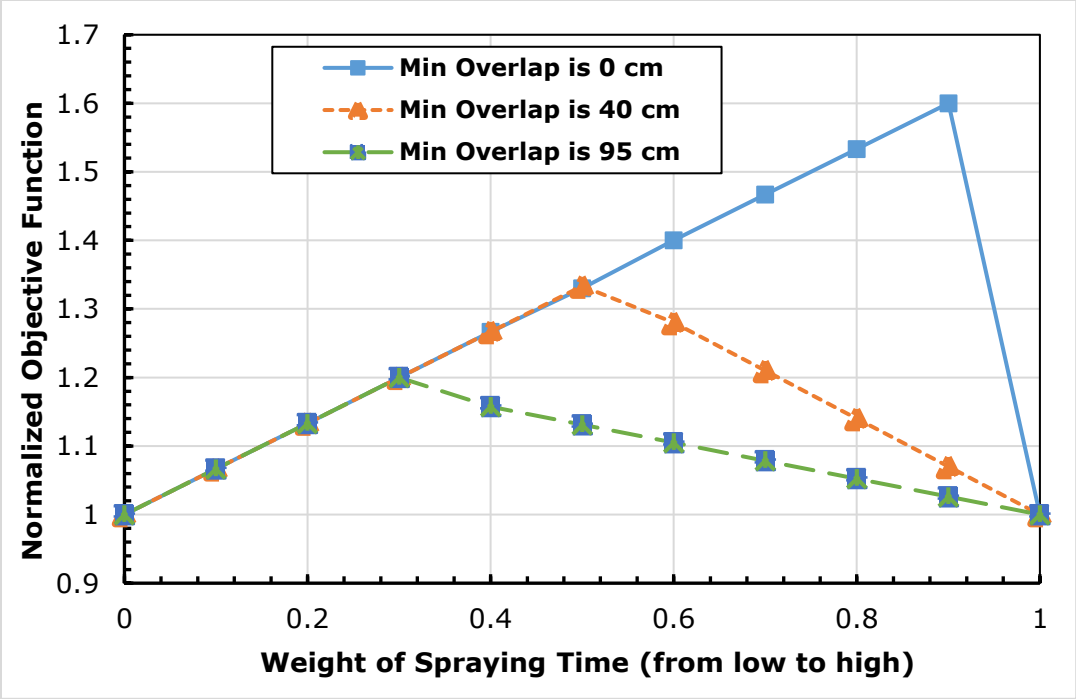

Figure 4-4: Sensitivity analysis on the weights of objective function

Figure 4-4 shows a sensitivity analysis of the weight used in the normalized objective function. For low weight values (i.e. spraying time is less valuable), the normalized objective function is similar for all three minimum overlapping values. For high weight values (i.e. spraying time is more valuable), the normalized objective function is lowest for the highest minimum overlap. Across all weight values, the normalized objective function is lowest for the highest minimum overlap meaning that this is the setting that gives the best trade-off between speed and drift regardless of the decision-maker's preferences.

In the experiments above, the model almost exclusively selected the low drift nozzle LD110.04 yielding results with low variability in the spray settings. In the following experiment, the three low drift nozzles are removed from the data and only the seven standard flat fan nozzles F80.02, F80.03, F80.04, F80.06, F65.03, F65.04, and

F65.06 are added to the existing four 110 degree flat fan nozzles. Using the observations from Al-Heidary et al. (2014) that drift losses were reduced by factors of 2 and 5 when going from 110 degrees spray nozzle to 80 and 65 degrees nozzles, respectively, we estimated the drift proportions for the new nozzles based on the values available for the 110 nozzles. The corresponding drift proportions are given in Table 4-3. Furthermore, linear interpolation is used to find the drift proportions for boom heights at 35, 45, 55 and 65 centimeters. The results obtained are displayed in Table 4-4 for minimum overlap values of 0, 0.1 and 0.4 meters and l=10cm.

Table 4-3: Relative drift proportion values

Nozzle type			Height of boom		
n	N_n	Δ_n^N (%)	j	H_j (m)	Δ_j^H (%)
1	N_1= F110 04	18	1	H_1= 0.30	0.0
2	N_2= F110 06	3.5	2	H_2= 0.35	0.8
3	N_3= F110 03	1.0	3	H_3=0.40	1.5
4	N_4= F110 02	1.5	4	H_4=0.45	2.3
5	N_5= F80 04	8.5	5	H_5=0.50	3.0
6	N_6= F80 06	1.5	6	H_6=0.55	4.0
7	N_7= F80 03	0.3	7	H_7=0.60	5.0
8	N_8= F80 02	0.5	8	H_8=0.65	6.5
9	N_9= F65 04	3.5	9	H_9=0.75	8.0
10	N_{10}= F65 06	0.5			
11	N_{11}= F65 03	0.0			

Table 4-4: Results of the weighted sums method for minimum overlapping of 0, 0.1, 0.4m.

Case # 4: 0m minimum overlap						
w	0	0.2	0.4	0.6	0.8	1
Z	1.00	1.13	1.27	1.40	1.53	1.00
T_S	2.20	2.20	2.20	2.20	2.20	1.32
H	0.30	0.30	0.30	0.30	0.30	**0.35**
O_V	0.055	0.055	0.055	0.055	0.055	**0.02**
A	0.1	0.1	0.1	0.1	0.1	**0.4**
n	F65.03	F65.03	F65.03	F65.03	F65.03	**F110.04**
s	6	6	6	6	6	**10**
Case # 5: 0.1m minimum overlap						
w	0	0.2	0.4	0.6	0.8	1
Z	1	1.13	1.27	1.4	1.53	1
T_S	2.202	2.202	2.202	2.202	2.202	**1.3212**
H	0.3	0.3	0.3	0.3	0.3	**0.75**
O_V	0.136	0.136	0.136	0.136	0.136	**0.157**
A	0.2	0.2	0.2	0.2	0.2	**1.7**
n	F80.03	F80.03	F80.03	F80.03	F80.03	**F110.04**
s	6	6	6	6	6	**10**
Case # 6: 0.4m minimum overlap						
w	0	0.2	0.4	0.6	0.8	1
Z	1.00	1.13	1.27	1.28	1.14	1.00
T_S	2.202	2.202	2.202	1.321	1.321	**1.321**
H	0.5	0.5	0.5	0.5	0.5	**0.75**
O_V	0.5	0.5	0.5	0.5	0.5	**0.86**
A	0.5	0.5	0.5	0.5	0.5	**1**
n	F110.03	F110.03	F110.03	F110.03	F110.03	**F110.04**
s	6	6	6	**10**	**10**	**10**

w = weight, *Z*= Normalized objective function, T_S= spraying/travel time (h), A= Nozzle Spacing (m), *H* = Boom height (m), O_V=Overlap (m), n = Nozzle Type, s= Speed (km/h)

The results in Table 4-4, show how the model moves from flat fan nozzle with the smallest top spray angle (65°) (Fig. 4-5) when there is no overlap required to the medium spray angle (80°) (Fig. 4-6) and finally to the highest spray angle (110°) (Fig. 4-7) when high overlap is required. Similar behavior is seen with the boom height. Trade-offs between speed and drift minimization appear in Case #6 at *w*=0.6.

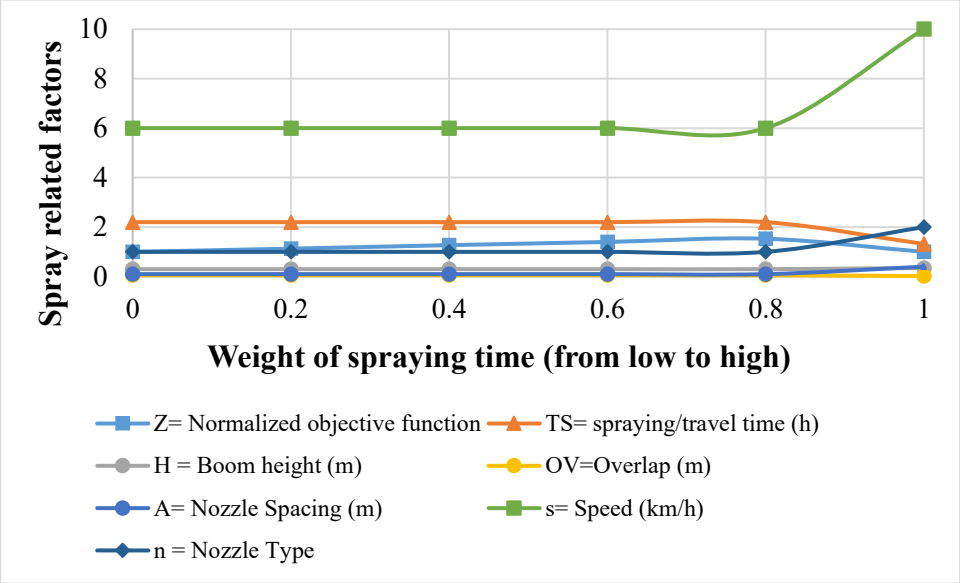

Figure 4-5: Weighted sum results of 0m minimum overlap

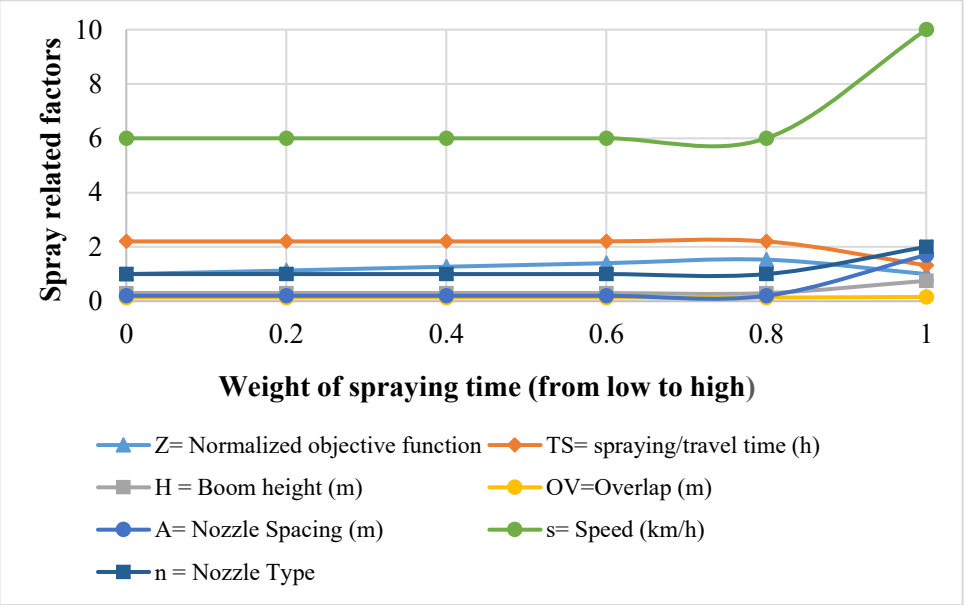

Figure 4-6: Weighted sum results of 0.1 m minimum overlap

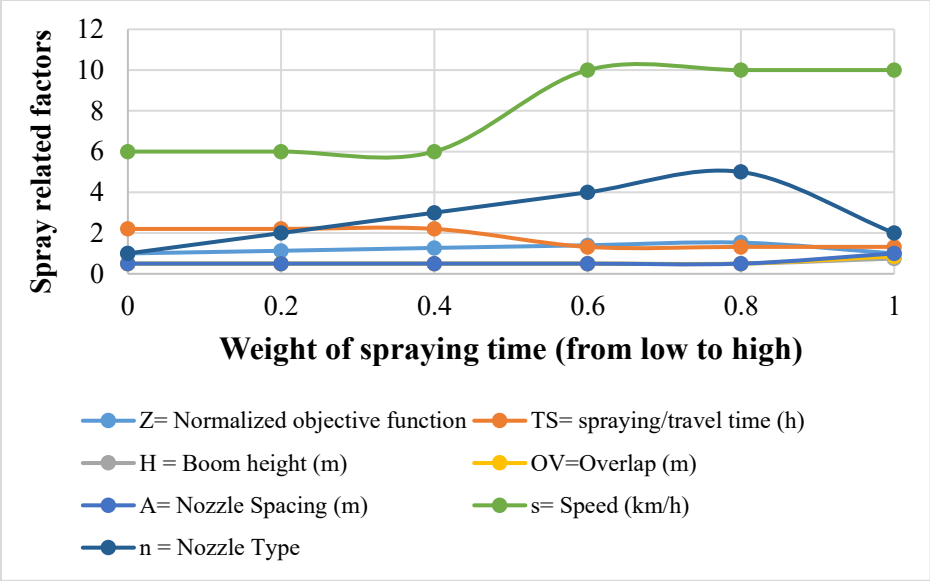

Figure 4-7: Weighted sum results of 0.4 m minimum overlap

4.5.2 Trade-off between drift reduction and spraying time using the ε-constraint method

In the epsilon constraint model, drift minimization is retained as the sole objective function and spraying time is constrained to be less than or equal to a specific value ε ($Z_1 \leq \varepsilon$). Table 4-5 presents the results obtained with the epsilon-constraint method with the dataset with 7 nozzles used at the beginning of Section 4.1 above and for three values of ε: 1, 2, 3 hours.

The maximum speed available is 10 km/h which allows to spray the farm in 1.32 hours. Thus, the model is infeasible when $\varepsilon = 1$. When the spraying time is constrained to be equal or less than 2 hours, the speed of 10 km/h is chosen with boom heights of 0.3m and 0.5m for minimum overlaps of 0 and 0.4 m respectively. When $\varepsilon = 3$, the travel speed is reduced to 6 km/h which yields the lowest drift proportion values.

Table 4-5: Results obtained with the Ɛ-constraint method.

	Ov_{min}=0.0m			Ov_{min}=0.4m		
Epsilon (hours)	**3.0**	**2.0**	**1.0**	**3.0**	**2.0**	**1.0**
Z_2	0.00	2.1	Infeasible	3.00	5.1	Infeasible
T_S	2.20	1.32		2.20	1.32	
H	0.30	0.30		0.50	0.50	
O_V	0.35	0.35		0.92	0.92	
A	0.508	0.508		0.508	0.508	
n	LD110.04	LD110.04		LD110.04	LD110.04	
P	2	2		2	2	
s	6	10		6	10	

Z_2= Normalized objective function, T_S= spraying/travel time (h), A= Nozzle Spacing (m), H = Boom height (m), O_V= Overlap (m), n = Nozzle Type, P= Nozzle Pressure (psi), s= Speed (km/h)

The parameters used in our numerical experiments are extracted from the field study conducted by Nuyttens et al., (2007b). Unfortunately, their field experiments were conducted with a very small number of settings for each factor considered in our study. Thus, the number of combinations of settings that the mathematical model can choose from is very limited resulting in low variation between solutions. All nozzles used had the same spray angle of 110 degrees, which did not allow for the model to change.

4.6 CONCLUSIONS

In this section of research, a mathematical model was developed to select settings for spraying operations with the dual goal of jointly minimizing spraying time and drift proportions. The obtained bi-objective mixed integer nonlinear programming model was solved for a case study example published in the crop protection literature. Optimal solutions were obtained using the weighted sums method and the epsilon-constraint approach. The results showed that valid and reasonable solution can be obtained by selecting the appropriate combination of boom height, nozzle spacing, nozzle type,

operating pressure and tractor travel speed. The mathematical model developed in this study could be extended to include more factors such as evaporation, spray run-offs and integrated into a mobile phone app to assist farmers into in selecting the settings for their spraying operations.

The current mathematical model does not consider any specific crop and other drift factors such as evaporation and droplet sizes. Future research initiatives should target the integration of these factors. It would also be useful to conduct extensive field experiments with the goal of obtaining more granular data to feed into the bi-objective model. Furthermore, the recent developments in the field of numerical simulation of drift losses can be leveraged to build joint simulation-optimization models to help farmers and decision makers in the selection of their spraying parameters.

CHAPTER 5: CONCLUSIONS AND FUTURE PERSPECTIVES

This dissertation is a thematic investigation of how spraying nozzle design and the configuration of the spraying apparatus can contribute to the reduction of spray losses in the context of sustainable agriculture.

5.1 Theme 1: Water quantification: PIV vs Imaging Processing Technique

Theme 1, in Chapter 2 of this thesis, investigated different water quantification methods for a flat fan nozzle. This study concluded that the PIV technique is an appropriate method for water quantification without intrusion. Most contact-based methods use in-contact instrument for water quantification, which interferes with the spray sheet and may affect its flow measurement. Validation of this PIV water quantification method with the manual method also strengthened this research methodology to extend in the field of precision irrigation (sprinkler irrigation, drip irrigation, central pivot irrigation systems) and fire sprinklers. The PIV system also provided insight about the velocity behavior of the sprayer nozzle flow: the field of velocity showed a uniform and symmetrical distribution on the entire spraying area.

Further improvements can be made in image processing system to reduce the absolute error while comparing the results of PIV and image processing systems, both for volume and velocity measurements. PIV system had a good potential to measure the velocity of nozzle flow for many complex nozzles where the physical velocity calculations are difficult. The volume and velocity measuring methods in this study could be used for drip and sprinkler irrigation systems to improve the irrigation efficiency. This study was designed to evaluate the conventional flat fan nozzle, used for applying agrochemicals in agriculture. The same study could be extended for other types of nozzles (hollow cone,

full cone, raindrop and air induction nozzles) used for applying agrochemicals and for the nozzles used in food industry for applying protective coating to improve their efficacy.

5.2 Theme 2: contribution to spraying nozzle study: a comparative investigation of imaging and simulation approaches

Under Theme 2, the research carried out under Theme 1 was further extended to study the velocity profile of the spray sheet under the nozzle in Chapter 3. This research step provided interesting results. It showed that the tip velocity of the sprayer nozzle changes with the change in operating pressure. As the operating pressure increases, the tip velocity of the nozzle increases. Increasing pressure does not mean that all the particles have uniform velocity distribution. For this purpose, the study was extended to investigate the velocity of the spray sheet not only at the tip of nozzle but also under the tip of nozzle at different locations using the ANSYS 16 simulation approach and PIV as an experimental approach. The results showed that the spray sheet had maximum velocity at its center. The particles present in the central region of spray sheet will have maximum kinetic energy and that region has the maximum probability to hit the right target. The spray particles present in the surroundings of the central part had less velocity that would lead to minimum kinetic energy. This part of spray would be the more sensitive part. There are maximum chances of off-target drift only on these parts. Due to low kinetic energy, these particles can move away from the targets surfaces easily even with very low wind velocity. The results showed that both PIV and mathematical modeling approaches are appropriate tools for the velocity profiling of flat fan nozzles and can be considered as reliable and cost-effective research methods for studying complex nozzle flows. There was substantial difference between PIV and ANSYS velocity at the tip of nozzle. The high turbulence flow could be the

potential reason for this difference. The overall results of this study showed that the edges of spray sheet and spray away from the tip of nozzle had low velocity and these parts are at high risk for drift. Spray from these parts have maximum probability to move away from the target. This off-target spray could cause soil and water contamination. To reduce this off-target spray, there is a need of comprehensive research on spray drift to consider all other possible factors, which can influence the spray drift.

The results of this study could be very useful for the uniform application of edible coating on fruits (an emerging food science topic) (Andrade et al., 2012) uniform protective coating for meat (Spraying system, 2013) fire sprinkler (Husted et al., 2009), sprinkler and drip irrigation (Yunkai et al., 2008) and to study the behaviour of nozzle injectors (Vimal and Gupta, 2015).

5.3 Theme 3: A bi-objective mathematical model to jointly minimize spraying time and drift losses

After the velocity profiling study, this dissertation dealt with the development of a mathematical model to reduce the drift losses and time of operation under Theme 3. A mathematical model was developed to select settings for spraying operations with the goal of jointly minimizing both spraying time and drift proportions. The obtained bi-objective mixed integer nonlinear programming model was solved for a case study example published in the crop protection literature. Optimal solutions were obtained using the weighted sum method and the epsilon-constraint approach. The results showed that valid, reasonable and sustainable spraying operations can be achieved by choosing the appropriate combination of boom height, nozzle spacing, nozzle type, operating pressure and tractor travel speed. The mathematical model developed in this study could be

expanded to include more factors such as evaporation, spraying flows and be integrated within a mobile phone application to help farmers select the parameters of their spraying operations. The current mathematical model does not consider any specific crop or other drifting factors such as evaporation and droplet size. Future research initiatives should target the integration of these factors. It would also be useful to conduct extensive field experiments in order to obtain more detailed data to feed the model with two objectives. In addition, recent developments in drift loss simulation can be used to create joint simulation optimization models to help farmers and decision-makers choose their spray parameters.

The results of this study highlighted the factors involved in the drift and spraying of operation and emphasized the development of commercial techniques to reduce the drift proportion and spraying time. A software package or mobile app could be developed with a user-friendly interface that will allow farmers to select the most appropriate setup/configuration parameters by inputting their preference levels between spraying time and drift losses. This software will allow the farmers to evaluate the trade-off between these factors.

REFERENCES

Adrian, R. J. 2005. Twenty years of particle image velocimetry. *Exp in Fluids.* 39(2), 159-169.

Albadawi, A., Donoghue, D. B., & Robinson, A. J. 2013. Influence of surface tension implementation in volume of fluid and coupled volume of fluid with level set methods for bubble growth and detachment. *Int. J. Multiphase Flow.* 53, 11-28.

Al-Heidary, M., Douzals, J. P., Sinfort, C., & Vallet , A. 2014. Influence of spray characteristics on potential spray drift of field crop sprayers: A literature review. *Crop Prot. 63,* 120-130.

Altimira, M., Rivas, A., Larraona, G. S. & Anton, R. 2009. Characteristics of fan spray atomizers through numerical simulation. *Int. J. Heat Fluid Flow.* 30, 339-335.

American Society of Agricultural and Biological Engineers. 2010. Spray nozzle classification by droplet spectra. Standard Technical Note - S572 Chart. ASABE, Saint Joseph, Missouri, United States of America.

Anantharamaiah N., Vahedi, H., & Pourdeyhimi, B. 2007. A simple expression for predicting the inlet roundness of micro-nozzles. *Int. J. Multiph Flow.* 59, 206-220.

Andrade, D.R., Skurtys, O. & Osorio, F.A. 2012. Atomizing spray systems for application of edible coatings. *Compr. Rev. Food Sci. Food Saf.* 11, 323-337.

Angui, L., Qin, E., Xin, B., Wang, G., & Wang, J. 2010. Experimental analysis on the air distribution of powerhouse of Hohhot hydropower station with 2D-PIV. *Energy. Convers. Manage.* 51(1), 33-44.

Arikan-Akdagli, Sevtap, Mahmoud Ghannoum, & Jacques Meis 2018. Antifungal Resistance: Specific Focus on Multidrug Resistance in Candida auris and Secondary Azole Resistance in Aspergillus fumigatus. *Journal of Fungi* 4.4, 129.

Arvidsson, T., 1997. Spray drift as influenced by meteorological and technical factors. A methodological study. Swedish University of Agricultural Sciences, Acta Universitatis Agriculturae Sueciae, Agraria. 71, pp. 1997-144.

Azadi, H., Ho, P., & Hasfiati, L. 2011a. Agricultural land conversion drivers: A comparison between less developed, developing and developed countries. *Land Degrad. Develop. 22,* 596-604.

Azadi, H., Schoonbeek, S., Mahmoudi, H., Derudder, B., De Maeyer, P., & Witlox, F. 2011b. Organic agriculture and sustainable food production system: main potentials. *Agric. Ecosyst. Environ. 144,* 92-94.

Bahrouni, H., Sinfort, C., & Hamza, E. 2008. Evaluation of pesticide losses during cereal crop spraying in Tunisian conditions. 10th International Congress on Mechanization and Energy in Agriculture, Antalya, Turkey; pp.1-7.

Bird, S.L., Esterly, D.M. & Perry, S.G. 1996. Off-target deposition of pesticides from agricultural aerial spray application. *J. Environ. Qual. 25,* 1095-1104.

Bown, M. R., MacInnes, J. M., Allen, R. W. K., & Zimmerman, W. B. J. 2006. Three-dimensional, three-component velocity measurements using stereoscopic. *Meas. Sci. Technol.* 2175-2185.

Canadian Cancer Statistics. 2015. Predictions of the future burden, Toronto, ON,: Retrived from:http://www.cancer.ca/en/cancer-information/cancer-101/canadian-cancer-statistics-publication. Accessed on January 15, 2016.

Cao, X., Liua, J., Jiangb, N., & Chena, Q. 2014. Particle image velocimetry measurement of indoor airflow field: A review of the technologies and applications. *Energy Build*. 69, 367-380.

Carlsen, S.C.K., Spliid, N.H. & Svensmark, B. 2006. Drift of 10 herbicides after tractor spray application: 2. Primary drift (droplet drift). *Chemosphere. 64,* 778-786.

Chao, F., Chengsheng, Z., Fanyu, K., & Jing, W. 2011. Effects of spray height and spray angle on spray deposition in tobacco plants" 6th IEEE Conference on Industrial Electronics and Applications, Beijing, 2011, pp. 2390-2393.

Chaudhary, K. C., & Maxworthy, T. 1980. The nonlinear capillary instability of liquid jet: Part 3. Experiments of satellite drop formation and control. *J. Fluid Mech*. 96, 275-286.

Cock, N. D., Massinon, M., Mercatoris, B. C. N., & Lebeau, F. 2014. Numerical modeling of mirror nozzle flow. ASABE and CSBE/SCGAB Annual International Meeting. Sponsored by ASABE. Montreal, Quebec Canada. July 13 – 16, 2014.

Dabiri, D. 2009. Digital particle image thermometry/velocimetry: a review. *Exp in Fluids*. 46(2), 191-241.

Dantec Dynamics. 2013. Dynamic Studio User Guide, 2nd Ed. Tonsbakken 18, DK-2740 Skovlunde., Denmark.

De Jong, A., Michielsen, J. M. G. P., Stallinga H., & Zande, V. D. J. C. 2000. Effect of sprayer boom height on spray drift. *Comm. Agric. Appl. Biol. Sci.* 65(2), 919-930.

De Jong, A., Michielsen, J. M. G. P., Stallinga, H., & Van de Zande, J. C. 2000a. Effect of sprayer boom height on spray drift. Gent: Mededelingen Univ.

Derksen, R.C., Zhu, H., Ozkan, H.E, Hammond, R.B., Dorrance, A.E. & Spongberg, A.L. 2008. Determining the influence of spray quality, nozzle type, spray volume, and air-assisted application strategies on deposition of pesticides in soybean canopy. *Trans. ASABE. 51,* 1529-1537.

Etheridge, R. E., Womac, A. R., & Mueller, T. C. 1999. Characterization of the spray droplet spectra and patterns of four venturi-type drift reduction nozzles. *Weed Technol*. *13*(4), 765-770.

Farm Bill. 1990. U.S. Congress. Food, Agriculture, Conservation, and Trade Act of 1990. Public Law 101–624: U.S. Farm Bill, 28 November 1990.

Farooq, M., Balachandar, R. Wulfsohn, D. & Wolf, T.M. 2001. Agricultural sprays in cross flow and drift. *J. Agric. Eng. Res. 78,* 347-358.

Gary, D., Jim, H., Andrew, H., Steve, A., & Barry, N. 2007. Modeling the Interaction of Plant Architecture and Spray Techniques. *ASABE Annual International Meeting, ASABE Minneapolis Convention Center Minneapolis, Minnesota*. 17-20 June, 2007.

Gary, J. D., Forsterb, W.A., Lisa, C.M., Scott, W.M., Daryl, M.K., Jim, H., Ian, W.T., John, A.B., Joseph, Y., & Jerzy A.Z. 2016. Spray retention on whole plants: modelling, simulations and experiments. *Crop Protection.* 88, 118-130.

Ghayebloo, S., Tarokha, M. J., Venkatadri, U., & Diallo Claver. 2015. Developing a bi-objective model of the closed-loop supply chain network with green supplier selection and disassembly of products: The impact of parts reliability and product greenness on the recovery network. *J. Mauf. Syst. 36,* 76-86.

Ghosh, S., & Hunt, J. C. R. 1998. Spray jets in a cross-flow. *J. Fluid Mech.* 365(1), 109-136.

Giles, D., Klassen, P., Niederholzer, F., & Downey, D. 2011. "Smart" sprayer technology provides environmental and economic benefits in California orchards. *Calif. Agric. 65*(2), 85-89.

Grant, I. 1997. Particle image velocimetry: A review. *J. Mech. Eng. Sci.* 211(1), 55-76.

Gueyffier, D., Li, J., Nadim, A., Scardovelli, R., & Zaleski, S. 1999. Volume of Fluid interface tracking with smoothed surface stress methods for three-dimensional flows. *J. Comput. Phys.* 152, 423-456.

Guler, H., Zhu, H., Ozkan, H. E., Derksen, R. C., Yu, Y., & Krause, C. R. 2007. Spray characteristics and drift reduction potential with air induction and conventional flat-fan nozzles. *Power Machinery Division of ASABE*. *50,* 745−754.

Hain, R., Kähler, C. J., & Tropea, C. 2007. Comparison of CCD, CMOS and intensified cameras. *Exp in Fluids.* 42(3), 403-411.

Harlow, F. H., & Welch, E. 1965. Numerical calculation of time-dependent viscous incompressible flow of fluids with free surface. *Phys. Fluids.* 8, 2182-2192.

Heijne, B., Wenneker, M., & Zande, V. D. J. C. 2002. Air inclusion nozzles don't reduce pollution of surface water during orchard spraying in The Netherlands. Aspects Appl. Biol. Intl. *Adv. Pest. Appl.* 66, 193-199.

Hilza, E., & Vermeer, A. W. P., 2013. Spray drift review: the extent to which a formulation can contribute to spray drift reduction. *Crop Prot.* 44, 75-83.

Hirt, C. W. and Nichols, B. D. 1981. Volume of Fluid (VOF) method for the dynamics of free boundaries. *J. Comput. Phys*. 39, 201-225.

Homma, S., J. Koga, S. Matsumoto, M. Song and G. Tryggvason. 2006. Breakup mode of an axi-symmetric liquid jet injected into another immiscible liquid. *Chem. Eng. Sci.* 61:3986-3996.

Huang, Y., Zhan ,W., Fritz, B. K., & Thomson, S. J. 2011. Optimizing selection of controllable variables to minimize downwind drift from aerially applied sprays. *Appl. Eng. Agric. ASABE.* 28(3), 307-314.

Husted, B. P., Petersson, P., Lund, I., & Holmstedt, G. 2009. Comparison of PIV and PDA droplet velocity measurement techniques on two high-pressure water mist nozzles. *Fire Saf. J. 44,* 1030-1045.

Hwang, C.L. and Masud, A.S.M., 1979. Methods for multiple objective decision making. In *Multiple Objective Decision Making—Methods and Applications* (pp. 21-283). Springer, Berlin, Heidelberg.

Iqbal, M., Ahmad, M., & Younis, M. 2005. Effect of Reynold's number on droplet size of hollow cone nozzle of environment friendly university boom sprayer. *Pak. J. Agri. Sci.* 42, 106-111.

Jan, C. V. D. Z., Huijsmans, J. F. M., Porskamp, H. A. J., Michielsen, J. M. G. P., Stallinga, H., & Holterman, H. J. 2008. Spray techniques: how to optimize spray deposition and minimise spray drift. *Environmentalist.* 28, 9-17.

Janine, M. D. A. R. K. 2011. Presence and levels of priority pesticides in selected canadian aquatic ecosystems, s.l.: Water Science and Technology Directorate.

Jiang, Y., Li, H., Xiang, Q., & Chen, C. 2017. Comparison of PIV experiment and numerical simulation on the velocity distribution of intermediate pressure jets with different nozzle parameters. *Irrig. & Drain.* 1-10. DOI: 10.1002/ird.2133.

Jonsen, T. 1992. Simulation and modeling of turbulence incompressible flows. Ph.D. diss., Dept. of Comput. Engg., Swiss Feder. Inst. of Technol., Lausanne, Switzerland.

Klein, R. N., & Johnson A. K. 2002. Nozzle tip selection and its effect on drift and efficacy. *Aspects Appl. Biol., Intl. Adv. Pest. Appl. 66*, 217-224.

Koohafkan, P., Altieri, M. A., & Gimenez, E. H. 2012. Green Agriculture: Foundations for biodiverse, resilient and productive agricultural systems. *Int. J. Agric. Sustain. 10,* 61-75.

Kuepper, G., & Sullivan, P. 2004. Organic alternatives for late blight control in potatoes. National Sustainable Agriculture Information Service. Retrieved from https://attra.ncat.org/attra-pub/download.php?id=123. Accessed on Oct 21, 2015.

Labchuk, S. 2012. Pesticide exposure Isl,&. Prevent Cancer Now. Retrieved from http://www.preventcancernow.ca/pei-pesticide-exposure-isl,&. Accessed on Oct 21, 2015.

Labchuk, S. 2013. Earth action on PEI pesticides. Prevent Cancer Now. Retrieved from http://www.preventcancernow.ca/earth-action-on-pei-pesticides. Accessed on Oct 21, 2015.

Lakdawala, A. M., Gada, V. H., & Sharma, A. 2014. A dual grid level set method based study of interface-dynamics for a liquid jet injected upwards into another liquid. *Int. J. Heat Fluid Flow.* 59, 206-220.

Lakehal, D., Meier, M. & Fulgosi, M. 2002. Interface tracking towards the direct simulation of heat and mass transfer in multiphase flows. *Int. J. Heat Fluid Fl. 23,* 242-257.

Lee, M. C., Jan-Mou, L., Chan, H. C., & Huang, W.C. 2010. The measurement of discharge using a commercial digital video camera in irrigation canals. *Flow Meas. Instrum. 21*(2), 150-154.

Lin, Y., & Schrage, L. 2009. The global solver in the LINDO API, *Optim Meth and Soft*, 24:4-5, 657-668.

Lin, S. P., & Reitz, R. D. 1998. Drop and spray formation from a liquid jet. *Annu. Rev. Fluid Mech.* 30, 85-105.

Liu, J., Li, Q. L., Wang, Z. G., & Wu, H. Y. 2011. Numerical simulation of flow field in pressure-swirl injector based on VOF interface tracking method. *J. of Aero. Power*. 26(9), 1986-1994.

Lv, X., Zou, Q. P., & Reeve, D. 2011. Numerical simulation of overflow at vertical weirs using a hybrid level set/VOF method. *Adv. Water Resour*. 34, 1320-1334.

MacRae, R. J., Hill, S. B., Henning, J., & Mehuys, G. R. 1989. Agricultural Science and Sustainable Agriculture: A Review of the Existing Scientific Barriers to Sustainable Food Production and Potential Solutions. *Biol. Agric. Hortic. 6,* 173-219.

Mandal, A., Jog, M. A., Xue, J., & Ibrahim, A. A. 2008. Flow of power-law fluids in simplex atomizers. *Int. J. Heat Fluid Flow.* 29, 1494-1503.

Marcal, A. R. S. and Cunha, M. 2008. Image processing of artificial targets for automatic evaluation of spray quality. *Trans. ASABE*. 51, 811-821.

Meinhart, C. D., Wereley, S. T., & Santiago, J. G., 1999. PIV measurements of a microchannel flow. *Exp in Fluids.* 27, 414-419.

Menter, F. R., Kuntz, M. & Langtry, R. 2003. Ten years of experience with the SST turbulence model. In: Proceeding of the fourth international symposium on Turbulence, Heat Mass Transfer, Antalya, Turkey. pp. 625-632.

Miller, P. C. H., & Butler, E. M. C. 2000. Effects of formulation on spray nozzle performance for applications from ground-based boom sprayers. *Crop Prot. 19,* 609-615.

Miller, P. C. H., & Smith, R. W. 1997. The effects of forward speed on the drift from boom sprayers. Proc. Brit. Crop Prot. Conf. Weeds, Alton, U.K.: BCPC. pp. 399-406.

Miller, P. C. H., Ellis, M .C. B., Lane, A. G., & Tuck, C.R. 2011. Methods for minimising drift and off-target exposure from boom sprayer applications. *Asp. Appl. Biol.* 106, 281-288.

Miller, P. C. H. and Butler E. M. C. 1997. A review of spray generation, delivery to the target, and how adjuvants influence the process. *Plant Prot. Quart. 12,* 33-38.

Morgan, R. G., Markides, C. N., Zadrazil, I., & Hewitt, G. F. 2013. Characteristics of horizontal liquid–liquid flows in a circular pipe using simultaneous high-speed laser-induced fluorescence and particle velocimetry. *Int. J. Multiph Flow*. *2*(49), 99-118.

Nadeem, M., Chang, Y.K., Venkatadri, U., Diallo C., Havard, P. & Nguyen-Quang, T. 2018. Water quantification from sprayer nozzle by using particle image velocimetry (PIV) versus imaging processing technique. *Pak. J. Agri. Sci.* 55, 203-210.

Najjar, F. M., Thomas, B. G., & Donald, E. H. 1995. Turbulent flow simulations in bifurcated nozzles: effects of design and casting operation. *Metall. Trans.* B. 26, 749-765.

Nuyttens, D., Baetens, K., De Schampheleire, M., & Sonck, B. 2007a. Effect of Nozzle Type, Size and Pressure on Spray Droplet Characteristics. *Biosyst. Eng. 97,* 333-345.

Nuyttens, D., Schampheleire, M. D., Baetens, K., & Sonck, B. 2007b. The influence of operator-controlled variables on spray drift from field crop sprayers. Trans. ASABE. 50, 1129-1140.

Nuyttens, D., Schampheleire, D., Verboven, M., Verboven, P., & Dekeyse, D. 2009. Droplet size and velocity characteristics of agricultural sprays. *Transactions of the ASABE. 5*(52), 1471-1480.

Oerke, E. C. 2006. Crop losses to pests. *J. Agric. Sci., 144*, 31-43.

OpenFOAM, L. 2015. OpenFOAM User Guide. [Online] Retrieved from: http://cfd.direct/openfoam/user-guide. Accessed 7 Jan, 2016.

Otsu, N. 1979. A threshold selection method from gray-level histograms. *IEEE Trans. Comput*. 9, 62-66.

Ozkan, H.E. 1998. Effects of major variables on drift distances of spray droplets. Fact Sheet AEX 525-98. Columbus, Ohio State University Extension, United State of America.

Ozkan, H.E., Miralles, H., Zhu, H., Reichard, D.R. & Fox, R.D. 1997. Shields to reduce spray drift. *J. Agric. Eng. Res. 67,* 311-322.

Pelletier, N., Arsenault, N., & Tyedmers, P. 2008. Scenario modeling potential eco-efficiency gains from a transition to organic agriculture: Life cycle perspectives on Canadian canola, corn, soy, and wheat production. *J. Environ. Manage. 42*, 989-1001.

Piggott, S. & Matthews, G.A. 1999. Air induction nozzles: A solution to spray drift? *Intl. Pest Cont. 41,* 24-28.

Pimentel, D. 2005. Environmental and economic costs of the application of pesticides primarily in the United States. Environ. *Dev. Sustain. 7*(2), 229-252.

Reganold, J. P., Papendick, R. I., & Parr, J. F. 1990. Sustainable Agriculture. *Sci. Am*. *262*, 112–120.

Rivera-Ferre, M., Ortega-Cerdà, M., & Baumgärtner, J. 2013. Rethinking Study and Management of Agricultural Systems for Policy Design. *Sustainability. 5*, 3858–3875.

Ryskin, G., & Leal, L. G. 1984. Numerical solution of free-boundary problems in fluid mechanics. Part 2. Buoyancy-driven motion of a gas bubble through a quiescent liquid. *J. Fluid Mech.* 148, 19-35.

Santiago, J. G., Wereley, S. T., Meinhart, C. D., Beebe, D. J., & Adrain, R. J. 1998. A particle image velocimetry system for microfluidics. *Exp in Fluids*. 25, 316-319.

Shih, T. H., Liou, W. W., Shabbir, A., Yang, Z., & Zhu, J. 1995. A new k-e eddy-viscosity model for high Reynolds number turbulent flows- model development and validation. *Comput. Fluid.* 24, 227-238.

Shirani, E., Jafari, A., & Ashgriz, N. 2006. Turbulence models for flows with free surfaces and interfaces. *AIAA J.* 44, 1454-1462.

simulation of heat and mass transfer in multiphase flows. *Int. J. Heat Fluid Fl. 23,* 242-257.

Sinha, A., Sridhar, B., & Shivasubramanian, G. 2015. A numerical study on dynamics of spray jets. *Indian Acad. Sci.* 40(3), 787-802.

Smith, D.B., Askew, S.D., Morris, W.H. & Boyette, M. 2000. Droplet size and leaf morphology effects on pesticide spray deposition. *Trans. ASAE. 43,* 255-259.

Spraying system. 2013. A guide to spray technology for food processing, solutions for coating, cleaning, drying, food safety & more. Available online with updates at https://spray-nozzles.co.za/wp-content/uploads/2014/06/B524D_Food_Processing.pdf

Sudheer, P. K. and Panda, R. 2000. Digital image processing for determining drop sizes from irrigation spray nozzles. Agr. Water Manag. 45, 159-167.

Sumner, H., & Herzog, G. A. 2000. Assessing the effectiveness of air-assisted and hydraulic sprayers in cotton via leaf bioassay. *J. Cotton Sci. 4*, 79-83.

Taylor, J.J. & Hoyt, J.W. 1977. Waves on water jet. *J. Fluid Mech. 83,* 119-127.

Taylor, W. A., Andersen, P. G., & Cooper, S. 1989. The use of air assistance in a field crop sprayer to reduce drift and modify drop trajectories. Proc. British Crop Prot. Conf. - Weeds, 6B-5, Alton, U.K.: BCPC. pp. 631-639.

Teske, M. E., & Thistle, H. W. 1999. A simulation of release height and wind speed effects for drift minimization. *Trans. ASAE.* 42(3), 583-591.

Theunissen, R., Schrijer, F. F. J., Scarano, F. & Riethmuller, M. L. 2006. Application of adaptive PIV interrogation in a hypersonic flow. In: Proceedings of the 13th international symposium on applications of laser techniques to fluid mechanics, Lisbon, Portugal. pp. 26-29.

Tilman, D., Cassman, K., Matson, P., Naylor, R., & Polasky, S. 2002. Agricultural sustainability and intensive production practices. *Nature. 418*, 671-677.

Tiwari, A. K., Ghosh, P., Sarkar, J., Dahiya, H., & Parekh, J. 2014. Numerical investigation of heat transfer and fluid flow in plate heat exchanger using nano-fluids. *Int. J. Therm. Sci*. 85, 93-103.

Tobi, I., Saglam, R., Kup, F., Sahin, H., Bozdogan, A. M., & Piskin, B. 2011. Determination of accuracy level of agricultural spraying application in Sanliurfa/Turkey. *Afri. J. Agri. Res.* 6, 6064-6072.

Van de Zande, J. C., Van Ijzendoorn, M. T., & Meier, R. 2000. The effect of air assistance, dose and spray interval on late blight control Phytophthora infestans in potatoes. In Brighton crop protection conference, 12–16 November 2000, Brighton, pp. 1087–1092.

Velten, S., Leventon, J., Jager, N., & Newig, J. 2015. What is sustainable agriculture? A systematic review. *Sustainability. 7*, 7833-7865.

Versteeg, H., & Malalasekera, W. 1995. An introduction to computational fluid dynamics. The finit volume method. 1st ed. New York: John Wiley ,& Sons Inc.,605 Third Avenue.

Vimal, K.P. and S. Gupta. 2015. Study of nozzle injector performance using CFD. *Int. J. Rec. Ad. Mech. Engineering.* 4, 153-160.

William, E., & Smith. 2004. Reducing Herbicide Spray Drift. New Agriculture, Tamworth Agricultural Institute.

Wolf, T. M., & Caldwell, B. C. 2001. Development of a Canadian spray drift model for the determination of buffer zone distances. Proceedings of the 2001 National Meeting, Edited by: Bernier, D., Campbell, D. R.A. and Cloutier, D. Québec, Canada: City of Québec, Saint Anne-de Bellevue.

Yarpuz, N. & Bozdogan, A.M. 2009. Comparison of field and model percentage drift using different types of hydraulic nozzles in pesticide applications. *Intl. J. Environ. Sci. Tech. 6,* 191-196.

Yeh, C. 2005. Turbulent flow investigation inside and outside plain-orifice atomizers with rounded orifice inlets. *Heat Mass Transf*. 41, 810-823.

Yunkai L., P. Yang, T. Xu, S. Ren, X. Lin, R. Wei and H. Xu. 2008. CFD and digital particle tracking to assess flow characteristics in the labyrinth flow path of a drip irrigation emitter. *Irrig. Sci.* 26, 427-438.

Zamir, A.Z., Mohd, S.S., Suraya, M.T., Yousuf, E.S., Mohamad, R.I., Abdul, A.H., Azizan A., Khairil, F.A.B., & Radhiyah, K. 2014. Effect of nozzle angleson spray losses reduction. *Appl. Mech. Mater.* 564, 216-221.

APPENDIX- A: DETAILS OF CALCULATIONS

Table A-1: Sample data sheet for manual water collection

	No. of Pictures	10	20	30	40	50
	kPa	**V (ml)**	**V (ml)**	**V (ml)**	**V (ml)**	**V (ml)**
1st replication	25					
	50					
	75					
	100					
	125					
	150					
	175					
	200					
2nd replication	25					
	50					
	75					
	100					
	125					
	150					
	175					
	200					
3rd replication	25					
	50					
	75					
	100					
	125					
	150					
	175					
	200					

Result of calculations done for measuring the spray volume using PIV and manually measured methods at different pressures

Table A-2. Result of calculations done for measuring the spray volume using PIV and manually measured methods at 50 kPa pressure.

No. of pictures	N_1	N_2	$V_{PIV\text{-}water}$ (ml)	V_{water} (ml)	% Error
10	1910659	9188047.766	114.91	108.00	6.40
20	3820488	10375579.44	129.76	132.67	2.18
30	5716947	11554797.64	144.51	139.67	3.47
40	7696117	12785445.55	159.90	153.00	4.51
50	9303731	13785059.94	172.40	164.00	5.12
60	11116028	14911946.21	186.50	184.00	1.36
70	13140992	16171068.83	202.25	194.00	4.25
80	14989167	17320264.04	216.62	207.33	4.48
90	16556575	18294878.34	228.81	230.00	0.51
100	18386225	19432554.71	243.042	240.00	1.26

** Where: N_1 = Number of white pixels, N_2 = Number of droplets measured through white pixels, $V_{PIV\text{-}water}$ = Predicted volume= Volume measured by using PIV ml, V_{water} = Manually measured volume (ml)*

*Same notations were used for table A-2 to table A-8

Table A-3. Result of calculations done for measuring the spray volume using PIV and manually measured methods at 75 kPa pressure.

No. of pictures	N_1	N_2	$V_{PIV\text{-}water}$ (ml)	V_{water} (ml)	% Error
10	2144163	10233965.81	127.99	132.33	3.27
20	4608473	11652176.21	145.73	146.00	0.182
30	6921694	12983434.9	162.38	158.00	2.774
40	9239490	14317326.5	179.06	179.33	0.1486
50	11637919	15697622.38	196.33	193.67	1.3752
60	14065280	17094568.64	213.80	209.00	2.2974
70	16232773	18341960.86	229.40	231.00	0.6913
80	18639764	19727184.18	246.72	253.33	2.6074
90	21616013	21440015.48	268.15	268.67	0.1922
100	23863498	22733443.1	284.32	282.33	0.7062

Table A-4. Result of calculations done for measuring the spray volume using PIV and manually measured methods at 100 kPa pressure.

No. of pictures	N_1	N_2	$V_{PIV\text{-}water}$ (ml)	V_{water} (ml)	% Error
10	1434320	10740117.02	134.32	140.67	4.50
20	2848358	12455627.93	155.78	163.33	4.62
30	4237592	14141046.61	176.86	188.33	6.09
40	5719493	15938888.91	199.34	206.33	3.38
50	7366935	17937565.54	224.34	228.33	1.746
60	9875835	20981363.02	262.41	250.00	4.965
70	10186288	21358004.6	267.12	267.33	0.078
80	11619755	23097086.77	288.87	294.67	1.96
90	13003175	24775451.91	309.86	324.67	4.55
100	14592260	26703329.83	333.97	345.33	3.28

Table A-5. Result of calculations done for measuring the spray volume using PIV and manually measured methods at 125 kPa pressure.

No. of pictures	N_1	N_2	$V_{PIV\text{-}water}$ (ml)	V_{water} (ml)	% Error
10	1440602	11607711.83	145.17	157.33	7.72
20	2894166	13229889.26	165.46	188.67	12.29
30	4391019	14900377.2	186.35	195.67	4.75
40	5893026	16576617.02	207.32	221.33	6.32
50	7430765	18292733.74	228.78	240.67	4.93
60	8946248	19984012.77	249.94	271.67	7.99
70	10474505	21689547.58	271.27	292.33	7.20
80	11997930	23389689.88	292.53	310.00	5.63
90	13359080	24908733.28	311.53	326.67	4.63
100	14926333	26657787.63	333.40	353.67	5.72

Table A-6. Result of calculations done for measuring the spray volume using PIV and manually measured methods at 150 kPa pressure.

No. of pictures	N_1	N_2	$V_{PIV\text{-}water}$ (ml)	V_{water} (ml)	% Error
10	2007716	12011932.2	150.23	155.33	3.28
20	3968836	13977170.56	174.81	184.00	4.99
30	6011453	16024077.05	200.41	207.67	3.49
40	7975757	17992506.09	225.03	235.33	4.37
50	9962695	19983616.66	249.93	254.00	1.60
60	12065774	22091112.13	276.29	311.33	11.25
70	14187548	24217341.85	302.88	328.33	7.75
80	16230258	26264341.54	328.48	335.00	1.94
90	18185686	28223875.94	352.99	358.67	1.58
100	20323692	30366371.75	379.79	401.67	5.44

Table A-7. Result of calculations done for measuring the spray volume using PIV and manually measured methods at 175 kPa pressure.

No. of pictures	N_1	N_2	$V_{PIV\text{-}water}$ (ml)	V_{water} (ml)	% Error
10	2319684	12511289.9	156.47	175.67	10.92
20	4509910	14882428.57	186.13	193.00	3.55
30	6007780	16504022.63	206.41	222.33	7.15
40	7816446	18462084.44	230.90	251.67	8.24
50	9795098	20604173.09	257.69	273.33	5.720
60	12274143	23287987.21	291.26	263.00	10.74
70	14547919	25749577.11	322.04	322.67	0.19
80	16348220	27698582.97	346.42	364.33	4.915
90	18550800	30083096.08	376.24	406.00	7.32
100	20565230	32263918	403.52	416.00	2.99

Table A-8. Result of calculations done for measuring the spray volume using PIV and manually measured methods at 200 kPa pressure.

No. of pictures	N_1	N_2	$V_{PIV\text{-}water}$ (ml)	V_{water} (ml)	% Error
10	2229876	12313496.35	154.00	198.33	22.35
20	4499193	14667912.74	183.45	227.33	19.30
30	6808518	17063837.43	213.41	230.67	7.47
40	9062462	19402304.33	242.66	275.67	11.97
50	11247265	21669037.44	271.014	287.33	5.67
60	13673302	24186050.83	302.49	309.33	2.21
70	15711660	26300847.25	328.94	346.00	4.92
80	18624659	29323083.71	366.74	401.00	8.54
90	20294840	31055896.5	388.41	421.00	7.73
100	22402382	33242471.33	415.76	465.67	10.71

Table A-9. Result of calculations done for measuring the spray volume using PIV and manually measured methods at different pressures.

Pressure (kPa)	No. of Pictures	Mean (% Error)	Pressure (kPa)	No. of Pictures	Mean (% Error)
200	10	22.220 a	50	70	4.3044 cde
200	20	19.271 ab	125	80	4.2329 cde
175	60	144.937 abc	125	100	4.2019cde
200	40	11.976 abcd	125	30	3.9503 cde
125	20	11.733 abcde	25	60	3.8850 cde
175	10	10.8557 abcde	125	50	3.8213 cde
200	100	10.7551 abcde	150	20	3.7088 cde
150	60	8.9564 bcde	175	10	3.5212 cde
200	80	8.5843 bcde	25	10	3.3504 cde
175	40	8.2079 bcde	100	40	3.3303 cde
50	40	8.2079 bcde	75	80	3.2700 cde
200	90	7.7806 bcde	100	100	3.2655 cde
200	30	7.4283 cde	75	10	3.1895 cde
125	10	7.2751cde	125	90	3.1592 de
175	90	7.3232 cde	150	10	3.0810 de
175	30	7.1514 cde	175	100	2.9929 de
50	80	7.0037 cde	100	50	2.9297 de
25	20	6.8154 cde	50	20	2.8329 de
125	60	6.8142 cde	75	30	2.7746 de
25	40	6.7863 cde	200	60	2.7233 de
50	10	6.4270 cde	50	90	2.6957 de
25	30	6.0339 cde	100	80	2.5746 de
100	30	5.9865 cde	150	100	2.4437 de
125	70	5.9185 cde	150	40	2.3560 de
50	30	5.7376 cde	75	60	2.3179 de
175	50	5.7006 cde	75	70	2.2457 de
200	50	5.6498 cde	150	30	1.7671 de

Table A-9. Result of calculations done for measuring the spray volume using PIV and manually measured methods at different pressures.

125	40	5.3614 cde	25	70	1.6295 de
50	50	5.1998 cde	75	100	1.5767 de
150	70	5.1791 cde	150	90	1.4255 de
50	60	5.1583 cde	75	50	1.3941 de
25	80	5.0776 cde	100	70	1.3583 de
100	60	4.9835 cde	150	50	1.2994 de
200	70	4.9598 cde	50	100	1.2726 de
175	80	4.9149 cde	150	80	1.1111 de
25	50	4.6513 cde	25	100	0.9754 de
100	20	4.5349 cde	25	90	0.9749 de
75	20	4.4630 cde	75	40	0.5454 de
100	10	4.4506 cde	75	90	0.2657 de
100	90	4.4486 cde	175	70	0.2110 e

Means with same grouping letter are not significantly different at the 5% level using LS mean

APPENDIX –B: PUBLICATIONS AND COPY RIGHT PERMISSION

Jan 23, 2019

Journal Articles
Pakistan Journal of Agricultural Sciences

Dear Sir/ Madam

I am preparing m PhD thesis for submission to the Faculty of Graduate Studies at Dalhousie University, Halifax, Nova Scotia, Canada. I am seeking your permission to include a manuscript version of the following paper(s) as a chapter in the thesis:

Nadeem M, Y. K. Chang, U. Venkatadri, C. Diallo, Havard, T. Nguyen-Quang. 2018. Water Quantification from sprayer nozzle by using Particle Image Velocimetry (PIV) versus Imaging Processing Technique. Pk. J. Agri. Sci. Vol. 55(1), 203-210.

Nadeem M, T. Nguyen-Quang, C. Diallo, U. Venkatadri, P. Havard, 2019. Contribution to spraying nozzle study: a comparative investigation of imaging and simulation approaches. Pk. J. Agri. Sci. Vol. 56(1), 215-224.

Canadian graduate theses are reproduced by the Library and Achieves of Canada (formerly National Library of Canada) through a non-exclusive, world-wide license to reproduce, loan, distribute, or sell theses. I am also seeking your permission for the material described above to be reproduced and distributed by the LAC (NLC). Further details about the LAC (NLC) thesis program are available on LAC (NLC) website (www.nlc-bnc.ca).

Full Publication details and a copy of this permission letter will be included in the thesis.

Yours Sincerely,

Muhammad Nadeem
PhD Candidate, Industrial Engineering,
Dalhousie University, Halifax, Canada

Permission is granted for:

The inclusion of the material described above in your thesis.

For the material described above to be include in the copy of your thesis that is sent to the library and Archives of Canada (formally National Library of Canada) for reproduction and distribution.

Name: **Prof. Dr. Jafar Jaskani** **Title - Managing Editor**

Signature: _____ **Dated: 25-01-2019**

APPENDIX –C: SNAPSHOTS OF ANSYS 16. FLUENT AND MPL 5.0

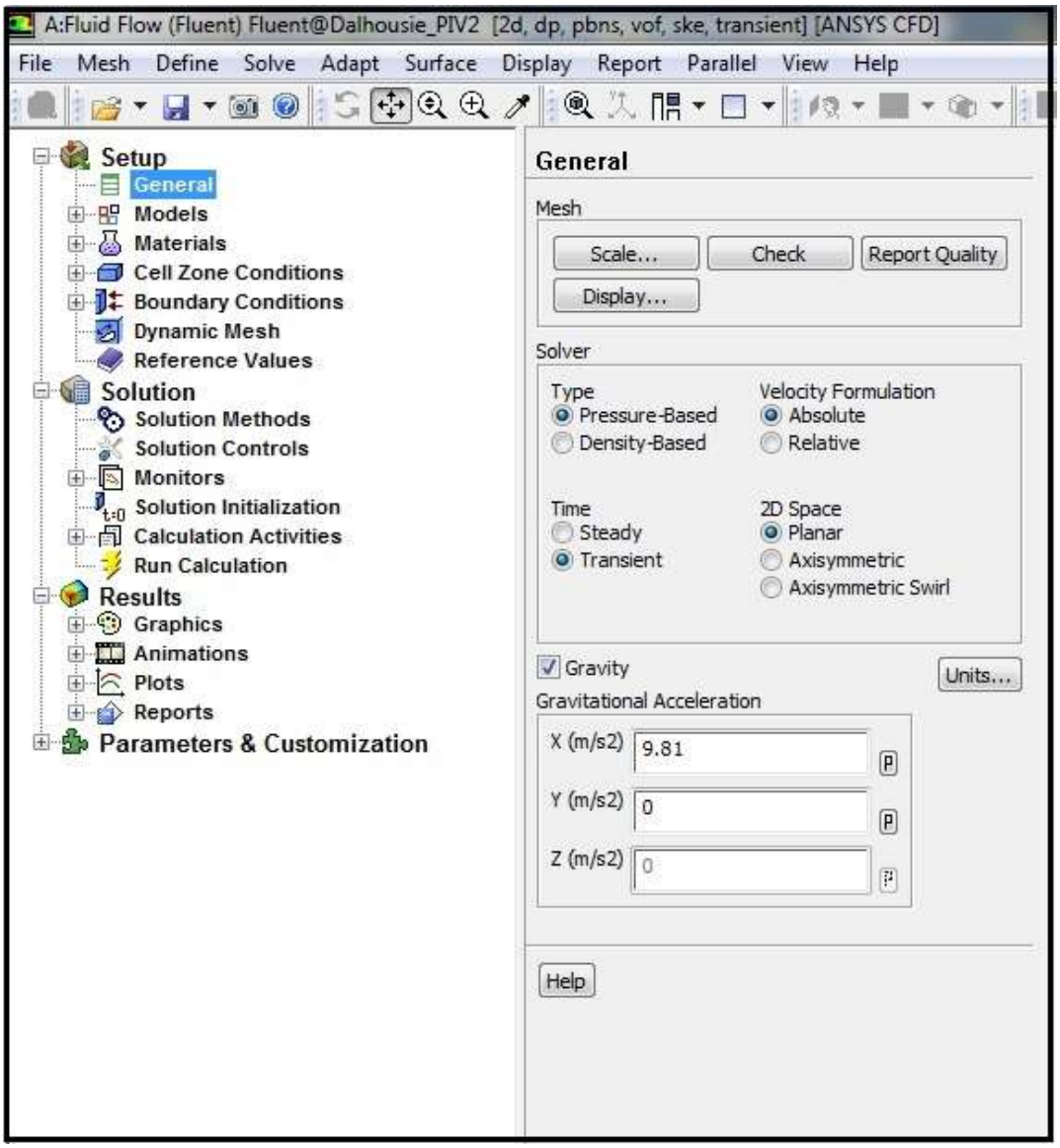

C-1. Selection of general parameters for simulation

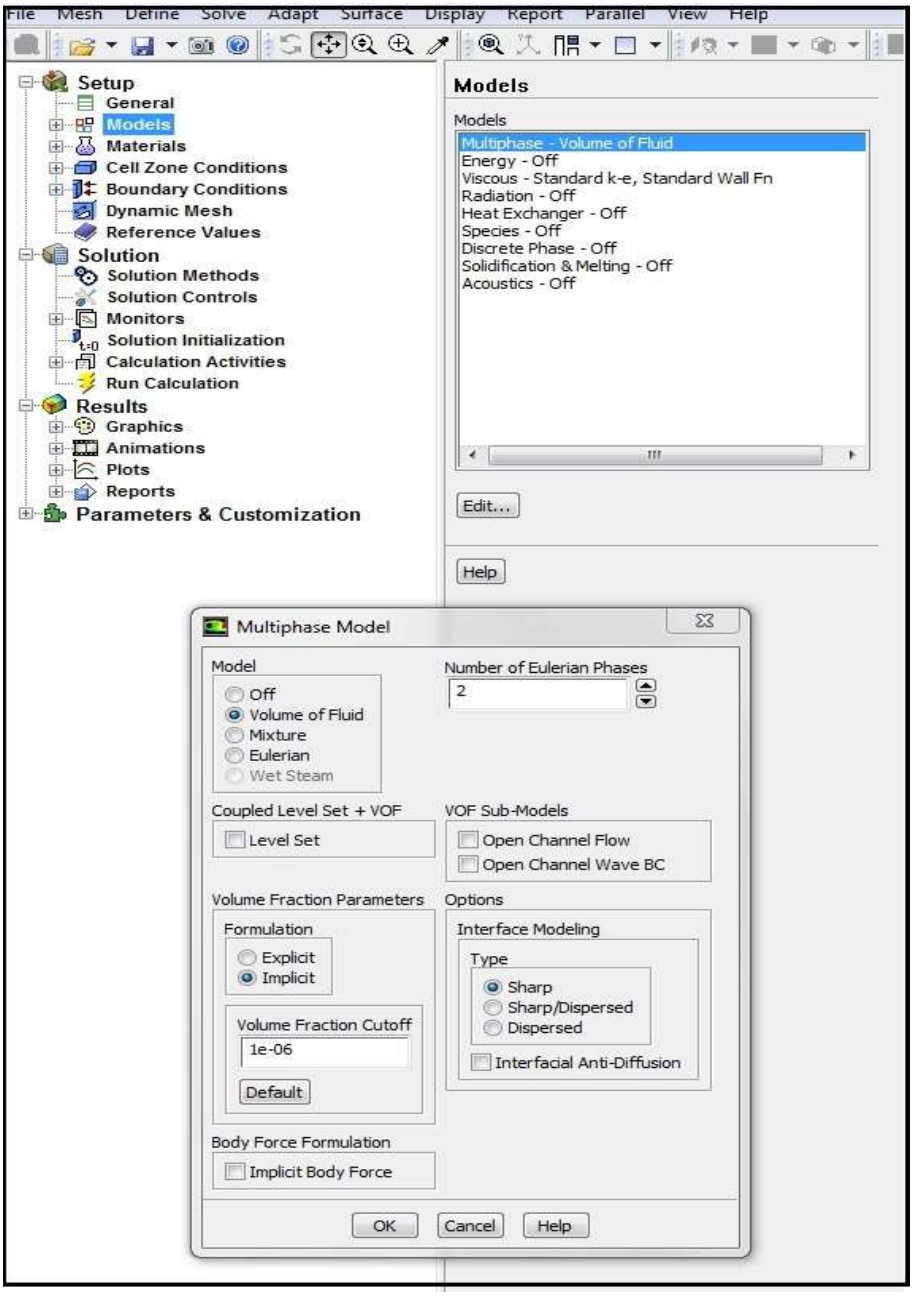

C-2. Selection of different parameters for Multiphase model (VOF)

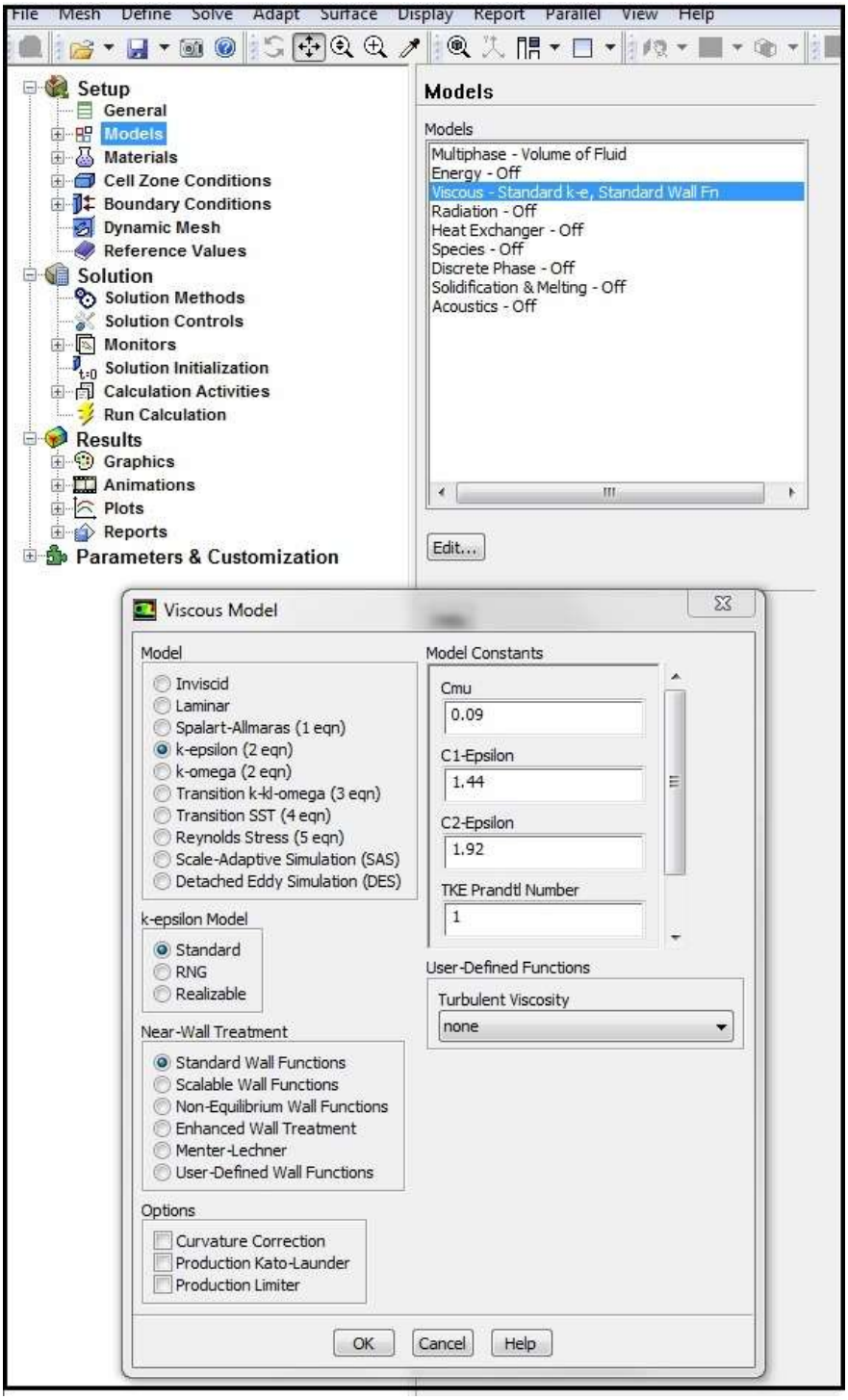

C-3. Selection of standard K-epsilon model

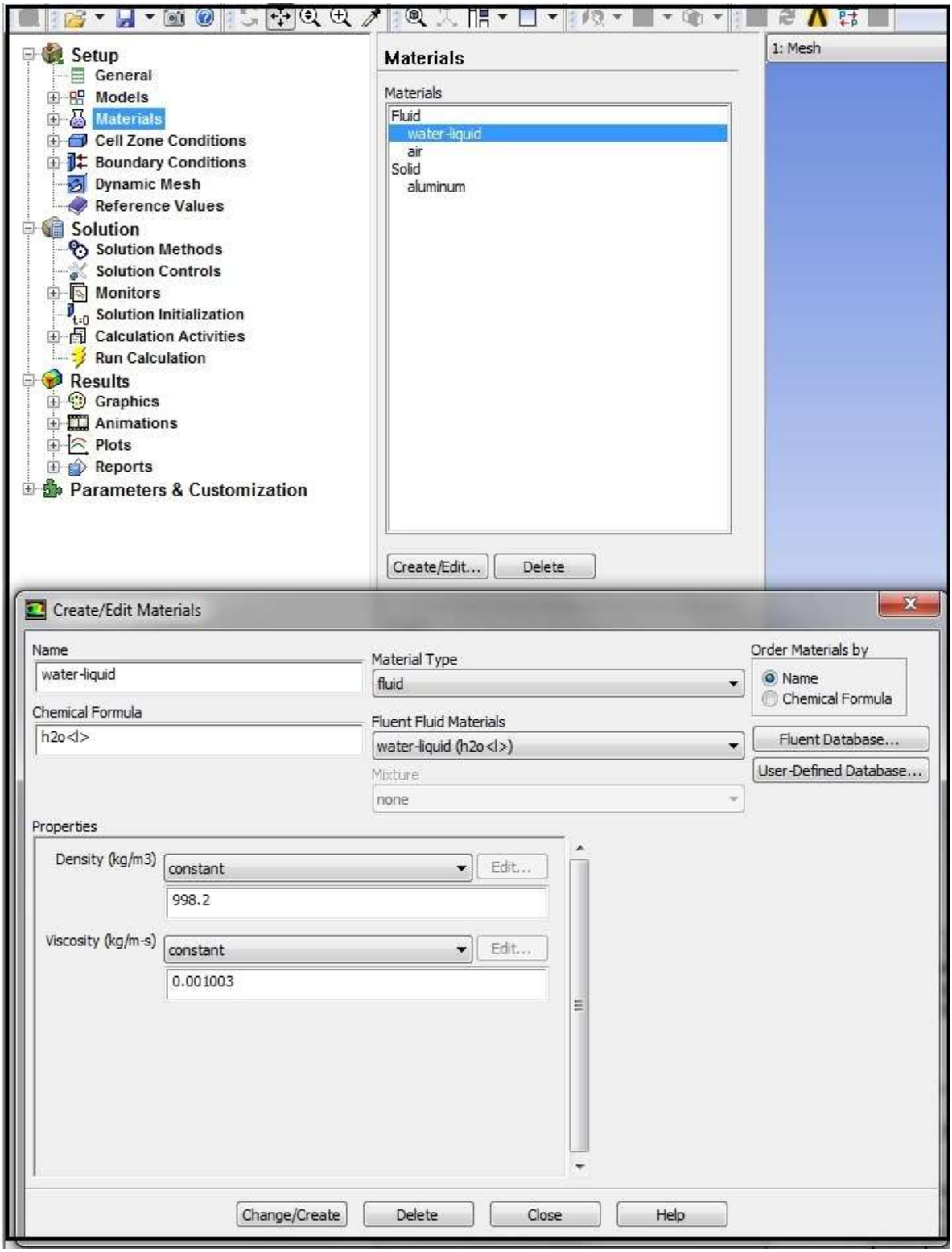

C-4. Assigning the density and viscosity to water and air phases.

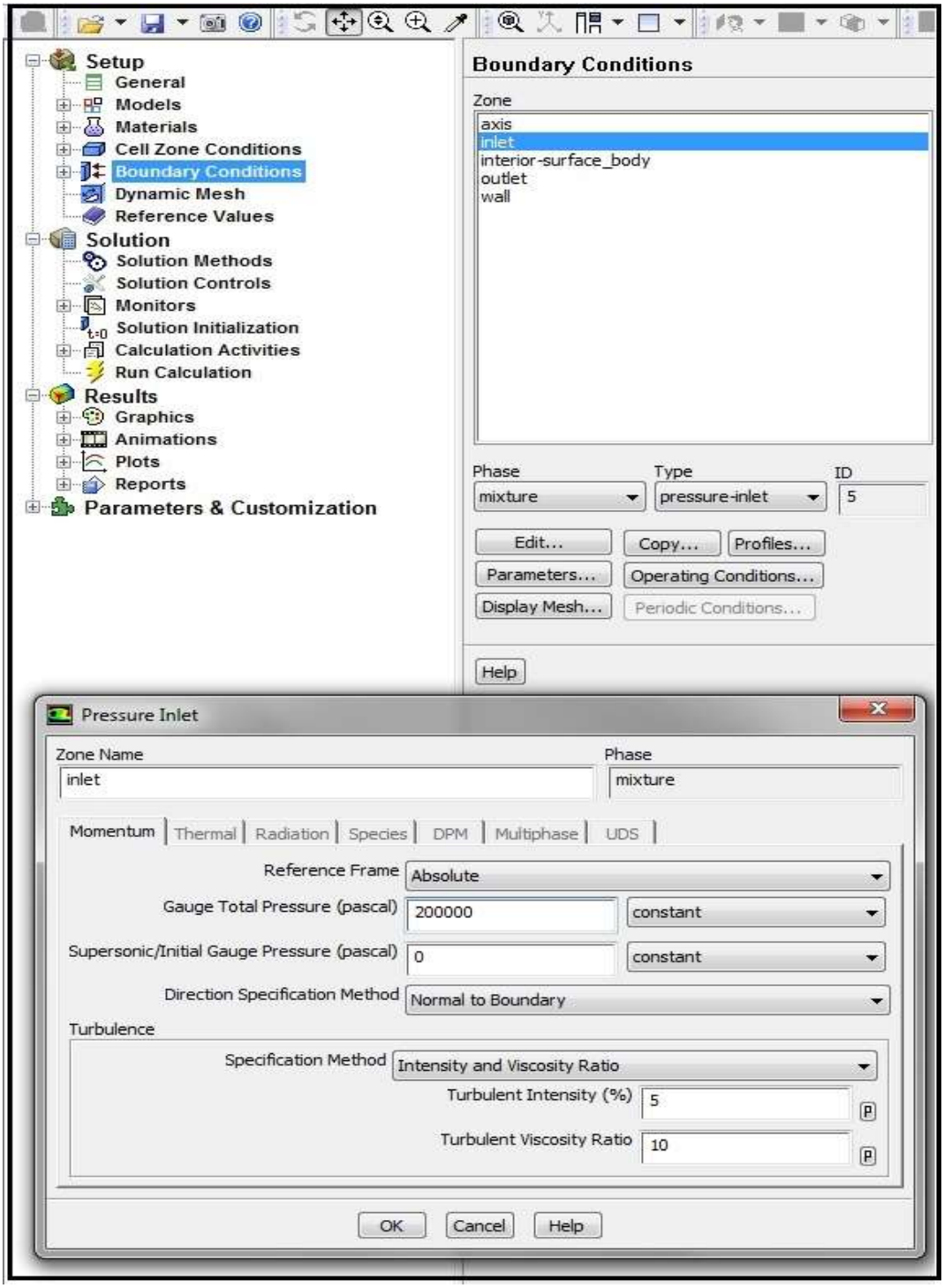

C-5. Boundary conditions selections for inlet.

C-6.

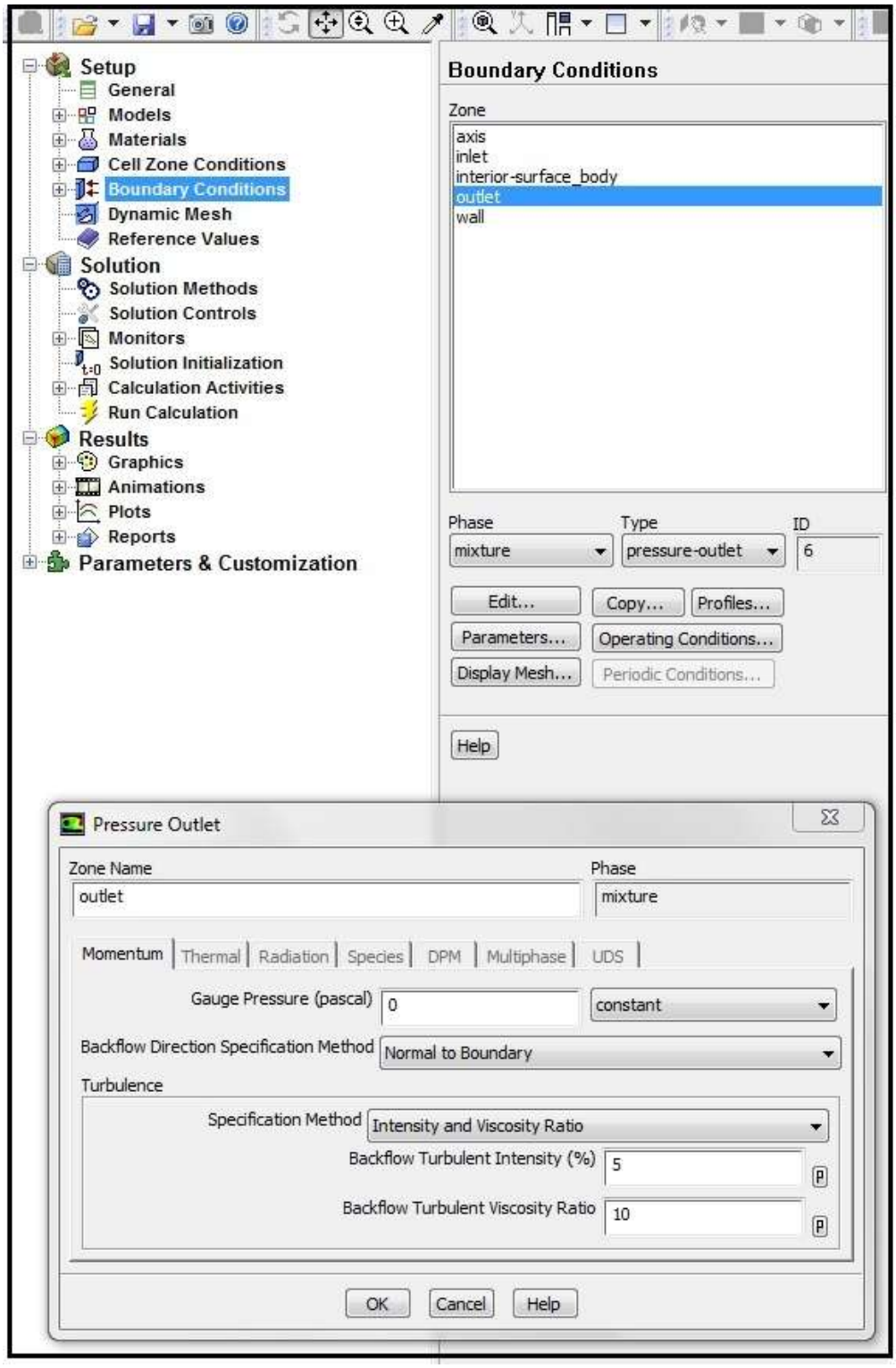

Boundary conditions selections for outlet.

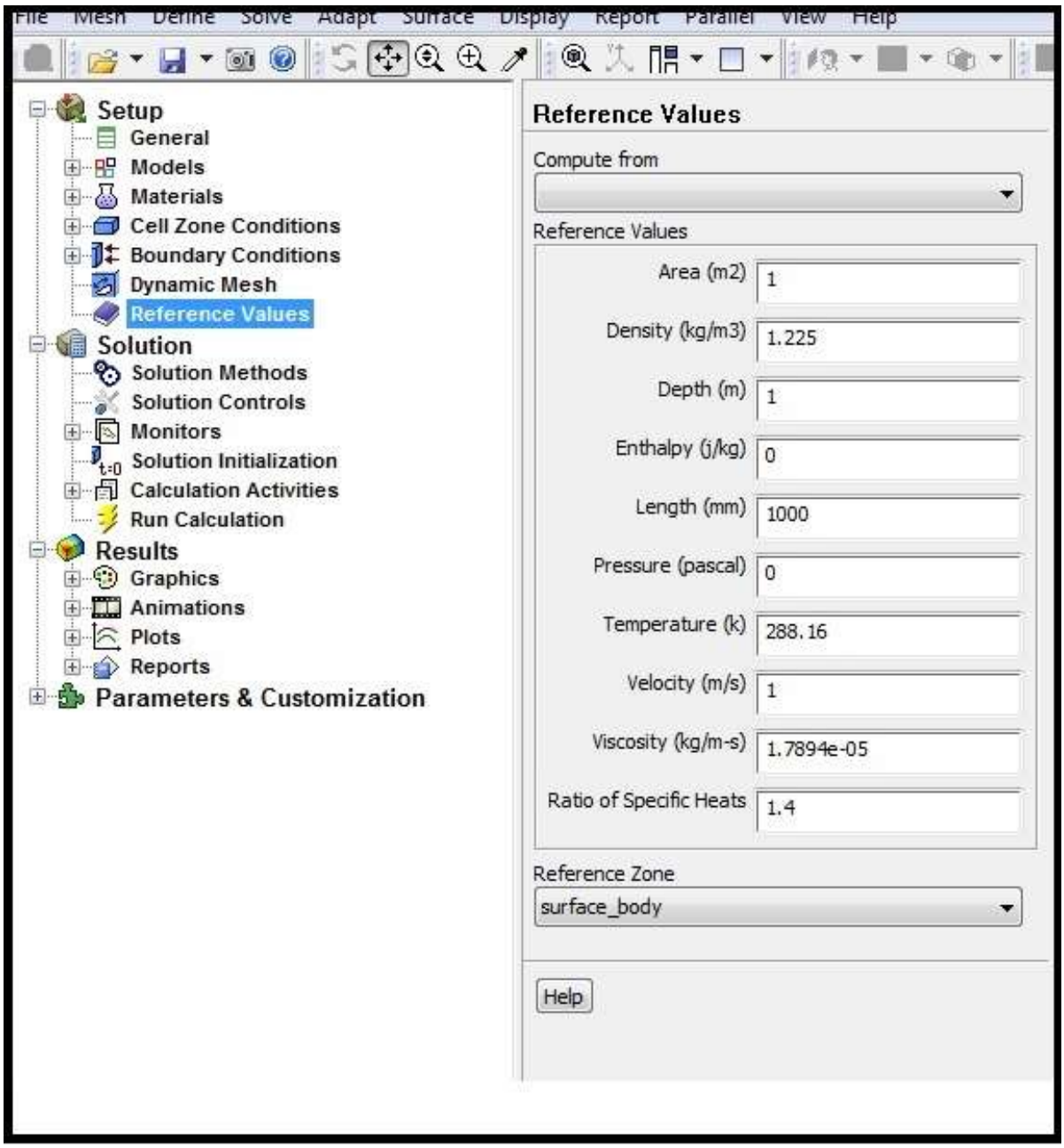

C-7. Selection of reference values before initialization of model.

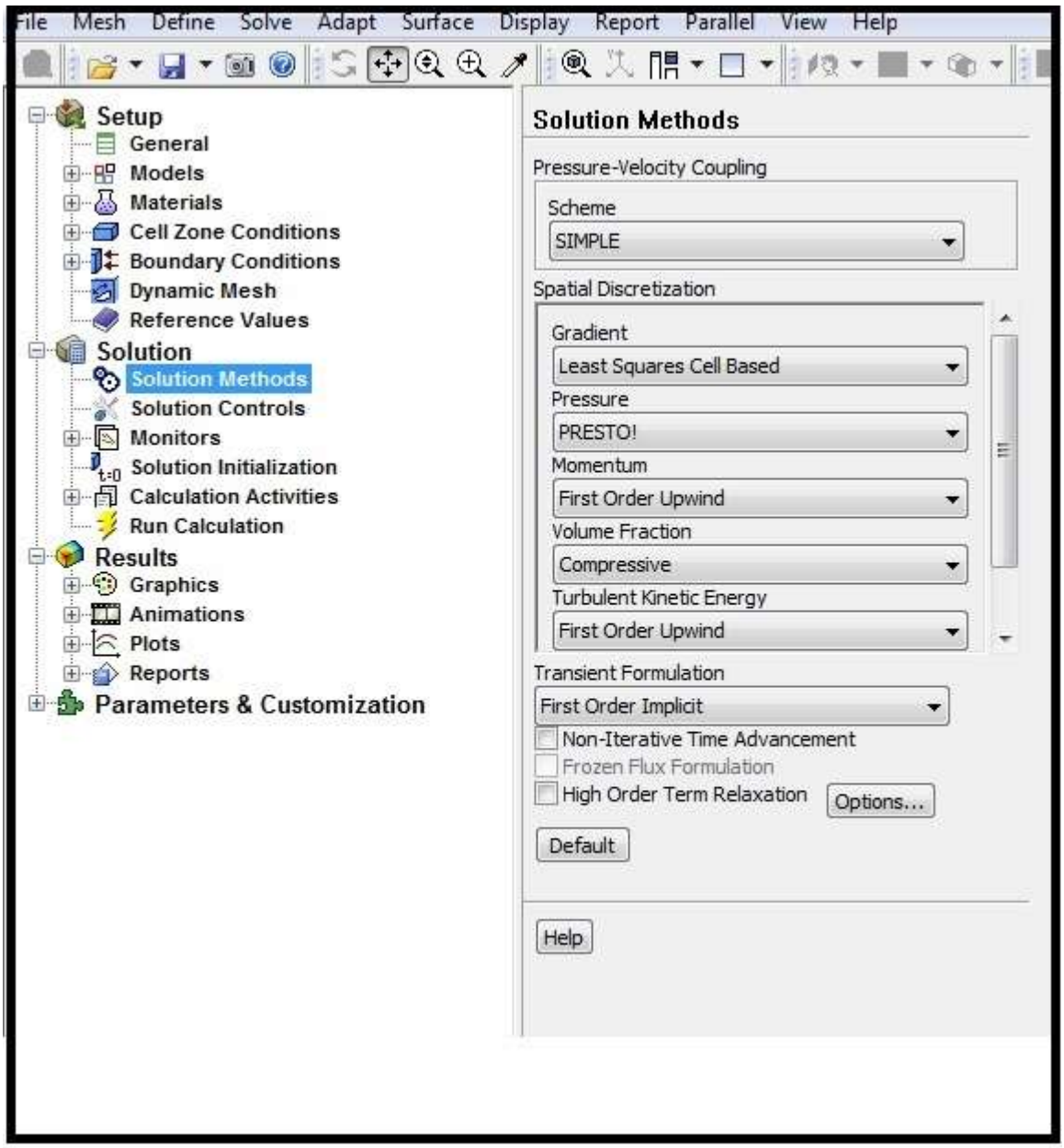

C-8. Solution method and spatial discretization.

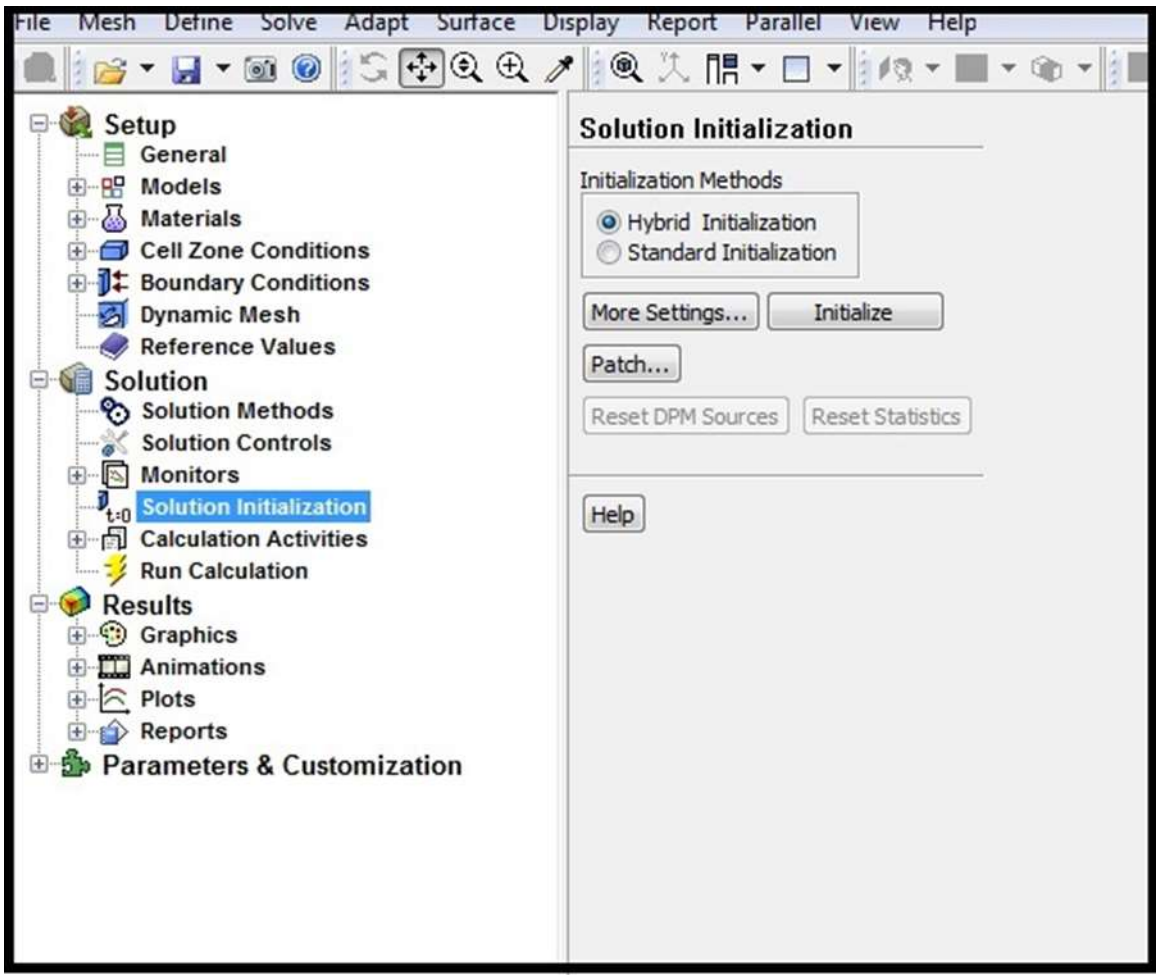

C-9. Initialization process

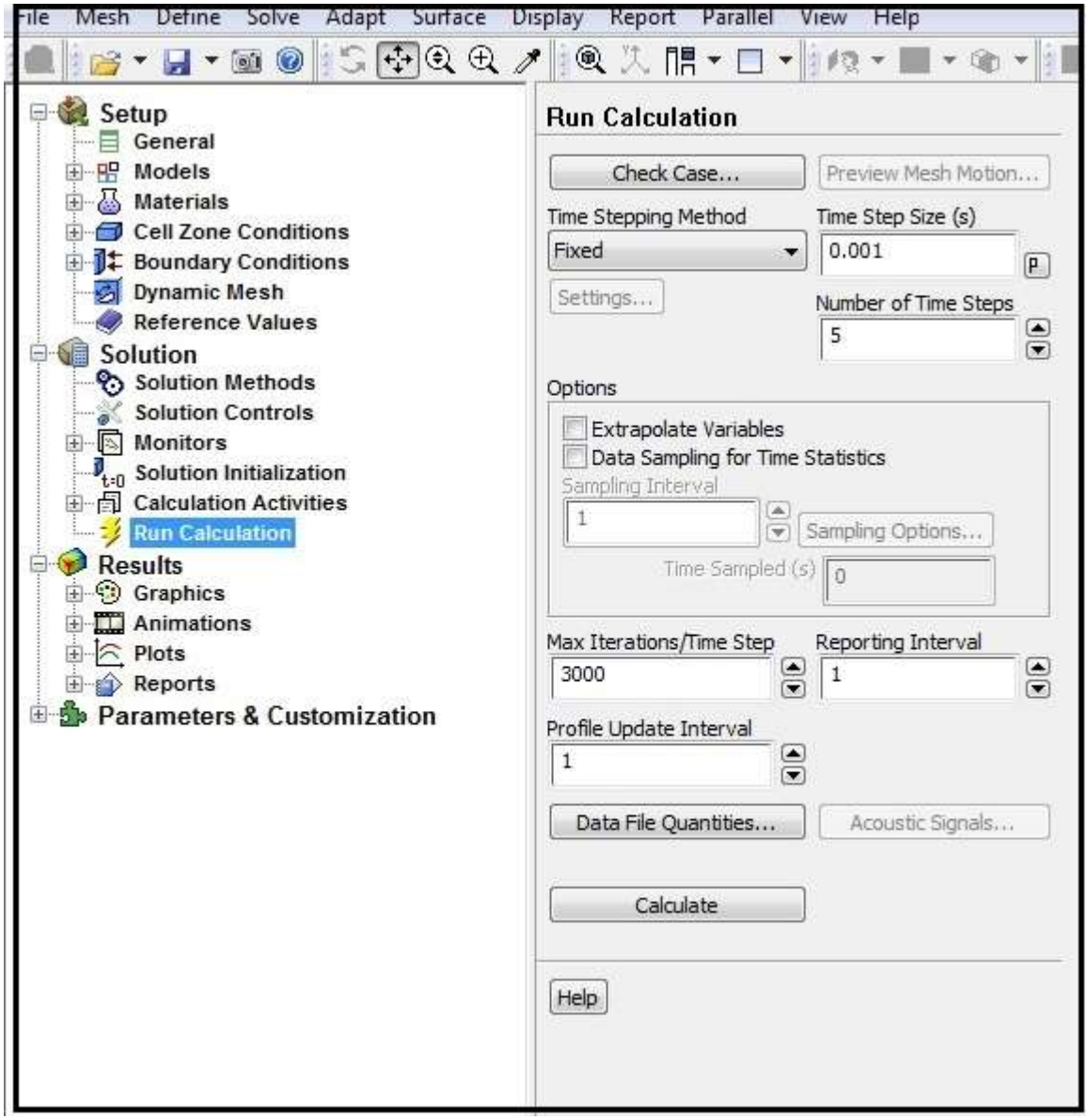

C-10. Section of time steps, maximum iteration, and run calculation.

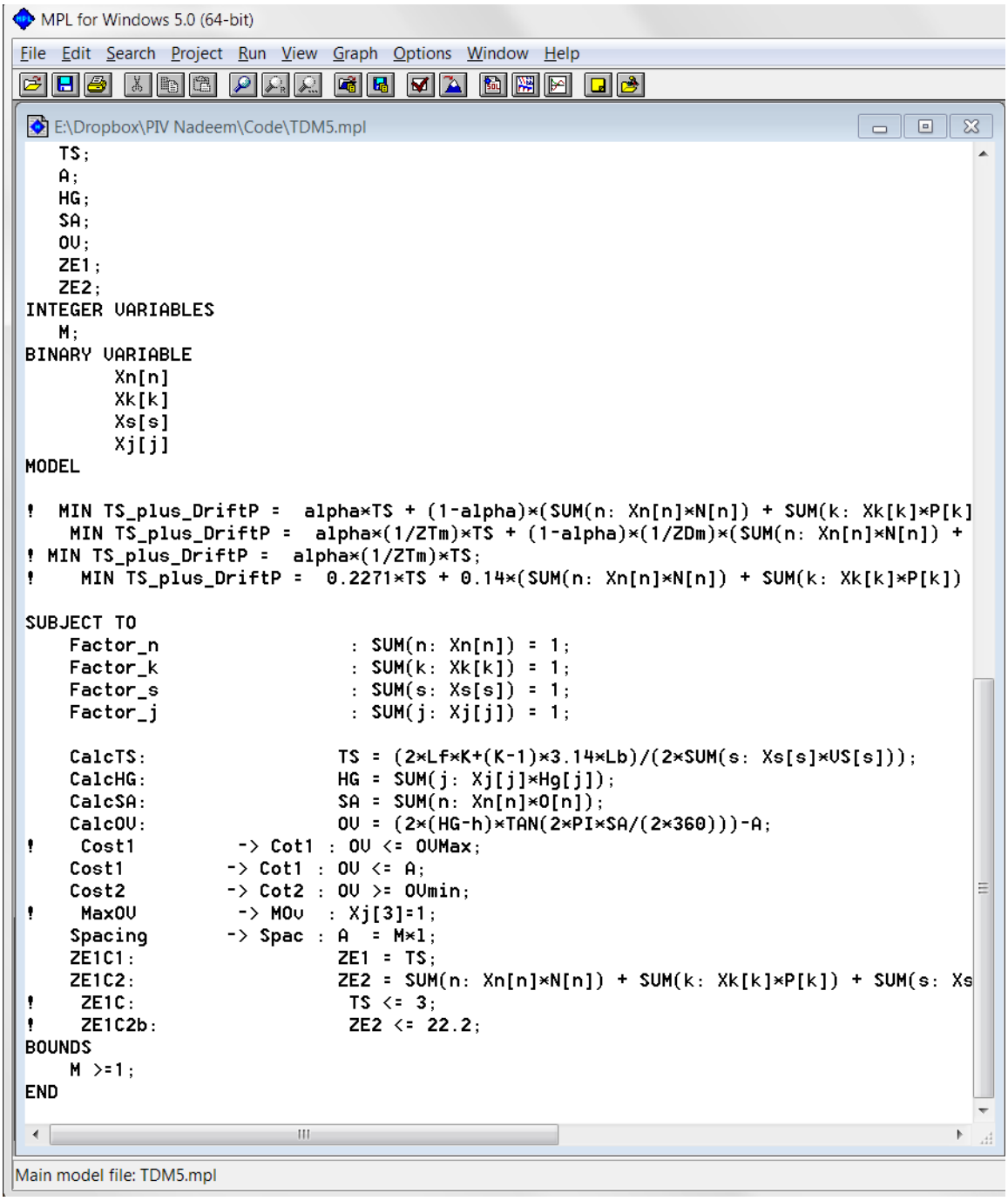

C-11. Bi-objective model, declaration of variables and constraints using MPL 5.0.

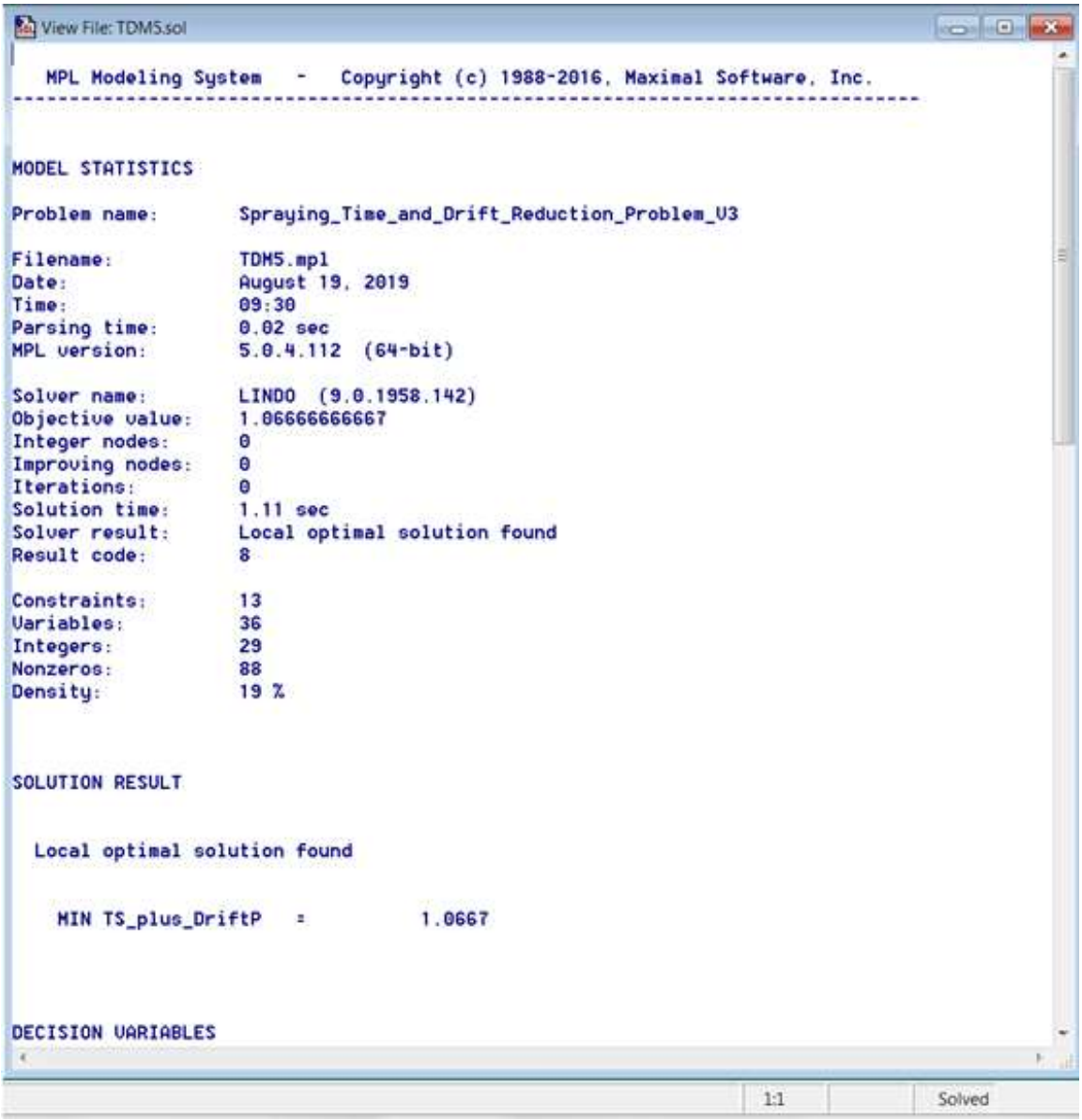

C-12. Bi-objective model statistics